RIVER AND STREAM TEMPERATURE IN A CHANGING CLIMATE

by

GRACE GARNER

A thesis submitted to the University of Birmingham for the degree of

DOCTOR OF PHILOSOPHY

School of Geography, Earth and Environmental Sciences

College of Life and Environmental Sciences

University of Birmingham

July 2014

Abstract

Driven by a changing climate and associated hydrological changes, the temperature of river water has changed worldwide and future change is anticipated. There is major concern that these river temperature changes will have profound impacts on freshwater ecosystems. To identify the rivers most sensitive to change and implement effective strategies to mitigate high thermal extremes, this thesis aims to improve understanding of the influences of hydrometeorology and riparian landuse on river temperature dynamics, controls and processes within a UK context. A multi-scale research design is adopted to address research gaps in four interlinked, key sub-themes. First, spatial patterns and inter-annual variability in the shape and magnitude of annual river temperature regimes are identified across England and Wales, and regime sensitivity to air temperature and river basin properties elucidated. Second, for a Scottish upland stream (the Girnock Burn), the prevailing hydrometeorological conditions are identified under which shading by riparian vegetation may be effective in mitigating river thermal variability and extremes. Third, a high-resolution water temperature model is applied to a 1050 m reach of the Girnock Burn to identify the processes driving cooling water temperature gradients in forested stream reaches. Fourth, the water temperature model is used to quantify the effects of riparian shading scenarios, channel orientation and water velocity on reach-scale stream temperatures dynamics. The main research outcomes are: (1) lowland streams in which contributions to streamflow are sourced predominantly from surface water are anticipated to be the most vulnerable to climate warming, (2) shading streams with semi-natural riparian vegetation is effective in mitigating thermal variability and extremes under high energy input, (3) shading headwater streams reduces the rate at which water warms as it flows downstream but water cools under very dense canopies only, and (4) afforesting southerly river banks with relatively sparse, over-hanging vegetation may be highly effective

in reducing high water temperature extremes. The results represent significant advancements towards making well-informed decisions concerning river thermal regimes and thus protecting freshwater ecosystems.

Acknowledgements

I thank David Hannah, Iain Malcolm, and Jon Sadler for their advice, sharing their enthusiasm, continual encouragement, and providing research training.

I thank the UK Natural Environment Research Council for funding my research through PhD Studentship NE/1528226/1. I also thank Marine Scotland Science Freshwater Laboratory for providing support in kind that enabled field data collection for Chapters 3, 4, and 5, and for the opportunity to work in the Girnock catchment.

I'm grateful to a number of organisations which provided me with data: the Environment Agency of England and Wales, the British Atmospheric Data Centre, Landmap UK, the British Geological Survey, and the Scottish Environmental Protection Agency.

I thank Luke Cooper for calculating the basin properties used in Chapter 2 and Anne Anckorn for drawing the maps in Chapters 3 and 4. R was used for remaining graphics, data analyses and modelling, and I'm grateful to countless Posters on online help forums for their advice on programming in this language. My sincere thanks also to: Freshwater Laboratory Staff who provided technical and field assistance, maintained and retrieved data from the weather stations and always made me feel welcome at the Lab, Colin Millar for suggesting and writing the code for the statistical methods employed in Chapter 3, Jason Leach and Dan Moore for generously sharing their net radiation model code that Chapters 4 and 5 rely heavily upon, and Nigel Mottram for valuable suggestions on how to write the water temperature model code. I also thank Harriet Orr who advised me on writing Chapter 2, five anonymous Reviewers, Anne Jefferson, Des Walling, Dan Moore, and Martijn Westhoff for comments made on versions of Chapters 1, 2, 3, and 4 during review processes in Progress in Physical Geography, Hydrological Processes, and Hydrology and Earth System Sciences, and finally Angela Gurnell and Nick Kettridge for thoughtful comments made during examination.

In addition, I thank Kieran Khamis, Ana Casado, and Phil Blaen for offering welcome advice on many aspects of this research. My thanks again to Kieran, Ana, and Phil, also Liliana Rose, Bryony Anderson, Megan Klaar, Faye Jackson, and everyone else in Geography 325 for their friendship, encouragement, many cups of tea and pieces of cake.

Finally I thank my Parents, who supported me unconditionally in this endeavour.

TABLE OF CONTENTS

LIST OF FIGURES

Figure 37. Water temperatures simulated throughout the reach under the scenario of 40 % canopy density under (a) channel orientation under which southerly sky-positions are not shaded and high flow velocity (b) channel orientation under which southerly sky-positions are shaded and high flow velocity (c) difference between a and b (d) channel orientation under which southerly sky-positions are shaded and low flow velocity (e) channel orientation under which southerly sky-positions are shaded and high flow velocity (f) difference between d and e (g) difference between a and d (h) difference between b and e. 136

LIST OF TABLES

CHAPTER ONE: INTRODUCTION

1.1 WATER TEMPERATURE: IMPORTANCE AND SENSITIVITY TO A CHANGING CLIMATE

Water temperature is recognised increasingly by scientists, environment managers and regulators as an important and highly sensitive 'master' variable of water quality (Hannah *et al.*, 2008). Temperature directly influences: distribution, (e.g. Boisneau *et al.*, 2008), predator-prey interactions (e.g. Boscarino *et al.*, 2007), survival (e.g. Wehrly *et al.*, 2007), growth rates (e.g. Jensen, 2003; Imholt *et al.*, 2010, 2011), timing of life history events (Harper and Peckarsky, 2006), and metabolism (e.g. Alvarez and Nicieza, 2005) of aquatic organisms in river systems. Indirectly, temperature controls in-stream processes such as rates of production, nutrient consumption and thus food availability, decomposition (e.g. Ormerod, 2009) and dissolved oxygen concentration (e.g. Sand-Jensen and Pedersen, 2005), which influence ecological processes further.

The desire to understand the effects of land management practices (particularly deforestation of conifer plantations) on cold-water adapted fish drove the earliest research into river and stream temperature (Moore *et al.*, 2005). More recently, interest has been motivated by the anticipation that water thermal regimes will be highly sensitive to a changing climate and anthropogenic impacts, with associated profound potential impacts on freshwater ecosystems as a whole (Ormerod, 2009). Instrumented records from recent decades demonstrate significant river temperature warming (e.g. Langan *et al.*, 2001; Durance and Ormerod, 2007; Kaushal *et al.*, 2010; Orr *et al.*, 2014) and, at some locations, cooling (e.g. Arismendi *et al.*, 2012; Isaak *et al.*, 2012). Future projections indicate further change (e.g. van Vliet *et al.*, 2013a; MacDonald *et al.*, 2014a). With these concerns in mind, process based understanding of the controls on space-time variability in water temperature is required urgently as an

important first-step towards making well-informed decisions concerning river thermal regimes and thus protecting freshwater ecosystems (Wilby *et al.*, 2010).

1.2 PROCESSES, CONTROLS, DYNAMICS AND DRIVERS OF CHANGE

1.2.1 Processes

Water temperature is controlled by dynamic energy (heat) and hydrological fluxes at the air-water and water-riverbed interfaces (Hannah *et al.*, 2008a). Land and water management impact on these drivers and, thus, modify river thermal characteristics (Webb *et al.*, 2008). Rivers are hierarchical systems (Montgomery, 1999) and therefore for a specific point on a river, water column temperature is determined initially by the mix of water source contributions (i.e. surface/ shallow sub-surface flows, groundwater, ice/snow melt etc.) and subsequently the energy gained or lost across the water surface and riverbed interfaces as the river flows downstream. Consequently, spatial and temporal variability in heat fluxes and hydrological processes create heterogeneity in water temperature at a range of scales (Webb, 1996).

Heat transfer within river systems occurs by a combination of: radiation, conduction, convection and advection (Webb and Zhang, 1997). These energy exchanges add and remove heat to and from the river. Energy inputs occur by: incident shortwave (solar) and longwave (downward atmospheric) radiation, condensation, and friction at the channel bed and banks. Energy losses occur by: reflection of solar radiation, emission of longwave (back) radiation and evaporation. Sensible heat and water column-bed energy transfers may cause gains or losses. In addition to these exchanges, energy may be advected by: in/out-flowing channel discharge, divergence of the longitudinal advective heat flux, hyporheic exchange, groundwater up/down-welling, tributary inflows and precipitation. The sum of these heat

fluxes is termed the river heat budget (or energy balance), which quantifies the total energy available to heat or cool the water-column (Q_n) at a given location (after Hannah *et al.*, 2004):

$$Q_n = Q_a + Q^* + Q_e + Q_h + Q_{bhf} + Q_f \qquad \text{(Equation 1)}$$

Q_a is advected heat due to groundwater inflow, hyporheic exchange, precipitation, and the divergence of the longitudinal advective heat flux, Q^* is net radiation, Q_h is sensible heat, Q_e is latent heat, Q_{bhf} is bed conduction and Q_f is friction at the stream bed and banks.

Changes in water temperature (*dTw*) may be calculated within either an Eularian (e.g. Caissie *et al.*, 2007; Hebert *et al.*, 2011) or a Lagrangian framework (e.g. Rutherford *et al.*, 2004; Leach and Moore, 2011; MacDonald *et al.*, 2014a). Within the Eularian framework, *dTw* is calculated as a function of time (*t*) (Equation 2) using a reference system (*i*) that is fixed in space and through which water flows:

$$\frac{dT_w}{d\mathrm{t}} = \frac{\mathrm{Q}^*_{(i,t)} + \mathrm{Q}_{e(i,t)} + \mathrm{Q}_{h(i,t)} + \mathrm{Q}_{bhf(i,t)} + \mathrm{Q}_{f(i,t)}}{\rho\, CD_{(i,t)}} \qquad \text{(Equation 2)}$$

Where ρ is density of water, *C* is specific heat capacity of water and *D* is river depth. Within the Lagrangian framework *dTw* is calculated as a function of space (*x*) (Equation 3) using a reference system that moves with the water:

$$\frac{dT_w}{dx} = \frac{W_{(i)}\left[\mathrm{Q}^*_{(i,t)} + \mathrm{Q}_{e(i,t)} + \mathrm{Q}_{h(i,t)} + \mathrm{Q}_{bhf(i,t)} + \mathrm{Q}_{f(i,t)}\right]}{C * F_{(i,t)}} \qquad \text{(Equation 3)}$$

Where *W* is width of the stream surface, and *F* is river discharge. The Eularian framework is most commonly used for temperature analysis and prediction in lowland waters (e.g. Caissie *et al.*, 2007; Hebert *et al.*, 2011), where temperatures are in dynamic equilibrium with meteorological conditions and longitudinal advection of heat does not dominate the energy budget. Conversely, the Lagrangian framework is used most frequently in headwater streams

(e.g. Rutherford *et al.*, 2004; Leach and Moore, 2011; MacDonald *et al.*, 2014a), where the energy budget is dominated by longitudinal advection of heat and local energy exchange processes have a minor influence on water temperature.

1.2.2 Controls and dynamics

Water thermal regimes exhibit marked spatio-temporal variability due to the heterogeneity of processes controlling temperatures at a range of different scales (Webb *et al.*, 2008; Imholt *et al.*, 2013a). Climate drives the thermal regime of rivers and, thus, it is the first-order control on regional patterns in the magnitude and timing of seasonal dynamics. Basin-wide characteristics are second order controls, for example: water sources, basin aspect, and precipitation regime may moderate the influence of climate and thus modify the timing and magnitude of water temperature dynamics. Reach specific controls, which interact with the water column as it moves through the catchment (such as topographic and riparian shading, reach-scale groundwater loss or gain, and hyporheic exchanges), may further moderate the influence of climate on water temperature dynamics. Hence, the cumulative effect of controls at each scale produces river temperature dynamics at a given location (Webb, 1996; Webb *et al.*, 2008).

The large number of potential controls on river temperature means that it is difficult to disentangle their multivariate influence on energy exchange, hydrological processes and, ultimately, river temperature. However, where water is sourced predominantly from groundwater (e.g. Erickson and Stefan, 2000; O'Driscoll and DeWalle, 2006; Tague *et al.*, 2007; Webb and Nobilis, 2007; Kelleher *et al.*, 2012), or snow/ice melt (e.g. Uehlinger *et al.*, 2003; Blaen *et al.*, 2013), or where frequent precipitation maintains thermal capacity (e.g. Webb and Nobilis, 2007) temperatures are typically cooler and much less variable. At smaller spatial scales, solar (shortwave) radiation inputs and so water temperatures are reduced by

channel orientation, and shading effects of topography (e.g. incised channels; Webb and Zhang, 1997) and riparian vegetation (e.g. forest cover, as reviewed by Moore *et al.*, 2005a). Finally, streamflow contributions associated with hyporheic exchange moderate minimum and maximum temperatures (e.g. Malcolm *et al.*, 2005a).

1.2.3 Drivers of change

There are a number of drivers of change that influence controls on the river energy budget, water fluxes, and thus river temperature. The impacts of forestry practice are the best documented; the somewhat contradictory findings are synthesised and evaluated by Moore et al., (2005a) with a UK focus provided by Hannah *et al.* (2008a). Land use change from riparian forest to grassland for agriculture may elevate river temperature in summer (e.g. Tait *et al.*, 1994; Isaak and Hubert, 2001) whereas afforestation may reduce summer maxima (Hrachowitz *et al.*, 2010; Lee *et al.*, 2012). Urbanisation is associated with increased river temperature compared with rural environments due to runoff of water across warmed paved surfaces (e.g. Herb *et al.*, 2008; Hester and Bauman, 2013; Xin and Kinouchi, 2013) and channel widening/ vegetation removal (i.e. exposure) to increase flow conveyance (Klein, 1979). Direct flow augmentation and abstraction change river thermal capacity, hence river temperature (Poole and Berman, 2001). Heated effluent from power plants and other point sources may have a profound warming impact (Maderich *et al.*, 2008; van Vliet *et al.*, 2012). The thermal effects of reservoirs are well documented for the UK, USA and elsewhere by Webb and Walling (1997), and, more recently, Casado *et al.* (2013) who report increases in temperature minima and decreases in temperature maxima.

In addition to these drivers, it is anticipated that climate change will have direct and indirect impacts on river temperature. Direct effects may occur due to shifts in the energy exchange and hydrological processes that determine river temperature. For example, longwave radiation

from the atmosphere, sensible heat (e.g. Ramanathan, 1981; Wild *et al.*, 1997; Andrews *et al.*, 2009) and groundwater temperature are anticipated to increase (e.g. Taylor and Stefan, 2009; Kurylyk *et al.*, 2013, 2014), while groundwater contributions to streamflow (e.g. Kurylyk *et al.*, 2014) and summer streamflow are anticipated to decrease (Capell *et al.*, 2013). Indirectly, river temperature may be affected by climate-induced alteration of riparian land use (Hrachowitz *et al.*, 2010) and, potentially, human response to reduced water security (van Vliet *et al.*, 2013b).

1.3 PRIORITY RESEARCH GAPS

It may be said with reasonable confidence that water temperatures are changing around the World and future change should be anticipated. Within the UK (the geographical focus of this thesis), mean annual water temperature increased on average by + 0.03 °C decade^{-1} at 86% of sites monitored by the Environment Agency within England and Wales between 1990 and 2006 (Orr *et al.*, 2014) and instantaneous maximum temperatures approach lethal-limits for sensitive species (e.g. salmonids, Malcolm *et al.*, 2008). For the year 2050 Webb and Walling (1992) predict a rise of +1.0 to +3.6°C in monthly mean water temperature throughout England Wales, given a scenario of monthly mean air temperature increase of + 3.0 °C.

Research on river temperature in the UK to date has investigated (Table 1): (1) point-scale heat fluxes that control fundamentally water temperature, (2) reach-scale variability in the water column and riverbed, (3) effects of forestry, and (4) spatial and temporal dynamics across river networks.

Table 1. Research on river and stream temperature in the UK

Author(s)	Study Scale & Location	Study Length	Key Findings	Controls & Processes
POINT-SCALE HEAT FLUXES CONTROLLING RIVER TEMPERATURE				
Webb and Zhang (1997)	11 sites in River Exe basin, Devon, southwest England	495 days across 18 study windows	Averaged over the entire dataset non-advective energy gain contributions = net radiation (56%), friction (22%), sensible heat (13%), condensation (6%) and bed heat flux (3%). Non-advective energy loss contributions = net radiation (49%), evaporation (30%), sensible heat (11%) and bed heat flux (10%). Magnitude and relative importance of heat fluxes varied in time and space.	Chanel morphology, valley topography, riparian vegetation, substratum composition hydrological conditions, and river regulation influence variability and magnitude of heat fluxes over time and between sites.
Evans *et al.* (1998)	1 site in English Midlands	8 days	On average, over 82% of the total energy transfers occurred at the air-water interface with 15% at the channel bed-water interface. Heat exchange at the channel bed varied considerably (max. 24%) in response to varying bed thermal, and periphyton and macrophyte cover.	Temporal heterogeneity in bed heat flux caused by varying riverbed albedo (due to seasonal changes in periphytion, macrophyte and silt cover) and relative contribution of surface- vs. ground-water.

Table 1. Continued

Author	Study Scale & Location	Study Length	Key Findings	Controls & Processes
POINT-SCALE HEAT FLUXES CONTROLLING RIVER TEMPERATURE (CONTINUED)				
Webb and Zhang (1999)	1 site in River Exe basin, southwest England	1 year	Net radiation contributed ~90% of energy gains during summer months. Sensible heat enhanced during summer. Bed heat flux reduced considerably at 1 site where weed growth extensive.	Sensible heat transfers enhanced in groundwater-fed streams during summer due to their lower water cf. air temperature. Macrophytes (lower thermal conductivity cf. sediment) decrease bed heat fluxes.
Hannah *et al.* (2004)	1 site, Cairngorms, northeast Scotland	7 months (autumn-spring)	Streambed (atmosphere) dominant energy source (sink) for heating (cooling) channel water	Groundwater upwelling advects heat into the bed. Friction important heat source in winter. Sensible heat primary atmospheric heat source when radiative transfers limited.
Webb and Zhang (2004)	4 sites in River Exe basin, southwest England	1 year	Sensible heat source (sink) in summer (winter). Bed heat sink (source) in summer (winter). Friction heat source. Evaporation heat sink. Differences between forested and non-forested sites, especially in terms of radiation.	Forest canopy reduces shortwave-radiation. Tree trunks and branches in deciduous forests cause shading effects even during winter.
Hannah *et al*. (2008a)	1 open moorland and 1 semi-natural forest site, Cairngorms, northeast Scotland	2 years	Net radiation greater summer (less winter) for moorland cf. forest. Magnitude and variability of turbulent fluxes greater for moorland cf. forest	Forest canopy shades in summer (but offsets net radiation loss in winter due to longwave emission) and sheltering effects on sensible and latent heat

Table 1. Continued

Author	Study Scale & Location	Study Length	Key Findings	Controls & Processes
REACH-SCALE TEMPERATURE VARIABILITY IN THE WATER-COLUMN AND RIVERBED				
Carling *et al.* (1994)	channel cross-sections, River Severn	< 1 day	Water temperature in dead zones of meanders 2°C warmer cf. flowing main channel	Shallower, slower flowing water warms more rapidly than deeper, faster flowing thalweg (i.e. atmospheric equilibration time)
Clark *et al*. (1999)	202 channel cross-sections, River Frome and Bere Stream, southwest England	< 1 day	0.2 -0.4°C vertical and/ or horizontal temperature contrasts across 78% of channel cross-sections	
Hannah *et al.* (2009)	Riffle-pool sequence, River Tern, English Midlands	22 months	Hyporheic temperature cooler (warmer) than water column in summer (winter), with convergence in spring and autumn. Temperature varies across and between riffles	River geomorphology alters groundwater-surface water interactions, hence thermal dynamics
Krause *et al*. (2011)	Riffle-pool sequence, River Tern, English Midlands	9 months (summer-winter)	Streambed temperature variability 0.75°C (3°C) over 16 m (0.4 m) longitudinally (vertically)	
FOREST EFFECTS ON RIVER TEMPERATURE				
Crisp (1999)	5 sites in 2 catchments, upper-Severn, mid-Wales (2 sites pre-clear-felled; 3 sites post-clearfelled)	15-52 months	Mean annual water temperature reduced by 0.4 °C and daily range lower pre-clearfelling. Greatest effects in summer.	

Table 1. Continued

Author	Study Scale & Location	Study Length	Key Findings	Controls & Processes
FOREST EFFECTS ON RIVER TEMPERATURE (CONTINUED)				
Weatherley and Ormerod (1990)	6 sites across clearfelled and afforested locations, upper River Severn, mid-Wales	1-2 years	Mean daily water temperature lower (higher) in forest cf. moorland in spring and summer (winter).	
Stott and Marks (1999)	1 site pre-clearfelling and 1 site post-clearfelling, River Severn, mid-Wales	28 months	Monthly mean temperature increased by 7°C in July and 5.3°C during August post-clearfelling.	
Malcolm *et al*. (2004a)	5 sites situated in open moorland and one in mixed (deciduous, coniferous) woodland	3 years	Riparian woodland reduced diurnal variability and extremes of temperature.	
Malcolm *et al*. (2008)	2 sites situated in open moorland sites and three sites in mixed woodland	35 months	Under forest: amplitude of annual temperature regime reduced, daily mean and maximum decreases, in daily minimum increases, and diurnal variability reduced	

Table 1. Continued

Author	Study Scale & Location	Study Length	Key Findings	Controls & Processes
FOREST EFFECTS ON RIVER TEMPERATURE (CONTINUED)				
Broadmeadow *et al*. (2011)	14 forested and 4 open-moorland sites in 2 catchments, New Forest, Southern England	3 years	Largest differences between forested and open sites during summer. Effects observed at canopy shading of 20-40%.	
Imholt *et al*. (2013b)	7 sites with the Tanar and 5 sites within the Girnock catchment, Dee river basin, northeast Scotland	13 months	Presence of semi-natural woodland reduces summer maximum (by up to 4 °C) and dial temperature range (by up to 6.6 °C)	
SPATIAL AND TEMPORAL DYNAMICS ACROSS RIVER NETWORKS				
Webb and Walling (1992)	3 sites on tributaries with contrasting land use, River Exe basin, southwest England	14 years	Significant increase in water temperature 0.05 to 0.092 °C y^{-1} associated with air temperature increases and removal of riparian vegetation shading	Climate and land use/ land cover influence long-term water temperature trends
Crisp *et al*. (1982)	7 streams (two watercress beds) in southern England	1-8 years	Surface water fed streams lower annual mean but greater cycle amplitude cf. groundwater fed streams.	Increased groundwater inputs, longer hydrological residence times and increased thermal capacity (flow volume) buffer influence of climate on water temperature
Webb and Walling (1986)	17 sites in River Exe basin, southwest England	5 years	Thermal variability buffered for larger basin areas and longer hydrological residence times	

Table 1. Continued

Author	Study Scale & Location	Study Length	Key Findings	Controls & Processes
SPATIAL AND TEMPORAL DYNAMICS ACROSS RIVER NETWORKS (CONTINUED)				
Webb *et al*. (2003)	Four sites draining basins of contrasting area, River Exe basin, southwest England	5 years	Air-water temperature relationships weaken with increased thermal capacity and longer residence times	See above
Hrachowitz *et al*. (2010)	25 sites, River Dee, northeast Scotland	2 years	Small, non-forested, inland, upland sites most sensitive to air temperature. Large, forested, lowland sites least sensitive air temperature.	
Johnson *et al*., (2014)	36 sites, Rivers Dive and Manifold, English Peak District	1 year	Upstream riparian shade and perennial spring inflows reduce sensitivity of water temperature to air temperature	
Imholt *et al*. (2013a)	26 sites across nested scales, River Dee, northeast Scotland	2 years	Least spatial variability at the sub-reach scale (0.3 °C difference between riffles and pools) with greatest variability between tributaries (8.1°C difference in diurnal range) and sub-catchments.	Thermal variability scale-dependent and related to river morphology, land use, altitude and forest cover. Notably, similar thermal patterns may be driven by different sets of physical controls.

The research presented within this thesis seeks to extend systematically our knowledge of the processes that control river and stream temperature at a number of spatio-temporal scales, that is *in space* inter-basin to inter-site, to reach scales, and *in time* from inter-annual, to annual, to monthly, to 15-minute (Figure 1). The literature is evaluated in detail in Chapters 2-5, from which the following specific research gaps are identified:

1. ***Annual and inter-annual thermal regime dynamics at the regional scale and beyond.*** Analytical tools are required that are capable of characterising large-scale spatio-temporal variability in river temperature regimes, climate-water temperature linkages and the modifiers of these relationships. Such tools and knowledge are essential for identifying river waters that are most sensitive to a changing climate across large geographical areas (Chapter 2).
2. ***Inter-annual variability in monthly mean water temperature in stream reaches of moorland and forest landuse.*** Improved understanding of long-term (i.e. > 2 years) variability in seasonal stream temperature dynamics beneath forest canopies as they relate to riparian microclimate and energy exchange conditions is required. Such research would yield new insights as to the hydrometeorological conditions under which riparian forest may be effective in mitigating river thermal variability and extremes under present and future climates (Chapter 3).
3. ***Processes generating sub-daily cooling water temperature gradients within forested stream reaches.*** The energy exchange processes that generate and drive the magnitude of daytime cooling gradients beneath forest canopies must be determined, especially in semi-natural woodland and in the absence of potentially confounding cool groundwater inflows. This knowledge is essential to inform process-based models, which may be used to plan future riparian planting strategies (Chapter 4).

4. ***Interactions between riparian vegetation density, channel and hydraulic characteristics and effects on sub-daily reach scale water temperature.*** Systematically derived, process based evidence is required on the density and extent of riparian tree planting required to produce suitable cool water refugia at the reach scale in channels of different orientation and hydraulic characteristics. This research will provide transferable information to inform the most effective riparian planting strategies at minimal cost (Chapter 5).

1.4 AIM AND OBJECTIVES

The primary aim of the research presented herein is to improve understanding of the influences of climate, hydrometeorology, and riparian landuse controls on stream temperature dynamics and associated processes at a number of spatio-temporal scales (Figure 1) within a UK context.

In response to the research gaps identified (see *Priority research gaps*), the specific objectives of the research are:

1. To assess spatial patterns and inter-annual variability of the shape and magnitude of annual river temperature regimes within England and Wales, their links with air temperature and how these links may be modified by static basin properties (Chapter 2).
2. To improve understanding of the conditions and processes that affect the magnitude of the forestry influence on water temperature, microclimate and energy exchange between years in an upland stream (Girnock Burn, a tributary of the Aberdeenshire Dee) (Chapter 3).

3. To determine the processes which generate and drive cooling gradients beneath forest canopies in an upland stream reach with no groundwater or tributary inputs (Chapter 4).
4. To quantify within a systematic framework the effects of riparian shading scenarios, channel orientation and water velocity on water temperature dynamics with an upland stream reach (Chapter 5).

1.5 THESIS STRUCTURE

The research is presented in the format of four self-contained research paper-type chapters (Chapters 2- 5) followed by a synthesis (Chapter 6) in which the key findings are summarised, implications discussed, and future research avenues proposed. Within each Chapter, the relevant literature is reviewed, and descriptions of data acquisition and detailed methodologies are provided. For brevity and to avoid repetition, where the same data are employed or methods are adopted in more than one Chapter then the Reader is referred to the relevant location in which these data or methods are first described. Figure 1 illustrates diagrammatically how each Chapter addresses specific objectives, the spatio-temporal scales with which each is concerned and inter-relationships between Chapters.

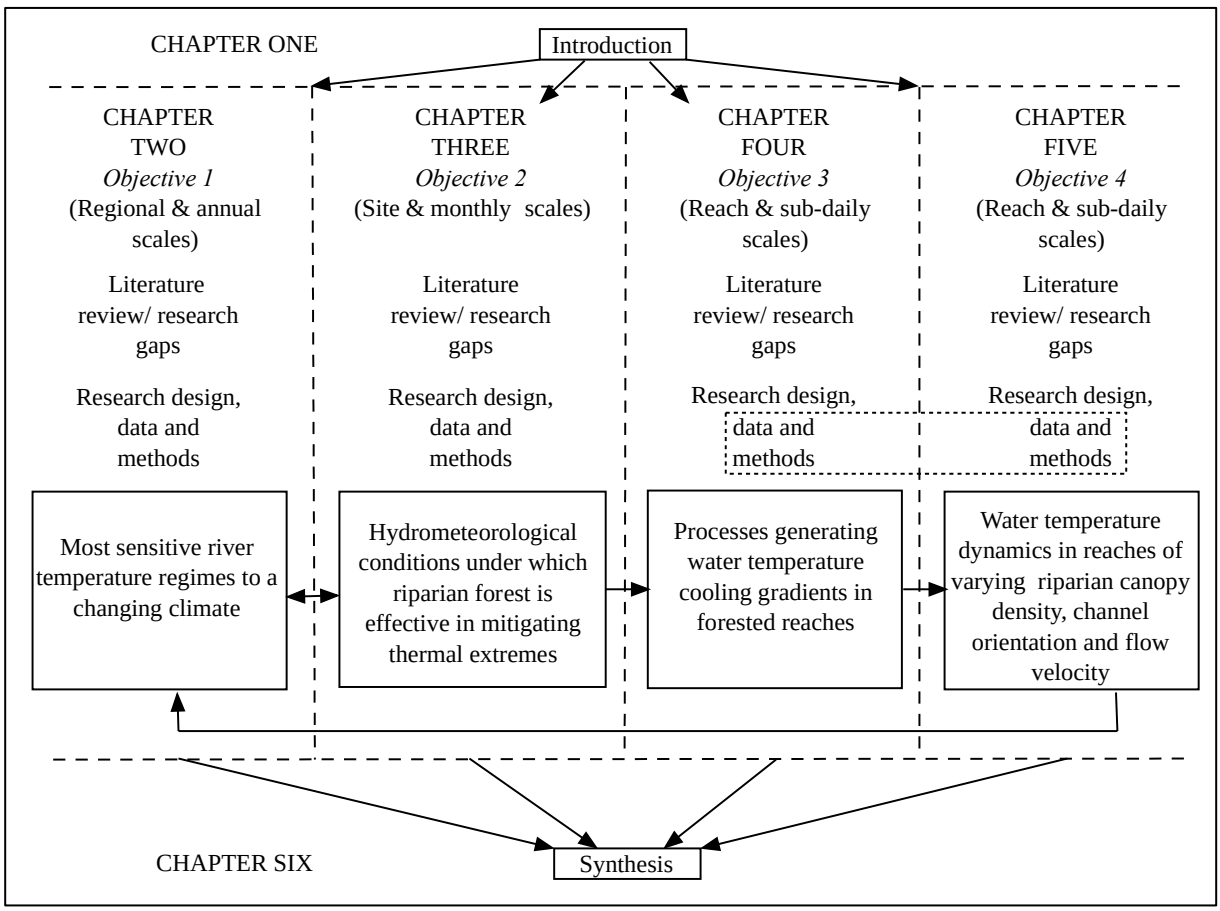

Figure 1. Thesis structure. [Arrows represent relationships between chapters.]

CHAPTER TWO: RIVER TEMPERATURE REGIMES OF ENGLAND AND WALES: SPATIAL PATTERNS, INTER-ANNUAL VARIABILITY AND CLIMATIC SENSITIVITY

2.1 ABSTRACT

Identification of the most sensitive hydrological regions to a changing climate is essential to target adaptive management strategies. This study presents a quantitative assessment of spatial patterns, inter-annual variability and climatic sensitivity of the shape (form) and magnitude (size) of annual river/ stream water temperature regimes across England and Wales. Classification of long-term average (1989-2006) annual river (air) temperature regime dynamics at 88 (38) stations within England and Wales identified spatially differentiable regions. Emergent river temperature regions were used to structure detailed hydroclimatological analyses of a subset of 38 paired river and air temperature stations. The shape and magnitude of air and water temperature regimes were classified for individual station-years; and, a Sensitivity Index (*SI*, based on conditional probability) was used to quantify the strength of associations between river-air temperature regimes. The nature and strength of air-river temperature regime links differed between regions. River basin properties considered to be static over the time-scale of the study were used to infer modification of air-river temperature links by basin hydrological processes. The strongest links were observed in regions where groundwater contributions to runoff (estimated by basin permeability) were smallest and water exposure time to the atmosphere (estimated by basin area) was greatest. These findings provide a new large-scale perspective on the hydroclimatological controls driving river thermal dynamics and, thus, yield a scientific basis for informed management and regulatory decisions concerning river temperature within England and Wales.

2.2 INTRODUCTION

In recent years, there has been an upsurge in river and stream temperature research (Hannah *et al.*, 2008b) as temperature is increasingly recognised as an important and highly sensitive variable affecting biological, chemical and physical processes in flowing waters (Caissie, 2006). Primary research challenges in the field of river temperature include improving understanding of thermal heterogeneity at different spatial and temporal scales, the nature of past variability, and likely future trends (Webb *et al.*, 2008). The analysis of spatial and temporal variability in river temperature regimes is vital to: (1) elucidate key controls and processes, (2) assess sensitivity to a changing climate, and (3) inform management of land-use, water resources and freshwater ecosystems (Moore *et al.*, 2005a). In part, river temperature has attracted growing attention because water thermal regimes may be highly sensitive to climate change. Instrumented records show significant river temperature warming (e.g. Webb and Walling, 1992; Kaushal *et al.*, 2010; Arismendi *et al.*, 2012; Isaak *et al.*, 2012) and cooling (e.g. Isaak and Hubert, 2001; Arismendi *et al.*, 2012; Orr *et al.*, 2014) over recent decades and future projections (e.g. Webb and Nobilis, 1994; Webb and Walling, 1992; Mohseni *et al.*, 2003; van Vliet *et al.*, 2011, 2013a) suggest profound potential impacts on freshwater ecosystems (Ormerod, 2009). Hence, environment managers and regulators need urgently information on space-time variability in river temperatures and a better understanding of the controlling factors as an important first step towards making well-informed decisions concerning the climatic sensitivity of river thermal regimes (Wilby *et al.*, 2010).

Drivers of river temperature dynamics are complex, with multivariate controls and process interactions spatially-nested at macro- (latitude, altitude and continentality), meso- (basin climate and hydrology) and micro- (micro-meteorology, channel geometry, riparian shading

and substratum conditions) scales (Webb, 1996). Research on river temperature within England and Wales has investigated: (1) point-scale heat fluxes that control fundamentally water temperature (Webb and Zhang, 2004; Hannah *et al.*, 2008a), (2) micro-thermal variability within the water-column (e.g. Clark *et al.*, 1999) and riverbed (e.g. Hannah *et al.*, 2004, 2008a; Krause *et al.*, 2011), (3) the effects of forest canopies and forest clear-felling (Stott and Marks, 1999; Hannah *et al.*, 2008a), and (4), spatial and temporal dynamics across river temperature networks (e.g. Webb and Walling, 1992). This UK-based research has been restricted to the sub-basin scale; thus, no research exists on spatial and temporal variability and controls on river temperature at a larger scale (i.e. inter-basin to region and beyond).

Regimes describe the behaviour of hydroclimatological variables over the annual cycle or hydrological year, and they are useful tools for characterising spatial and temporal variations in timing and magnitude of seasonal patterns (Bower *et al.*, 2004). The importance of the entire flow regime for maintaining and protecting the integrity of fluvial systems, rather than considering only the maximum, minimum or mean values is well recognised with regard to the management of river discharge (e.g. Poff *et al.*, 1996; Harris *et al.*, 2000; Kennard *et al.*, 2010) . However, for river temperature, single metrics (particularly maxima, e.g. Picard *et al.*, 2003) and isolated months or seasons are used most commonly. These approaches consider the magnitude of thermal condition, which may limit aquatic stream organisms, but ignore other potentially relevant characteristics, particularly the timing and duration of warmer and cooler episodes over the annual cycle (Chu *et al.*, 2010; Arismendi *et al.*, 2013). Spatial variability in multiple aspects of annual regime magnitude has been explored over a single calendar year in the Great Lakes Basin, Canada (Chu *et al.*, 2010), but, typically, consideration of river temperature variability across multiple years has been restricted to trend analyses (e.g. Webb and Walling, 1992; Webb and Nobilis, 1994, 2007; Kaushal *et al.*, 2010).

Inter-annual variability/stability in the character of the entire river thermal regime has not been investigated to date. Therefore, there is a clear need to develop methods to assess the key attributes of annual river temperature regimes and their year-to-year dynamics.

To explore linkages between climate and river temperature, air temperature is commonly used as a proxy for net heat exchange at the air-water interface (Webb *et al.*, 2003). Across space, air-water temperature relationships are weaker for: (1) upper headwater streams (Brown *et al.*, 2005; Hrachowitz *et al.*, 2010; Kelleher *et al.*, 2012); (2) locations with increased thermal capacity and longer water travel times (Webb and Nobilis, 2007); and (3) at sites with major groundwater or anthropogenic inputs (Erickson and Stefan, 2000; O'Driscoll and DeWalle, 2006; Tague *et al.*, 2007; Webb and Nobilis, 2007; Kelleher *et al.*, 2012). The strength of the relationship between air and water temperature increases from sub-daily to monthly timescales but is weakest for annual samples (Webb *et al.*, 2008) because river temperature displays less year-to-year variability than air temperature (Pilgrim *et al.*, 1998; Erickson and Stefan, 2000; Webb *et al.*, 2003). There is a need to advance methods for rigorous, systematic analysis of dynamic air-water temperature links and to explore the controls on space-time patterns in the climatic sensitivity of river temperature.

Although there is a growing body of river temperature research there remains limited understanding of large-scale spatial and temporal variability in climate-water temperature associations, and the modifiers of these relationships. Such research is essential for identification of the most temperature sensitive river waters and to understand the controls on thermal sensitivity. To address these research gaps, this paper aims: (1) to provide the first quantitative assessment of spatial patterns and inter-annual variability of the shape (timing) and magnitude (size) of annual river temperature regimes across England and Wales; and (2) to assess the climatic sensitivity of river temperature regimes and understand the controls on

river thermal sensitivity, including the potential moderating role of static basin properties. In addition to providing a new large-scale, long-term perspective and understanding of English and Welsh river temperature, this paper seeks to make methodological innovations by testing a classification tool for annual regimes (Hannah *et al.*, 2000) on water temperature and a climatic Sensitivity Index (Bower *et al.*, 2004) for air-river temperature associations. Notably, this study represents the first application of the classification scheme and sensitivity index to annual river temperature regimes.

2.3 STUDY AREA CLIMATE

The countries of England and Wales have a temperate maritime climate. Highest air temperature is observed in July-August with the lowest air temperature in January-February. Air temperature is coldest in northern England and north-west Wales and warmest in south-eastern England, which reflects relief. High seasonality of the annual air temperature regime is observed inland; whereas in coastal locations air temperature is warmer but seasonality is reduced (Bower *et al.*, 2004).

2.4 DATA

2.4.1 River temperature

Time series of river water temperature from monitoring stations across England and Wales were extracted from the Environment Agency's Freshwater Temperature Archive. The Archive and its data holdings are described in detail by Orr *et al.* (2010). Sites were selected from the Archive to provide a robust analysis with optimal spatio-temporal coverage across England and Wales. A total of 88 sites were identified that had water temperature observations in ≥ 90% of all months over a common 18-year period (1989-2006 inclusive; Figure 2); water temperature was sampled on average 11.1 times per month over this time

span. Monthly mean water temperature (°C) was calculated for each site for each month over the entire record to characterise annual thermal regimes and their year-to-year variability.

The potential influence of sampling frequency on the estimation of monthly means was evaluated systematically using data collected at the site monitored at the highest temporal resolution (i.e. River at Pont Mwnwgl Y Llyn, 15-minute intervals over 13 years). Means calculated from all possible combinations of three samples in each month for all years (> 4.5 M resamples for each month in each year) were calculated; and results indicated sampling frequency to have minimal impact on shape and magnitude of annual river temperature regimes (Figure 3).

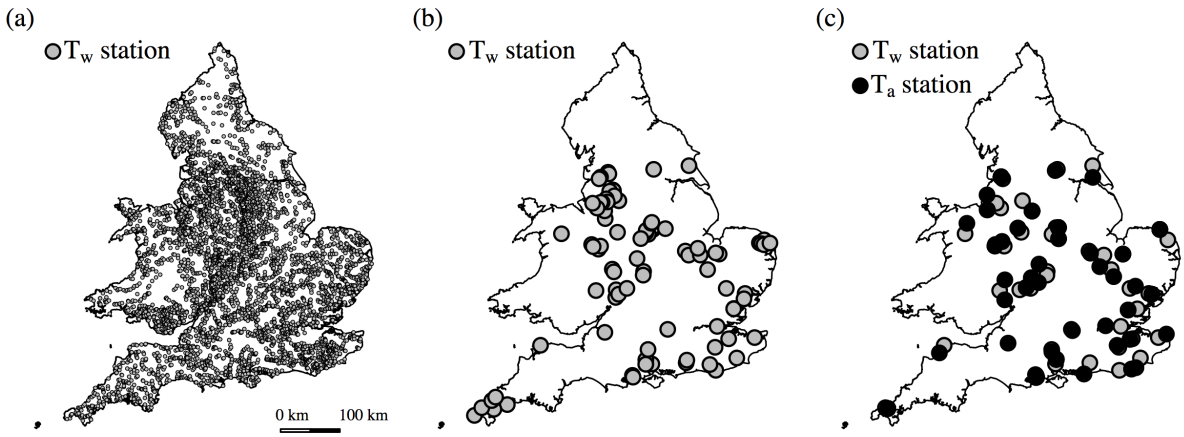

Figure 2. Maps of England and Wales showing (a) water temperature stations during the 1989–2006 common period, (b) water temperature monitoring stations within the common period with temperature samples in >90% of months and (c) paired air–water temperature monitoring stations

2.4.2 Air temperature

Observations of daily minimum and maximum air temperature for the common data period (1989-2006) were obtained from the British Atmospheric Data Centre, MIDAS Land Surface Stations data set (UK Meteorological Office, 2006). River temperature sites were paired with the closest climate station, which yielded a total of 38 air temperature locations (Figure 2). The mean of minimum and maximum values for each station day provided estimates of daily averages (Bower *et al.*, 2004); monthly averages of mean daily air temperature (°C) were calculated to characterise annual regimes and their temporal stability.

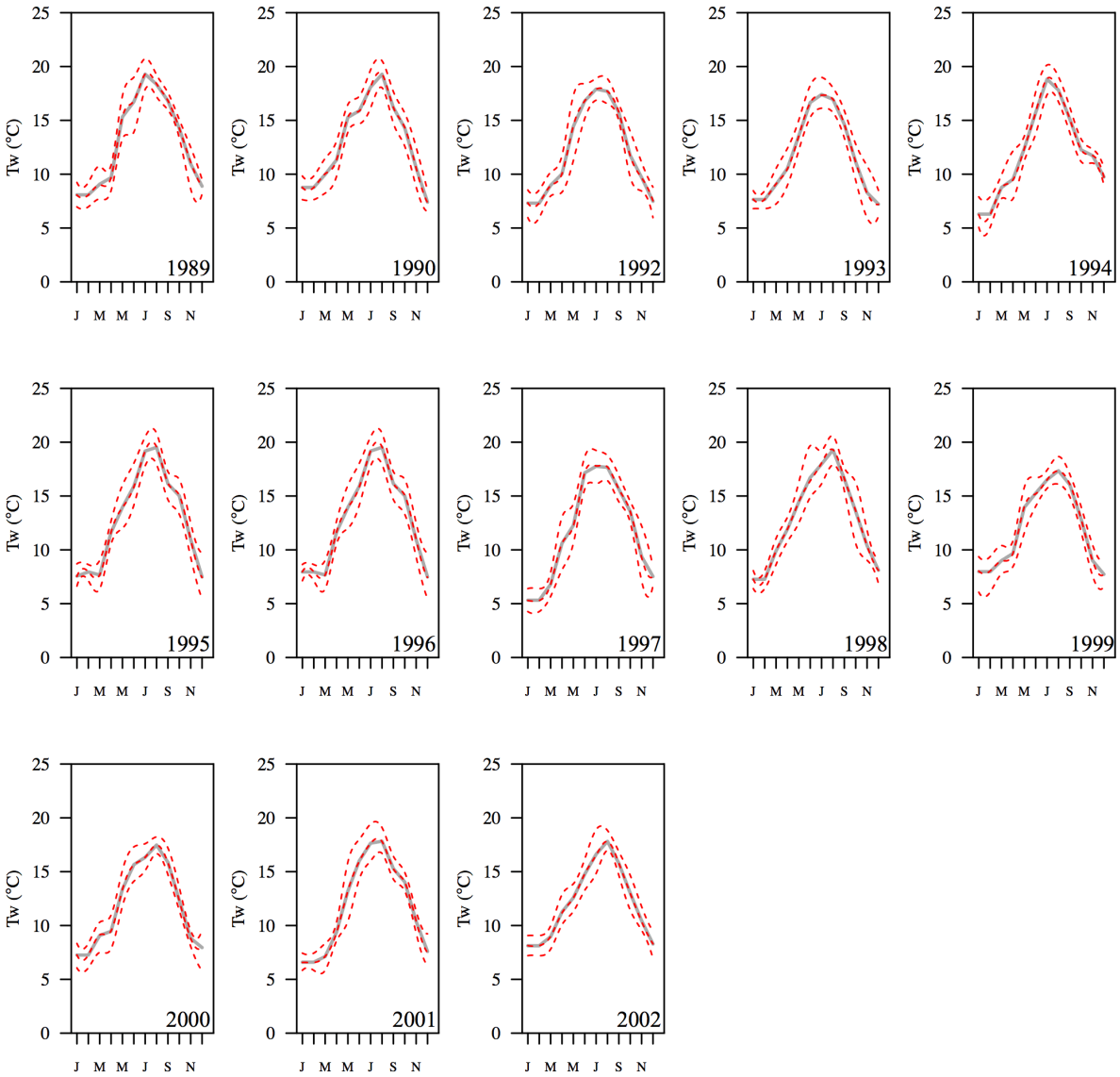

Figure 3. Influence of sampling frequency on the shape and magnitude of the annual river temperature regime for 13 years at Pont Mywnwygl Y Llyn on the River Dee, Wales. [Grey lines illustrate annual regimes based on monthly means calculated from continuous data recorded at 15 min intervals. Red lines show the 50th (median), 97.5th and 2.5th percentiles of monthly means calculated from all possible combination of 3 samples in each month in each year.]

2.4.3 Basin properties

River basin properties were selected to assess the potential role of hydrological controls in moderating spatial river temperature pattern and air-water temperature sensitivity. Properties were derived from two sources: (1) a 25 m resolution digital elevation model of England and Wales (University of Manchester/ University of London, 2001) that was used to calculate basin area (km^2) and mean basin elevation (m above sea level); and (2) the British Geological Survey (BGS) Bedrock Permeability Index of England Wales that was used to characterise average basin permeability as a measure of basin water storage and hydrological response time (Laize and Hannah, 2010). Basin properties for the 38 rivers selected for analysis of air-river temperature regime associations are summarised in Table 2.

Table 2. Properties of 38 river basins selected for analysis of air–water temperature associations [River basins are listed in alphabetical order.]

Station Name (river at site)	Mean Basin: Elevation (masl)	Mean Basin: Permeability	Basin Area (km^2)	Sampling frequency ($month^{-1}$)
Ditton Brook at Dart Bridge	98.1	3.5	179.8	3.7
Hundred Foot R. at Earith Bridge	14.2	2.0	1034.6	4.2
Moors R. at Hurn Bridge	48.6	3.6	7964.1	3.1
R. Ant at Wayford Bridge	30.9	3.0	4160.4	3.0
R. Avon at Lower Evesham	12.2	2.8	936.8	2.9
R. Avon at Stoneleigh Park	23.3	2.4	534.7	2.6
R. Chelmer at Langford	75.7	2.3	13867.1	5.3
R. Cuckmere at Sherman Bridge	17.1	1.9	4009.1	4.6
R. Darwin at Blue Bridge	65.8	2.5	423.4	6.1
R. Dee at Pont Mwnwgl Y Llyn	46.1	3.4	589.0	593.7
R. Derwent at Coultauds	73.2	3.0	3603.5	2.5
R. Eden at Clappers	19.3	2.0	4451.1	4.1
R. Erewash at Shipley Gate	69.3	2.4	22223.6	2.5
R. Goyt above Tame	98.0	2.8	1166.5	4.4
R. Hull at Hempholme	106.8	2.1	6153.5	10.5
R. Itchen at Gaters Mill	110.3	3.9	1441.7	3.9
R. Leam at Prince's Drive	45.6	2.6	65000.0	2.3
R. Mardyke at Thurrock	82.5	2.8	5614.1	4.5
R. Medway above Allington	45.1	2.0	3834.2	5.9
R. Nene at Littleport	86.8	2.9	9915.3	3.7
R. Perry at Mytton	40.3	2.4	14942.6	2.4
R. Roden at Roddington	107.3	1.5	19057.4	2.2
R. Rother at Blackwall Bridge	40.3	2.1	14942.6	4.4
R. Rother at Hardham	212.5	3.7	1918.2	6.9
R. Severn at Upton on Severn	160.9	2.6	4515.3	2.7
R. Stour at Bretts Bailey Bridge	255.0	3.6	1642.7	5.2
R. Stour at Iford Bridge	275.7	3.7	3289.5	4.7
R. Stour at Ingham	82.5	3.1	5614.1	5.7
R. Stour at Wixhoe	60.5	2.6	428.5	6.8
R. Test at Wherwell	35.4	3.9	2622.1	3.8
R. Thames at Caversham	127.5	2.9	4680.7	13.9
R. Trent at Yoxall Bridge	71.8	3.6	496.2	2.8
R. Umber above beach	31.0	2.7	210.0	2.7
R. Welland at Tinwell	132.0	2.7	496.9	4.8
R. Wharfe above Tadcaster	85.3	2.9	2589.6	6.6
R. Wye at Victoria Bridge	219.9	3.0	3173.9	3.5
Red R. at Gwithian Towans	3.5	3.2	115.2	4.8
Ten Mile R. at Denver	23.9	3.1	3448.0	4.4

2.5 METHODS

The analytical procedure was divided into five linked stages: (1) regionalisation of long-term average regimes for river and air temperature, (2) classification of annual regimes for each station-year, (3) quantification of inter-annual regime stability and (4) application of the Sensitivity Index (*SI*) to quantify linkage between air-river temperature classes.

2.5.1 Regime classification

As it was important to assess the timing (seasonality) and size of the annual river temperature regime, a hierarchical, agglomerative cluster analysis based classification approach was used to group intra-annual patterns for river and air temperature according to two key regime attributes: shape and magnitude. The regime classification procedure was developed by Hannah *et al.* (2000) and subsequently extended and evaluated for application to annual river flow and climate regimes (e.g. Harris *et al.*, 2000; Bower *et al.*, 2004). The shape classification identified stations (for regionalisation) or station-years (to assess inter-annual regime variability) with similar regime forms, regardless of their magnitude. For the regionalisation process, shape regimes were determined from long-term mean monthly values (i.e. the mean of observations in each month over the entire study-period) standardised separately for each station using *z*-scores (mean= 0, standard deviation= 1). To classify inter-annual shape regimes, monthly mean values (i.e. means of observations in months for individual years) were standardised for each station prior to classification.

The magnitude classification was based on four indices (i.e. the mean, minimum, maximum and standard deviation), regardless of their timing. For regionalisation, the indices were derived from long-term mean monthly values at each station; and stations with similar magnitude regimes were grouped. Each index was *z*-scored to control for differences in relative magnitudes. Index values for inter-annual magnitude regimes were determined from

monthly mean values in each station-year; and station-years with similar magnitude regimes were grouped. Each index was *z*-scored over the entire study-period for each station to control for between-station differences in the indices. Classification of regime shape and magnitude was performed separately for air and river temperature over the common data period (1989-2006). This is the first application of these methods to classify annual river water temperature regimes.

It is important to note that the methods applied herein yielded two separate sets of regime classifications: (1) the *regionalisation* procedure grouped stations to examine spatial patterns, and (2) the *inter-annual classification* grouped annual regimes for each station-year to identify patterns of year-to-year variability. Together, the two classification modes characterised spatial and temporal regime dynamics. The *regionalisation* of long-term regimes provided a basis for structuring analyses of between- and within region patterns in inter-annual regime variability. The long-term average regime for a station was estimated from mean monthly values across all years for all 88 river temperature sites. *Annual regimes for each station-year* were characterised using monthly mean values for each station-year for a subset of 38 river temperature sites (i.e. closest locations paired with the 38 climate stations; Figure 2). Thus, regime shape and magnitude classes were identified for 702 station-years for both river and air temperature. It is also important to note that: (1) regime classes are not interchangeable between long-term and station-year regime classifications and (2) magnitude classes for regionalisation identify absolute differences between stations whereas magnitude classes for station-years identify relative inter-annual variations at a station (Bower *et al.*, 2004). For all classifications performed: (1) inspection of the cluster dendrogram and agglomeration schedule identified the number of classes and (2) Ward's algorithm yielded the most robust (Kalkstein *et al.*, 1987) and evenly sized classes.

2.5.2 Quantification of inter-annual regime stability and climatic sensitivity

The stability of inter-annual regimes at each site was assessed using the concept of equitability (*E*), which was a measure (values range from 0 to 1) of the probability of observing each regime shape or magnitude class against all the possible regime classes (Bower *et al.*, 2004) (Equation 4). Higher values indicated greater equitability (evenness).

$$E = \frac{-\sum_{i=1}^{n} P_i \, ln \, P_i}{\ln n} \text{ (Equation 4)}$$

The *SI*, which quantifies the strength and direction of associations between air and river temperature, was adapted by Bower *et al.* (2004) from an ecological index (Kent and Coker, 1992). Based upon the concept of equitability the *SI* considers the conditional probability, $P(Y_j|X_i)$, of observing a particular river temperature Y_j regime under each air temperature regime X_i and also the conditional probability, $P(X_i|Y_j)$, of a given air temperature regime prevailing for each river temperature regime. Equations (5) and (6) were used to calculate the equitability of regimes as the probability, $P(Y_j)$ and $P(X_i)$, of observing a particular river temperature and air temperature regime, Y_j and X_i, respectively.

$$E(Y) = -\sum_{j=1}^{n_y} \left(\frac{PY_j \ln PY_j}{\ln n_y} \right) \text{ (Equation 5)}$$

$$E(X) = -\sum_{j=1}^{n_x} \left(\frac{PX_j \ln PX_j}{\ln n_x} \right) \text{ (Equation 6)}$$

The ratio of *E*(Y): *E*(X) identified one of two scenarios to produce an *SI* ranging from -1 to +1. Where *E*(Y) ≥ *E*(X), Equation (7) (positive scenario) returned an *SI* value between 0 and +1, which indicated that water temperature was more variable than air temperature. Where *E*(Y) ≤ *E*(X), Equation (8) (negative scenario) yielded an *SI* value between 0 and -1, which indicated that air temperature was more variable than water temperature. Values close to 0

indicated greater river temperature sensitivity to air temperature than those closer to +/- 1 (Bower *et al.*, 2004).

$$SI = \frac{1}{2(n_x n_y)}\left[-\sum_{i=1}^{n_x}\left[\left(\frac{PX_j \ln PX_j}{\ln n_x}\right) + \left(\frac{PY_j \ln PY_j}{\ln n_y}\right)\right]\right] \text{ (Equation 7)}$$

$$SI = -1 - \frac{1}{2(n_x n_y)}\left[-\sum_{i=1}^{n_x}\left[\left(\frac{PX_j \ln PX_j}{\ln n_x}\right) + \left(\frac{PY_j \ln PY_j}{\ln n_y}\right)\right]\right] \text{ (Equation 8)}$$

2.5.3 Influence of basin properties on air-river temperature sensitivity

To assess potential modification of air-river temperature associations by basin properties, (1) the 38 paired water and air temperature stations were grouped by the long-term average river temperature regions and (2) equitability, *SI* and basin properties were compared within- and between-regions.

2.6 RESULTS

Results are presented in three sections: (1) regionalisation of long-term shape and magnitude regimes for river and air temperature, to explore spatial patterns and identify regions that structure further analyses, (2) inter-annual river and air temperature shape and magnitude regimes, to assess between- and within-region regime dynamics and air-river temperature sensitivity and (3) analysis of the influence of basin properties on air-water temperature regime sensitivity between- and within-regions.

2.6.1 Regionalisation of long-term regimes

Regime shape and magnitude were classified using long-term (1986-2006) mean monthly river and air temperature for 88 and 38 stations, respectively. The correspondence between river and air temperature was explored for 38 paired stations.

Long-term regime shape

One river temperature and one air temperature regime were identified across all of England and Wales. Both regimes had similar forms of annual cycle. River temperature regimes peaked in July with minima in January; air temperature regimes exhibited an extended July-August maxima and January-February minima (Figure 4). Air temperature regimes demonstrated less variability between sites than river temperature (*cf.* composite averaged regime; Figure 4), indicating that air temperature was more spatially conservative than river temperature.

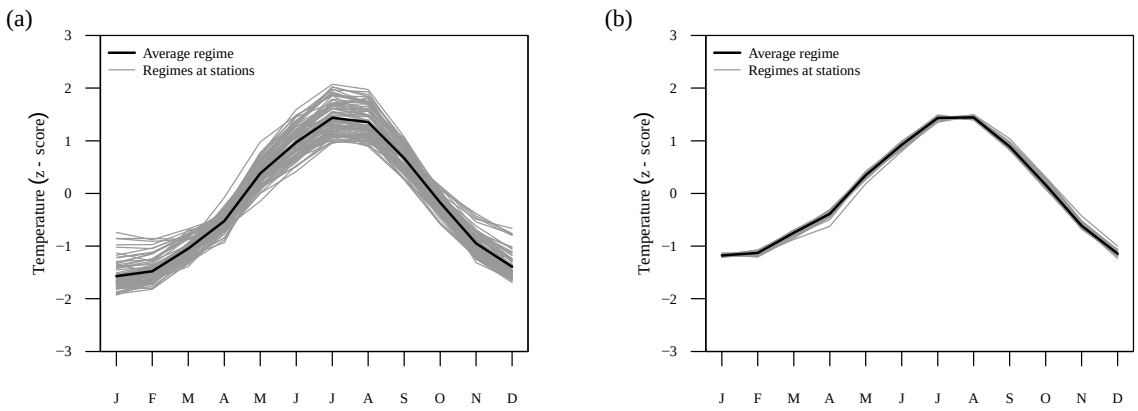

Figure 4. Long-term (1989–2006) average standardised (*z*-scores) mean monthly temperature values for all (a) river temperature and (b) air temperature stations

Long-term regime magnitude

Four and three clusters respectively provided a robust classification of the magnitude of air and river temperature regimes. The four river temperature regime classes (R-Tw_x) were characterised by variation in the indices as follows (Figure 5):

R-Tw₁ Cool- lowest mean and minimum and second lowest maximum and standard deviation (8 sites, 9%).

R-Tw₂ Moderate- moderate mean and lowest maximum, moderate minimum and standard deviation (30 sites, 34%).

R-Tw₃ Warm with low seasonality- highest mean and minimum, lowest maximum and standard deviation (17 sites, 19%).

R-Tw₄ Warm with high seasonality- second highest mean, moderate minimum, highest maximum and high standard deviation (33 sites, 38%).

Three air temperature classes were identified (Figure 5):

Ta₁ Cool- lowest mean and minimum, moderate maximum and high standard deviation (23 sites, 59%).

Ta₂ Warm with low seasonality- second highest mean, highest minimum, lowest maximum and lowest standard deviation (3 sites, 8%).

Ta₃ Warm with high seasonality- highest mean, moderate minimum, highest maximum and standard deviation (13 sites, 33%).

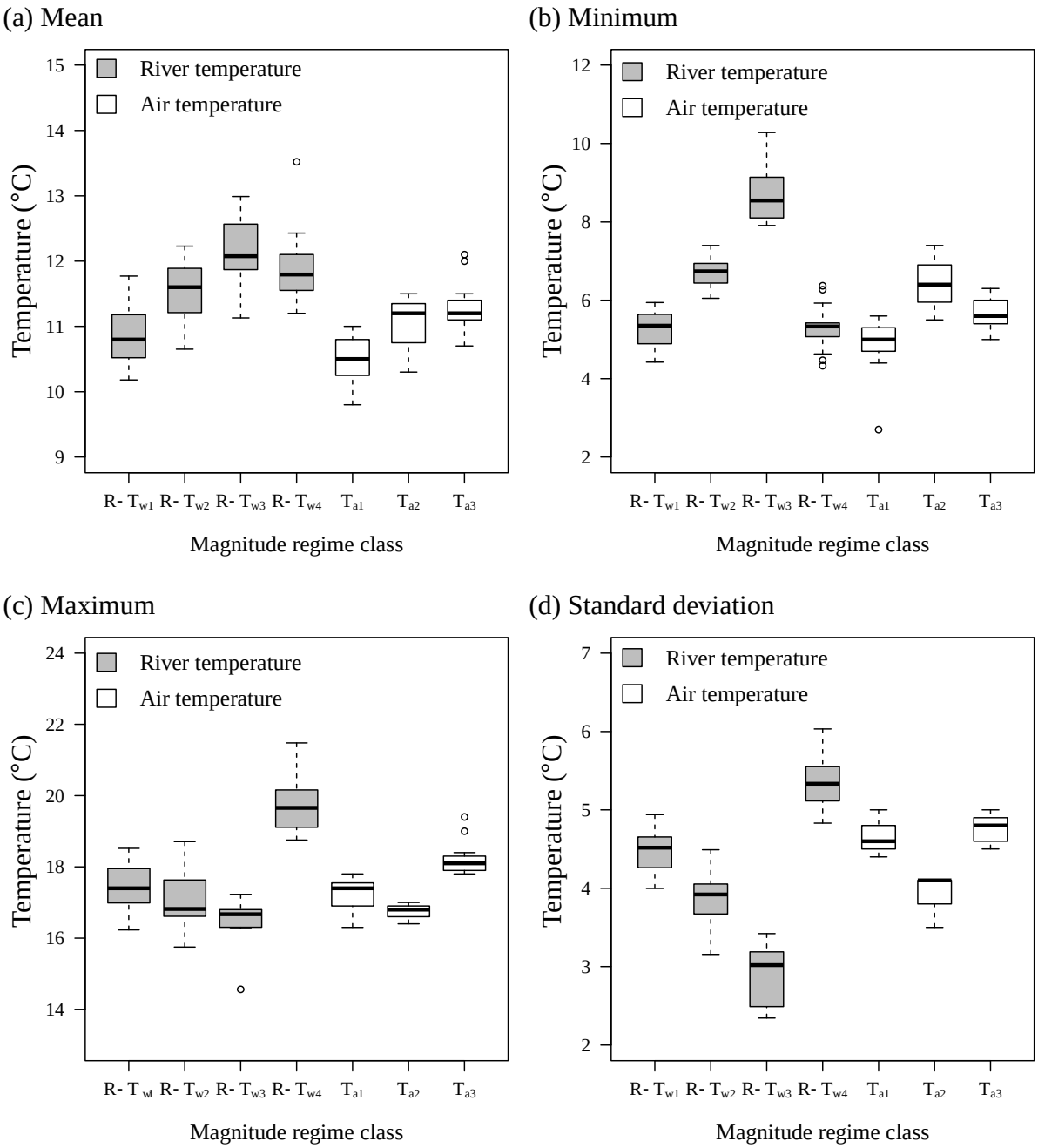

Figure 5. Box plots of annual (a) mean, (b) minimum, (c) maximum and (d) standard deviation for long-term average river and air temperature magnitude regime classes

Long-term regimes: spatial patterns and air-river temperature associations

Regionalisation produced only one air and one river temperature class, indicating no spatial variability in long-term river or air temperature shape regimes across England and Wales.

Therefore, the focus is on spatial patterns and air-river temperature associations for long-term magnitude regimes.

River and air temperature magnitude regimes displayed clear spatial differentiation across England and Wales (Figure 6); and dynamics of paired air-river temperature stations corresponded with the exceptions of central, southern England and two sites in the north-west. The coldest regimes were observed in the north (Ta_1 and R-Tw_1, n=13); whereas those in the south displayed higher means and greater seasonality (Ta_3 and R-Tw_3, n=13). Regimes in the south-west were characterised by high means and low seasonality (Ta_3 and R-Tw_4, n=2). Three combinations of air and river temperature classes occurred for which air temperature contrasted with river temperature (Figure 6): (1) Ta_2 *and* R-Tw_2 (n=8), that was warm and highly seasonal air temperature with moderate river temperature (2) Ta_1 and R-Tw_3 (n=1), that was cold air temperature with warm and highly seasonal river temperature and (3) Ta_1 and *R-*Tw_4 (n=1), that was cold air temperature with warm and less seasonal river temperature.

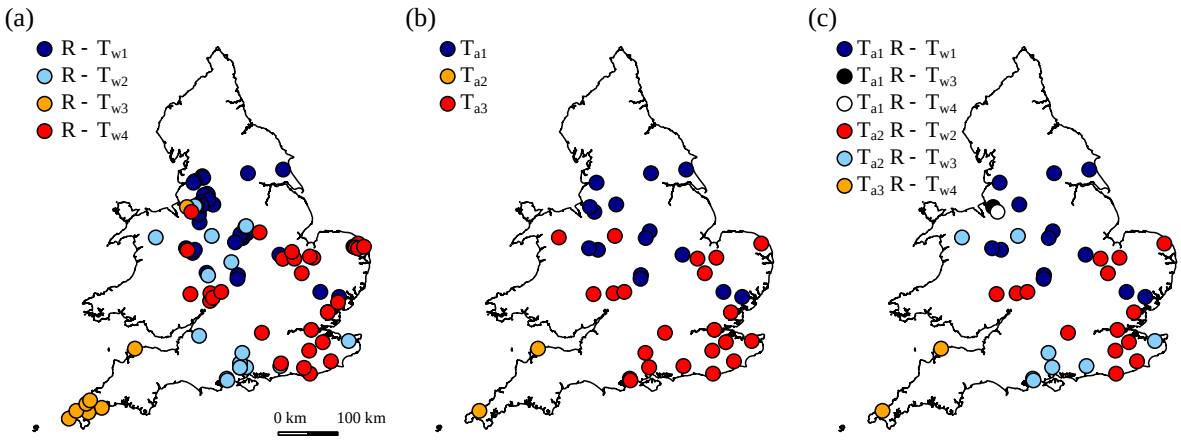

Figure 6. Maps of England and Wales showing distribution of long-term average (a) river temperature regime classes, (b) air temperature regimes classes and (c) associated air–river temperature regime classes at paired air–river temperature stations

2.5.2 Inter-annual regimes: variability and air-river temperature associations

Regime shape and magnitude of river and air temperature were classified using monthly means for each year (1989-2006) across the 38 paired stations (i.e. 702 station-years). These regime classes provided the basis for: (1) quantification of inter-annual stability and (2) test application of the *SI* for linking air and river temperature regimes. The regionalisation results (presented above) structured analyses of between- and within region inter-annual regime variability. As stated in the methodology, the long-term and annual regime classes were not the same; it must be noted that classes for regionalisation were absolute (between-stations) while classes for inter-annual regimes were relative (between-years at a station).

Inter-annual shape regimes

Three inter-annual river temperature and four inter-annual air temperature shape regime classes were identified. River temperature shape regime classes (*IA-Tw*$_x$) were identified as follows (Figure 7):

IA-Tw$_A$ Extended June-August maximum and January minimum with gradual warming and rapid autumn cooling (157 station-years, 22%)

IA-Tw$_B$ July maximum and January minimum with rapid warming and gradual cooling (270 station-years, 38 %)

IA-Tw$_C$ August maximum and December minimum with gradual warming and rapid cooling (275 station-years, 39%)

Four inter-annual air temperature shape regimes (*IA-Ta*$_x$) were identified as follows (Figure 7):

IA-Ta$_A$ Extended June-August maximum and November-February minimum with very rapid rate of cooling (37 station-years, 5%)

IA-Ta$_B$ July maximum and December minimum (240 station-years, 34 %)

IA-Ta$_C$ August maximum and December minimum (269 station-years, 39%)

IA-Ta$_D$ August maximum and January minimum (156 station-years, 22%)

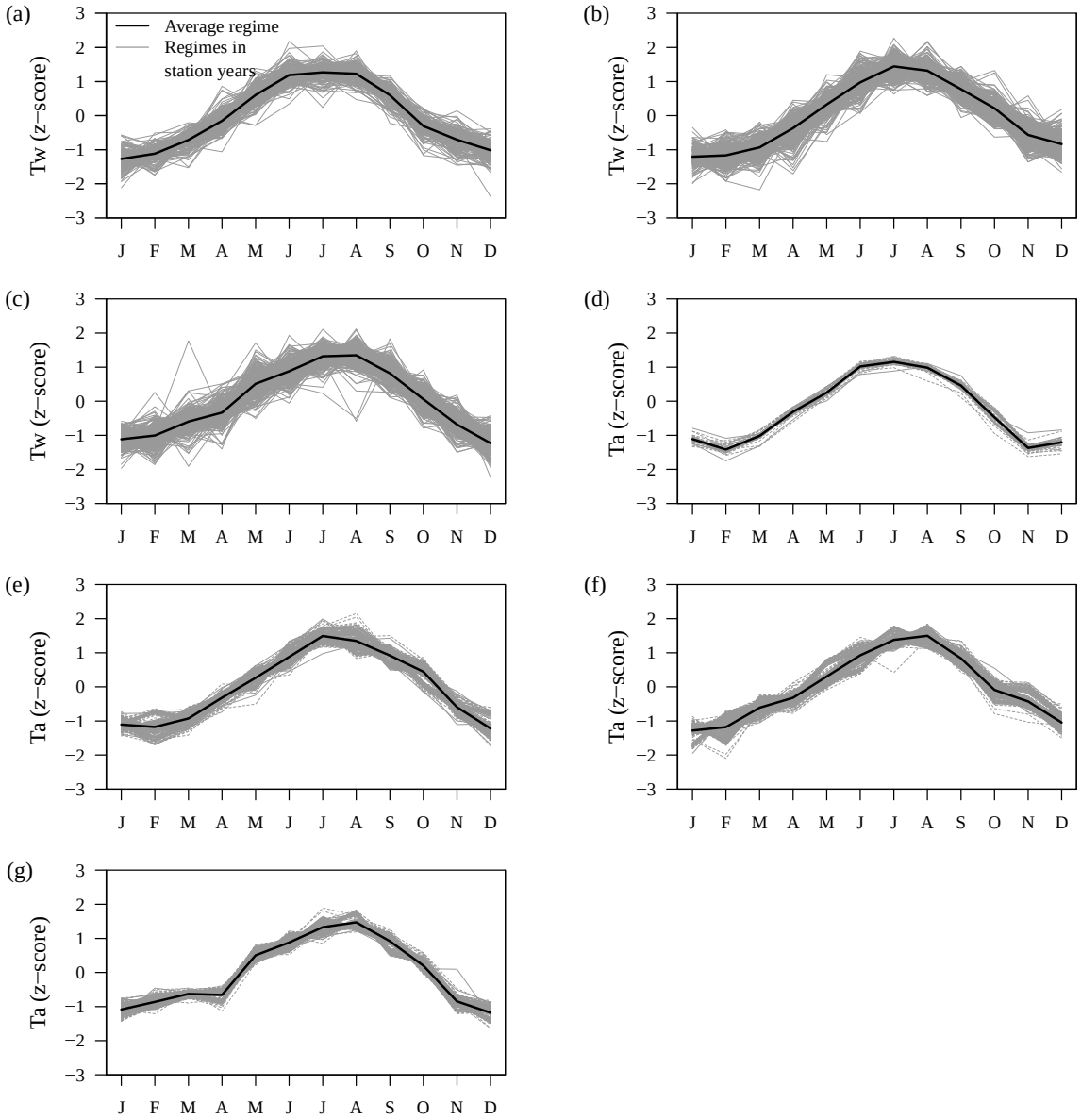

Figure 7. Standardized (*z*-score) monthly average temperature values for regimes in station-years (a) *IA-Tw*$_A$, (b) *IA-Tw*$_B$, (c) *IA-Tw*$_C$, (d) *IA-Ta*$_A$, (e) *IA-Ta*$_B$, (f) *IA-Ta*$_C$ and (g) *IA-Ta*$_D$

Associations between inter-annual air and river temperature shape regimes

As the regionalisation identified single long-term average river and air temperature shape regimes, stations were not subdivided for analysis of associations between inter-annual classes. Annual frequencies of river and air temperature regime shape classes are summarised in Figure 8. There was no evidence of a trend in the occurrence of either river or air temperature regimes over the 18-year study period. Very limited spatial differentiation was observed in patterns of air temperature shape regime occurrence across all sites in each year of the study period. In any given year, one of the four air temperature shape regimes predominated at >90% of stations. Regime *IA-Ta*$_C$ predominated in seven years, *IA-Ta*$_D$ in six years, *IA-Ta*$_B$ in four years and *IA-Ta*$_A$ in one year only. Greater spatial differentiation was observed in patterns of river temperature shape regimes (*cf.* air temperature), although a predominant river temperature shape regime was identified across > 50-92% of stations in all years except 1997, 2003 and 2004. Regime *IA-Tw*$_C$ predominated in six years, *IA-Tw*$_A$ in seven years and *IA-Tw*$_B$ in two years. Equitibility (*E)* quantified the evenness of regime occurrence at each station. Values of *E* were on average very high with 0.87 +/- 0.2 and 0.89 +/- 0.5 for river and air temperature regimes, respectively. This indicated that river and air temperature shape regime occurrence was highly variable between-years and that all regimes occurred reasonably evenly at each station over the study period.

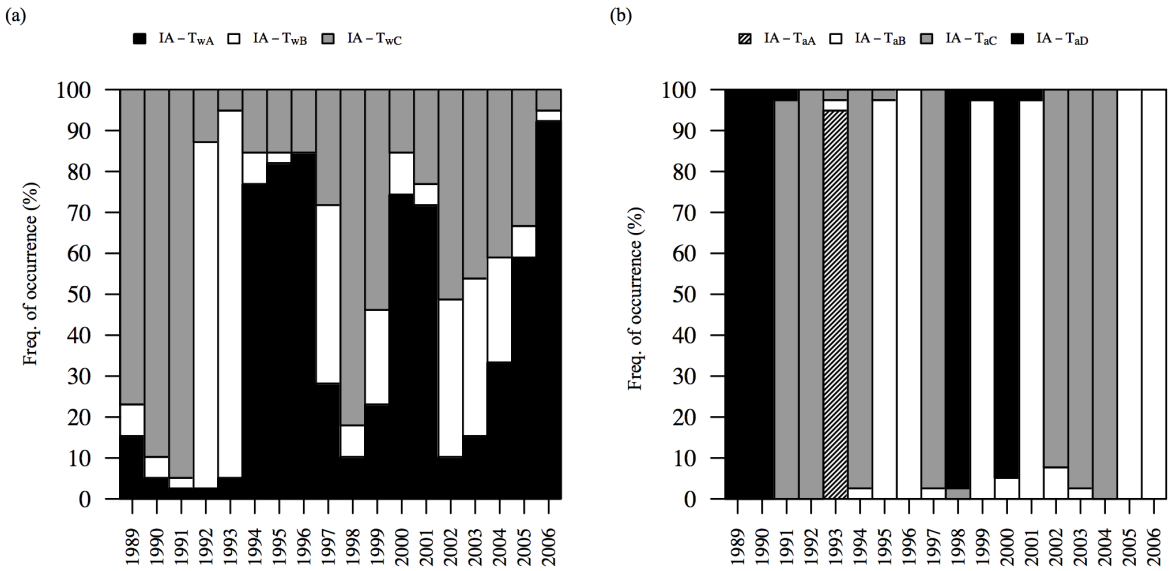

Figure 8. Percentage frequency of occurrence of each inter-annual shape regime in each study year for (a) river temperature and (b) air temperature

The *SI* quantified the strength and direction of the association between air and river temperature regimes. *SI* values were positive at all stations indicating that river temperature regime shape was more variable than air temperature regime shape. Absolute magnitude of *SI* values averaged 0.35 +/- 0.3, which indicated moderate sensitivity of river temperature to air temperature.

Inter-annual magnitude regimes

Five inter-annual river temperature and four inter-annual air temperature magnitude regime classes were identified. Inter-annual river temperature magnitude regime classes (*IA-Tw*$_x$) were identified as follows (Figure 9):

IA-Tw$_1$ Cool- low mean, low maximum, minimum and moderate standard deviation (133 station-years, 19%).

IA-Tw$_2$ Moderate- moderate mean, lowest maximum, highest minimum, lowest standard deviation (175 station-years, 25%)

IA-Tw$_3$ Moderate with high seasonality- moderate mean, high maximum, lowest minimum and high standard deviation (71 station-years, 10%)

IA-Tw$_4$ Warm- moderate mean, high maximum, moderate minimum and standard deviation (224 station-years, 32%)

IA-Tw$_5$ Warm with high seasonality- highest mean and maximum, moderate minimum and highest standard deviation (99 station-years, 14%).

Inter-annual air temperature magnitude regimes (*IA-Ta*$_x$) were identified as follows (Figure 9):

IA-Ta$_1$ Cool- lowest mean, low maximum, low minimum, moderate standard deviation (198 station-years, 28%).

IA-Ta$_2$ Moderate- moderate mean, moderate maximum, high minimum, moderate standard deviation (158 station-years, 23%).

IA-Ta$_3$ Warm- highest mean, high maximum, high minimum, moderate standard deviations (182 station-years, 26%).

IA-Ta$_4$ Warm with greatest seasonality- High mean, high maximum, low minimum, highest standard deviation (164 station-years, 23%).

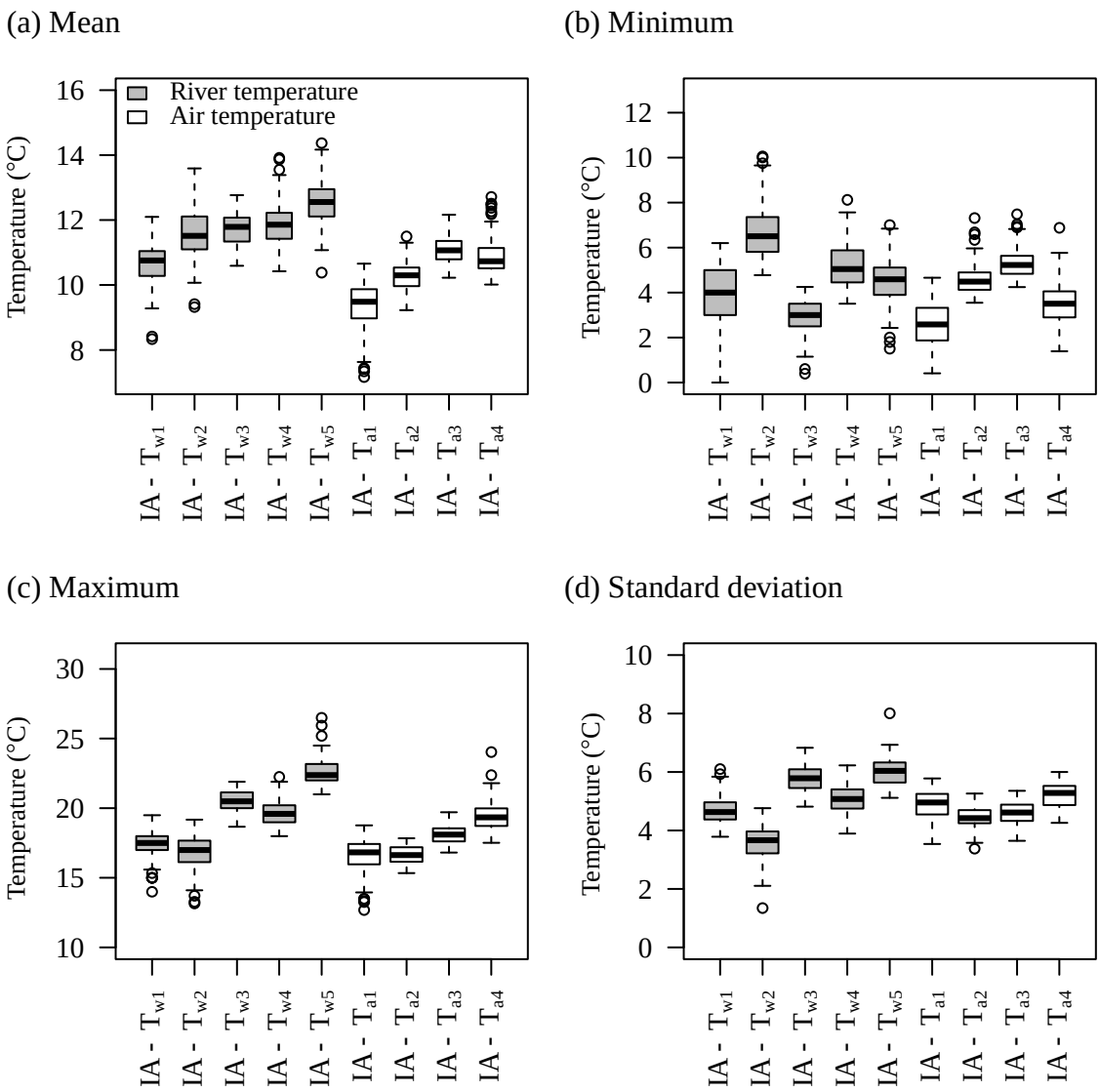

Figure 9. Box plots of annual (a) mean, (b) minimum, (c) maximum and (d) standard deviation for inter-annual river and air temperature magnitude regime classes

Associations between inter-annual air and river temperature magnitude regimes

Regionalisation identified four long-term average river temperature regions (*R-Tw$_1$-R-Tw$_4$)*; for which stations were pooled for analysis of associations between inter-annual regimes of river and air temperature magnitude. Annual frequencies of river and air temperature magnitude classes in each region are summarised in Figure 10. There was no apparent trend in either river or air temperature regime magnitude for any region.

Distinct differences in the frequency of occurrence of inter-annual river temperature magnitude regimes were observed between regions (Figure 10). All inter-annual magnitude regimes occurred within *R-Tw*$_1$ only; *IA-Tw*$_1$ occurred most frequently, followed by *IA-Tw*$_4$, *Ia-Tw*$_2$, *IA-Tw*$_3$ and *IA-Tw*$_5$ (Figure 10). Within region *R-Tw*$_2$, all inter-annual regimes except *IA-Tw*$_3$ occurred; *IA-Tw*$_2$ occurred most frequently, followed by *IA-Tw*$_4$, *IA-Tw*$_1$ and *IA-Tw*$_5$ (Figure 10). Within region *R-Tw*$_3$, all regimes except *IA-Tw*$_2$ were observed; *IA-Tw*$_4$ occurred most frequently, followed by *IA-Tw*$_5$, *IA-Tw*$_3$ and *IA-Tw*$_1$ (Figure 10). Within region *R-Tw*$_4$ regime *IA-Tw*$_2$ predominated across the majority of stations and station-years, followed by *IA-Tw*$_4$ (Figure 10). Consequently, equitability was greatest within region *R-Tw*$_1$ (0.71 +/- 0.11), followed by *R-Tw*$_3$ (0.70 +/- 0.07), *R-Tw*$_2$ (0.49 +/- 0.11) and *R-Tw*$_4$ (0.18+/- 0.32).

For air temperature, all inter-annual magnitude regimes occurred in each region; equitability was high and varied little between regions (*cf.* river temperature regimes). Equitability was greatest within *R-Tw*$_3$ (0.88 +/- 0.14), followed by *R-Tw*$_4$ (0.86 +/- 0.13), *R-Tw*$_1$ (0.81 +/- 0.27) and *R-Tw*$_2$ (0.74 +/- 0.33). Differences in the frequency of regimes were observed between regions (Figure 10) but were not as pronounced as differences for river temperature. In *R-Tw*$_1$ regime *IA-Ta*$_1$ occurred most frequently, followed by *IA-Ta*$_2$, *IA-Ta*$_4$ and *IA-Ta*$_3$ (Figure 10). The frequency of inter-annual air temperature regime occurrence was similar in regions *R-Tw*$_2$ and *R-Tw*$_3$ (Figure 10) because stations within these regions formed the same long-term average air temperature region (Figure 6); *IA-Ta*$_1$ occurred most frequently followed by *IA-Ta*$_3$, *IA-Ta*$_2$ and *IA-Ta*$_4$. In *R-Tw*$_4$, inter-annual regime *IA-Ta*$_1$ occurred most frequently, followed by *IA-Ta*$_2$, *IA-Ta*$_3$ and *IA-Ta*$_4$.

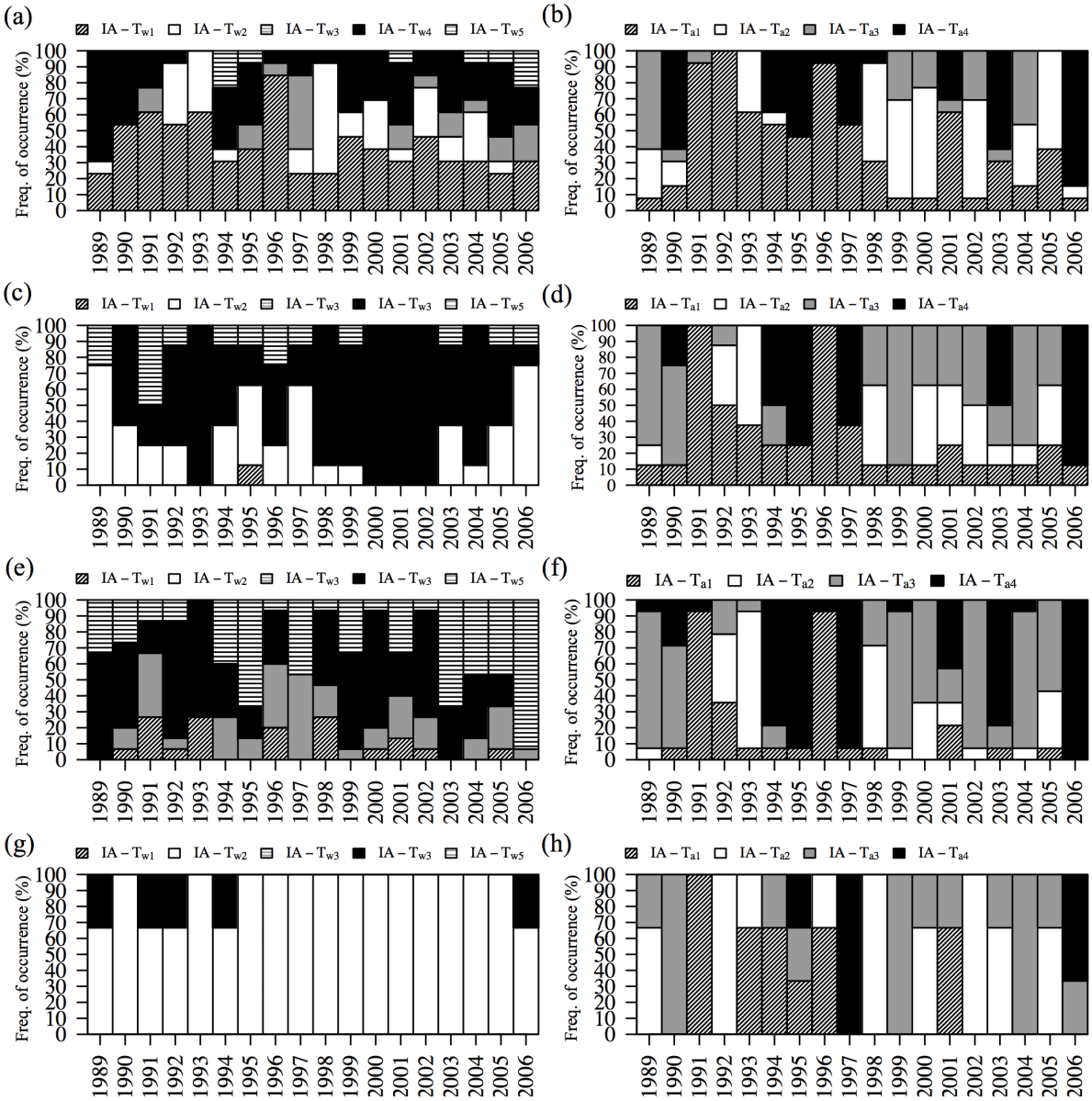

Figure 10. Percentage frequency of occurrence of each inter-annual magnitude regime in each study year for river temperature in (a) *R-Tw*$_1$, (b) *R-Tw*$_2$, (c) *R-Tw*$_3$ and (d)*R-Tw*$_4$ and air temperature in (e) *R-Tw*$_1$, (f) *R-Tw*$_2$, (g) *R-Tw*$_3$ and (h) *R-Tw*$_4$

The strength and direction of inter-annual associations between river and air temperature regime magnitude were quantified using the *SI* and the number of synchronous air-river temperature regime switches. All stations within regions *R-Tw*$_1$, *R-Tw*$_2$ and *R-Tw*$_3$ were associated with negative *SI* values; therefore, river temperature was not as variable year-to-

year as air temperature. Within region *R-Tw*$_2$, 12 stations had negative *SI* values but two stations had positive *SI* values, thus at a minority of stations river temperature was more variable than air temperature between-years. Region *R-Tw*$_3$ was associated with the greatest absolute *SI* values (Figure 11) and the least synchrony of air-river temperature regime switches from year-to-year, five on average. Region *R-Tw*$_2$ had an *SI* of 0.68 and displayed an average of nine synchronous air-river temperature switches. Regions *R-Tw*$_1$ and *R-Tw*$_4$ had the lowest *SI* values and the most synchronous air-river temperature regime switches; on average, stations within *R-Tw*$_1$ had an *SI* value of 0.56 and displayed 10 synchronous switches. Stations within *R-Tw*$_3$ had an *SI* value of 0.52 and displayed 11 synchronous switches.

2.5.3 Influence of basin properties on air-water temperature regime sensitivity

Mean basin permeability (a measure of basin water storage and response time), basin area and mean basin elevation were compared across the four long-term average river temperature regions for magnitude (Figure 11). For basin area, stations within *R-Tw*$_4$ were characterised by the smallest basins and lowest sensitivity to air temperature. Region *R-Tw*$_2$ was associated with the most permeable geologies and was the second least sensitive to air temperature. *R-Tw*$_4$ was situated on the second most permeable geologies. Regions *R-Tw*$_1$ and R-Tw$_3$ were situated on the least permeable geologies and contained the largest basins. For mean basin elevation, a considerable range of values were observed for all regions, especially *R-Tw*$_2$.

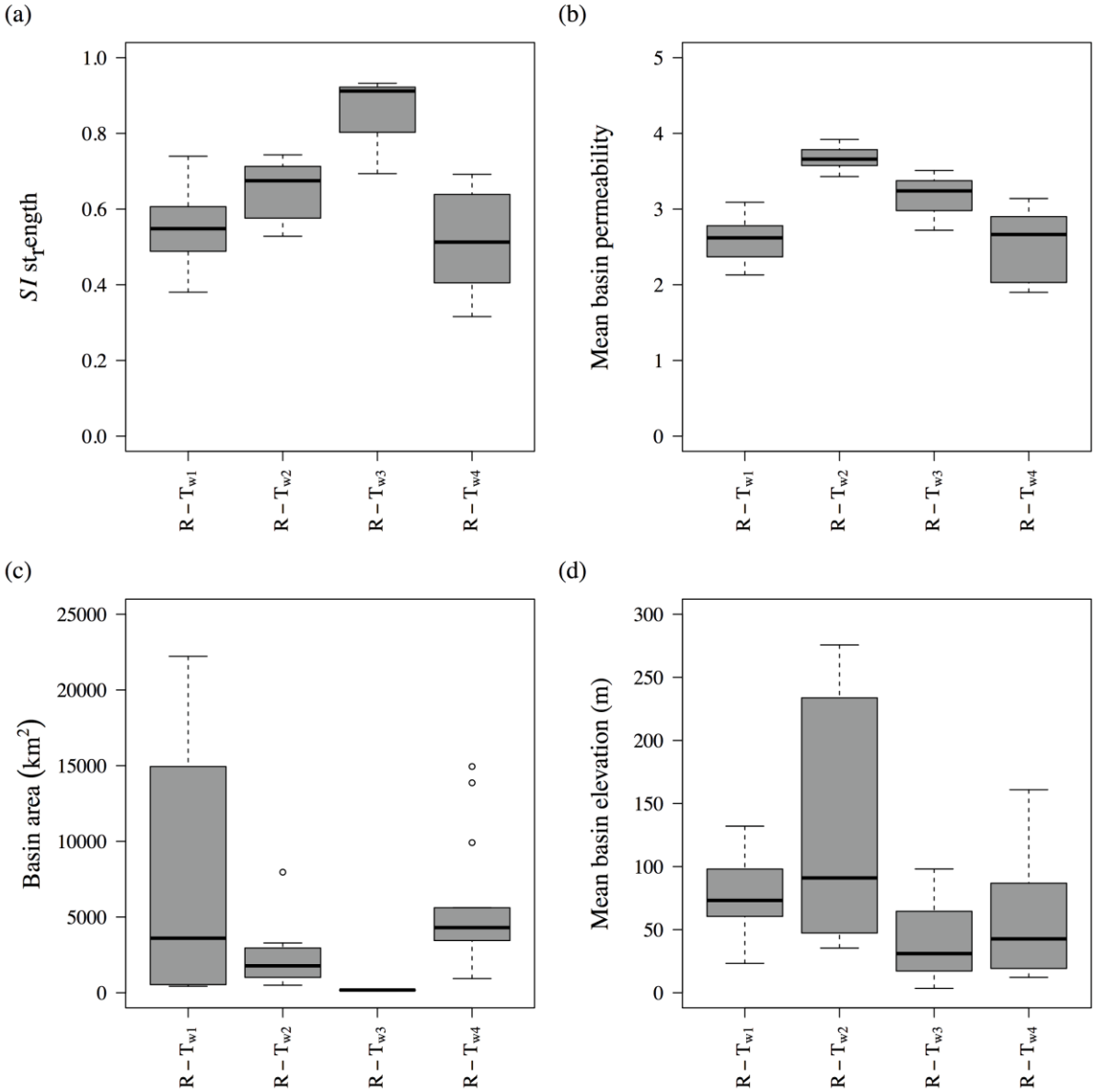

Figure 11. Box plots showing (a) *SI* strength, (b) mean basin permeability, (c) basin area and (d) mean basin elevation for river temperature stations in each region

2.6 DISCUSSION

This paper has quantified the space-time links between the shape and magnitude of air and river temperature regimes within England and Wales and identified the role of static basin properties in modifying these associations. Static basin properties were not found to influence

river temperature shape regimes; therefore, the discussion of the role of the river basin in modifying river temperature is confined to regime magnitude.

2.6.1 Shape regimes

No spatial differentiation of regime shape occurred within England and Wales as only one river and one air temperature regime were identified in the regionalisation process. Broad temporal correspondence of air and river temperature dynamics was observed both intra- and inter-annually. For long-term regimes, river and air temperature displayed maxima in July and minima in January, but air temperature maxima (minima) continued into August (February). The observed discrepancy between the timing of maximum and minimum regime features is attributable probably to the dominance of summer river flow by baseflow (i.e. groundwater) contributions (Tague *et al.*, 2007; Marsh *et al.*, 2007; Payn *et al.*, 2012). The thermal dynamics of groundwater are influenced little by intra-annual variability in air temperature; whereas runoff is influenced by intra-seasonally variable meteorological conditions (O'Driscoll and DeWalle, 2006; Tague *et al.*, 2007; Herb and Stefan, 2011;). Hence, maximum air temperature continued through August, whereas river temperature declined from its annual maximum in July potentially because of changing hydrological sourcing of river flow.

Inter-annually, river temperature regimes varied more than air temperature regimes and the *SI* quantified moderate links between air and river temperature. Moderate correspondence suggests that basin controls modified links between air and river temperature, but since the regionalisation process did not discern regional scale variability in long-term average regime it is likely that these controls were basin specific and that the strength of their influence was variable between years (i.e. they were not static), explaining also why river temperature varied more than air temperature. Inter-annually variable discharge and hydrological sourcing

of river flow (i.e. from runoff or groundwater) would generate varied thermal capacity and initial water temperature for atmospheric warming/ cooling (Poole and Berman, 2001). Therefore, responsiveness of river temperature to air temperature would be varied between-years. A lack of previous research on the variability of river temperature seasonality and links with air temperature hampers the comparison of these results for regime shape with studies conducted elsewhere.

2.6.2 Magnitude regimes and their modification by basin properties

For regime magnitude, spatially distinct regions of long-term average air and river temperature dynamics were observed. Bower *et al.* (2004) (and Chu *et al.*, 2010) also observed variability of air (and river temperature) magnitude at regional scales. Intra-annual dynamics of air and river temperature regimes corresponded broadly within most regions, although some exceptions occurred. Air temperature regimes were warmer and varied less between seasons across a north to south-west gradient within England and Wales in response to reducing altitude and continentality (as observed by Bower *et al.*, 2004). River temperature regimes became warmer and varied less between seasons across a north to south-west gradient too, with the exception of moderate regimes within *R-Tw*$_2$ (located in the south-east) that were observed under warm and highly seasonal air temperature regime *Tw*$_2$. Stations within *R-Tw*$_2$ were located on the most permeable geologies (i.e. predominantly on the Chalk in central southern England; Marsh *et al.*, 2000) and received larger influxes of groundwater. Groundwater contributions in these regions would have contributed cooler water to river flow during summer and warmer water during winter (Story *et al.*, 2003; Hannah *et al.*, 2004; O'Driscoll and DeWalle, 2006; Tague *et al.*, 2007; Chu *et al.*, 2010; Kelleher *et al.*, 2012) and so dampened the magnitude and inter-seasonal variability of the long-term average annual river temperature regime.

Inter-annually, clear regional spatial differentiation was observed in the occurrence of river temperature magnitude regimes and in the strength of links between air and river temperature. River temperature regimes were least stable between-years and displayed the strongest (yet weaker *cf.* shape) links with air temperature in regions *R-Tw*$_1$ and *R-Tw*$_4$, where stations were situated on the least permeable and also the largest basins. River temperature regimes were most stable and displayed the weakest links with air temperature in regions *R-Tw*$_2$ and *R-Tw*$_3$, where stations were located on the most permeable geologies and smallest basins, respectively. These results were consistent with studies conducted on North American and continental European rivers. Runoff sourced from groundwater in Pennsylvanian and Oregon streams, USA, was less variable and less sensitive to variability in air temperature in comparison to those sourced from shallow sub-surface flows (O'Driscoll and DeWalle, 2006; Tague *et al.*, 2007). Reduced sensitivity of headwater streams to air temperature was observed in the Aberdeenshire Dee, Scotland (Hrachowitz *et al.*, 2010), River Danube, Austria (Webb and Nobilis, 2007) and small Pennsylvanian streams were shown to be less sensitive to changes in air temperature than larger streams, USA (Kelleher *et al.*, 2012). The thermal dynamics of headwater streams were similar to those of groundwater because they were likely to be located closer to the river source and water had insufficient exposure time to equilibrate with the atmosphere (Edinger *et al.*, 1968; Poole and Berman, 2001; Tague *et al.*, 2007; Kelleher *et al.*, 2012). Furthermore, stations on small headwater catchments may be forested (e.g. Hrachowitz *et al.*, 2010), so that downstream warming may have been reduced or interrupted (Poole and Berman, 2001; Moore *et al.*, 2005).

Although more sensitive to air temperature than smaller basins, thermal dynamics in larger basins did not exhibit strong links with air temperature as would be expected if they had reached dynamic atmospheric equilibrium. Only moderate air-river temperature links were

observed, for which a number of causes may be hypothesised: (1) dynamic basin properties (e.g. discharge and changing hydrological sourcing of runoff, see *Discussion* section on *Shape regimes*) varied the strength of air-river temperature between-years, (2) larger basins within England and Wales (i.e. predominantly 'mesoscale basins', 10^2-10^3 km^2 in size; Cappel *et al.*, 2012) were smaller than so-called large river basins in continental Europe (e.g. Webb and Nobilis, 2007) and North America (e.g. Kelleher *et al.*, 2012) and thus due to shorter travel times (Mohseni et al., 1999) river temperature may not have enough time to fully equilibrate with the atmosphere, (3) thermal capacity was greater at stations on larger basins owing to higher discharge (Poole and Berman, 2001) and thus response to air temperature variations was weakened (as demonstrated by Webb *et al.*, 2003 in the Exe basin, UK).

2.7 SUMMARY

This study is innovative in presenting: (1) an assessment of large-scale spatial and temporal variability of the shape (timing) and magnitude (size) of annual river temperature regimes within England and Wales, (2) a quantification of their associations with air temperature regimes, and (3) the identification of basin controls that modified the strength of air-river temperature links.

The application of a regime classification methodology (after Hannah *et al.*, 2000) and Sensitivity Index (after Bower *et al.*, 2004) proved to be useful tools for identifying spatial and temporal patterns in annual air and river temperature regimes and assessing the strength of air-river temperature links. Observed patterns of, and associations between, river and air temperature regimes within England and Wales were explained by physically meaningful basin controls, which modified the climatic signal in similar ways to those observed in North American (e.g. Tague *et al.*, 2007; Kelleher *et al.*, 2012) and continental European rivers (e.g. Webb and Nobilis, 2007). Thus, the methods applied herein to annual river temperature

regimes have wide potential applicability for the assessment of large-scale hydroclimatological interactions.

Future changes in river temperature are anticipated in response to a changing climate (Webb and Walling, 1992; Webb and Nobilis, 1994; Mohseni *et al.*, 2003; van Vliet *et al.*, 2011). This study represents an important first step in identifying the locations within England and Wales, and dynamics of annual river temperature regimes, which may be impacted most (i.e. those most sensitive to air temperature change). The results suggest that regime shape will be most sensitive to a changing climate, followed by regime magnitude in the largest and least permeable basins. Regime magnitude in the smallest and most permeable basins is anticipated to be least sensitive. The outcomes of this study contribute new knowledge to the scientific basis for making informed regulatory and management decisions regarding river temperature within England and Wales.

CHAPTER THREE: INTER-ANNUAL VARIABILITY IN THE EFFECTS OF RIPARIAN WOODLAND ON MICRO-CLIMATE, ENERGY EXCHANGES AND WATER TEMPERATURE OF AN UPLAND SCOTTISH STREAM

ABSTRACT

The influence of riparian woodland on stream temperature, microclimate and energy exchange was investigated over seven calendar years. Continuous data were collected from two reaches of the Girnock Burn (a tributary of the Aberdeenshire Dee, Scotland) with contrasting landuse characteristics: (1) semi-natural riparian forest and (2) open moorland. In the moorland reach, wind speed and energy fluxes (especially net radiation, latent heat and sensible heat) varied considerably between years as a consequence of variable riparian microclimate coupled strongly to prevailing meteorological conditions. In the forested reach, riparian vegetation sheltered the stream from meteorological conditions which produced a moderated microclimate and thus energy exchange conditions which were relatively stable between years. Net energy gains (losses) in spring and summer (autumn and winter) were typically greater in the moorland than the forest. However, when particularly high latent heat loss or low net radiation gain occurred in the moorland, net energy gain (loss) was less than that in the forest during the spring and summer (autumn and winter) months. Spring and summer water temperature was typically cooler in the forest, and characterised by less inter-annual variability due to reduced, more inter-annually stable energy gain in the forested reach. The effect of riparian vegetation on autumn and winter water temperature dynamics was less clear due to the confounding effects of reach-scale inflows of thermally stable groundwater in the moorland reach, which strongly influenced the local heat budget. These findings provide new insights as to the hydrometeorological conditions under which semi-natural riparian forest may be effective in mitigating river thermal variability, notably peaks, under present and future climates.

3.1 INTRODUCTION

Thermal dynamics in streams are driven by energy and hydrological fluxes at the air-water and water-riverbed interfaces (Gu and Li, 2002; Hannah *et al.*, 2004; Malcolm *et al.*, 2004a) and may be modified by land and water management (Poole and Berman, 2001; Webb *et al.*, 2003; Webb and Nobilis, 2007; Hannah *et al.*, 2008a). A changing climate, linked to elevated greenhouse gas concentrations, is expected to yield increased long-wave radiation flux from the atmosphere and consequently elevated air temperatures (Ramanathan, 1981; Wild *et al.*, 1997; Andrews *et al.*, 2009), increased sensible heat fluxes from the atmosphere (Leach and Moore, 2010) and elevated groundwater temperatures (Meisner *et al.*, 1988; Leach and Moore, 2010). Hence, there is growing concern that a changing climate may be associated with increases in stream temperature (Langan *et al.*, 2001; Hari *et al.*, 2006; Durance and Ormerod, 2007; Webb and Nobilis, 2007; Huguet *et al.*, 2008; Kaushal *et al.*, 2010; van Vliet *et al.*, 2011, 2013a), which may have profound impacts on physical, chemical and biological processes in flowing waters (Poole and Berman, 2001; Caissie, 2006; Webb *et al.*, 2008) and consequently on freshwater ecosystems (Webb and Walsh, 2004; Wilby *et al.*, 2010).

Stream energy budgets are driven primarily by diurnal and seasonal variability in solar radiation (Beschta *et al.*, 1987). Thus shading at the stream surface by riparian vegetation represents one potential measure for mitigating thermal variability and extremes (Malcolm *et al.*, 2004a; Moore *et al.*, 2005a.; Gomi *et al.*, 2006; Hannah *et al.*, 2008; Imholt *et al.* 2010; 2012*)*. In North America, 'best' management practice is to protect streams against direct insolation using wooded riparian buffer strips (Cole and Newton, 2000; Young, 2000; Hannah *et al.*, 2008a). In the UK, the Forest and Water Guidelines recommend the provision of shading by native woodland where salmonids prevail (Forestry Commission, 2011). However, despite riparian forest being advocated as an effective way to mitigate river temperature

(notably extremes), there is limited process-based evidence to support such recommendations since research to date has often been: (1) short-term (i.e. less than two calendar years; Hannah *et al.*, 2008a), and (2) focused primarily on the effects of forest harvesting on summer maximum temperatures (Malcolm *et al.*, 2008).

No previous studies provide a process based understanding of inter-annual variability in seasonal stream temperatures as they relate to riparian microclimate and energy exchange. Johnson and Jones (2000) investigated water temperature variability in a coniferous forest catchment and two clear-cut catchments in the western Cascades, Oregon over a six-year period. They observed that weekly maximum summer water temperatures varied by up to 1 °C under forest cover and up to 4 °C in clear-cuts between years. Differences between shaded and unshaded sites were greatest during periods of high solar radiation gain and lower during periods of high cloud cover (i.e. low solar radiation gain). This suggests that microclimate and energy exchange conditions may control water temperature variability and extremes in forested reaches; perhaps because the microclimate of un-shaded riparian zones is coupled more strongly to prevailing climatic conditions, as observed by Guenther *et al.* (2012).

To address the above research gaps, this paper compares stream temperature, riparian microclimate and energy exchange dynamics between a moorland (no-trees) reach and a semi-natural forested reach in the Scottish Cairngorms over seven calendar-years. The study aims to improve understanding of the conditions and processes that affect the magnitude of the forestry influence (as indicated by inter-site differences in temperature) between years. Specifically, the following hypotheses are tested:

1. Inter-annual variability in microclimate, net energy exchange and stream temperature is greater in the moorland than under forest cover.

2. Inter-annual variability in microclimate and associated net energy exchange is of greater relative importance than the forest effect in determining the extent of between-reach differences in stream temperature.
3. Inter-annual variability in net energy exchange in the moorland reach is driven by energy fluxes coupled strongly to prevailing meteorological conditions, while a more stable microclimate under the forest canopy weakens the influence of prevailing meteorological conditions.

3.2 STUDY AREA AND SITES

The study catchment, Glen Girnock, is located in a semi-natural, upland basin that drains into the Aberdeenshire Dee, northeast Scotland (Figure 12). The altitude of the catchment ranges from 230 to 862 m, covering 30.3 km^2. Full details of the catchment are found in Tetzlaff *et al*. (2007). In brief, soils are composed of primarily of peaty podsols with a lesser coverage of peaty gleys. Land use is dominated by heather (*Calluna*) moorland, although areas of commercial and semi-natural forest are present in the lower catchment composed of birch (*Betula*), Scots pine (*Pinus*), alder (*Alnus*) and willow (*Salix*) (see Imholt *et al.*, 2013b). Granite at higher elevations and schists at lower elevations, both of which have poor aquifer properties, dominate geology; groundwater movement is mainly by fracture flow (Tetzlaff *et al.*, 2007). The riverbed is composed of a series of gravel-cobble riffles.

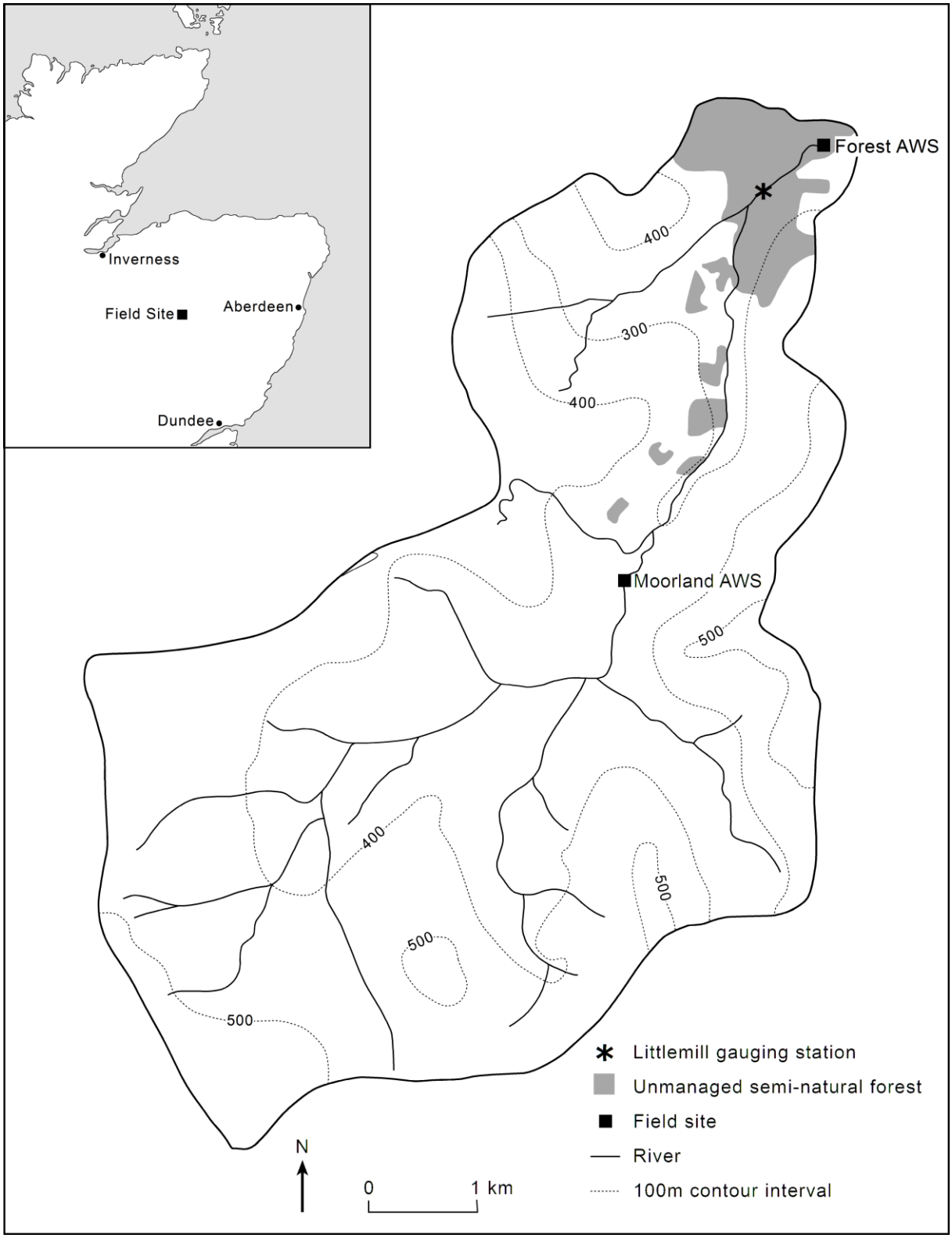

Figure 12. Location map of the Girnock Burn

Study reaches were established with contrasting riparian cover: (1) heather moorland (no trees) and (2) semi-natural woodland. Sites had no tributary inflows. Sediment calibre was similar between reaches, with a median particle size (D_{50}) of ~ 21 mm and a mean fines (particles < 1 mm diameter) content of ~ 5 %. Groundwater-surface water interactions are described by Malcolm *et al.* (2005b) and provide background to interpret the influence of such interactions on stream heat exchange and temperature. Groundwater discharge is highly heterogeneous but spatially constrained. Hyporheic conditions in the forest reach were characterised predominantly by downwelling surface water, while those in the moorland reach were influenced by longer residence groundwater contributions with a greater thermal stability. The moorland and forest reaches had a respective elevation of 310 and 230 m, catchment area of 20.7 and 31.0 km^2, mean channel bankfull width of 9.5 and 7.6 m and channel gradient of 0.01 and 0.02 m m^{-1}.

Inter-annual variability in stream temperature, micro-climate and energy exchange was investigated using observations from two identical automatic weather stations (AWSs), one in each reach. AWSs were micro-sited to reduce risk of damage by ice and debris transported at high flow, and where the channel water was mixed well. In the moorland reach, the AWS was located on a lateral bar/ riffle feature beyond a pool. Previous studies of hydrochemistry and hydraulic head conducted immediately upstream of this site indicate that groundwater discharge dominates; however discharge patterns are highly spatially and temporally variable (Malcolm *et al*., 2004, 2010). Therefore, larger scale catchment controls are considered more influential on controlling groundwater-surface water interactions than localised channel morphology in the moorland reach. In the forest reach, the AWS was located on a lateral bar as it transitions into a riffle. Previous studies of hyporheic hydrochemistry at this site have

shown that it is dominated by surface water exchange (Malcolm *et al.*, 2005b) with no evidence of any substantial groundwater discharge.

3.3. DATA AND METHODOLOGY

3.3.1 Data collection

Data were collected across seven calendar years between 1 January 2003 and 31 December 2009. All sensors were cross-calibrated prior to installation and correction factors applied if required. Sensors were sampled at 10-second intervals, with averages logged every 15-minutes. Measured hydrometeorological variables included air temperature and water colum temperature (°C), relative humidity (%), wind speed (ms^{-1}), net radiation and bed heat flux (Wm^{-2}) (Table 3). Meteorological measurements were made ~2 m above the stream surface in each reach. The bed heat flux plate and thermistor (for water temperature measurement) were located directly below each AWS. The heat flux plate was buried at 0.05 m depth to avoid radiative and convective errors. The heat flux plate provided aggregated measurements of convective, conductive and radiative heat exchanges between the atmosphere and the riverbed and the riverbed and the water column (Hannah *et al.*, 2008a).

Table 3. Variables monitored and instruments employed in hydrometeorological field data collection

Variable	Instrument	Location	Instrument error
Air temperature	Campbell HMP35AC temperature and humidity probe	~ 2 m above water surface	0.2 °C
Water column temperature	Campbell 107 thermistor	0.05 m above stream bed	0.2 °C
Net radiation	NR lite net radiometer	~ 1.75 m above water surface	5%
Bed heat flux	Hukseflux HFP01 SC soil heat flux plate	0.05 m below stream bed	3%
Relative humidity	Campbell HMP35AC temperature and humidity probe	~ 2 m above water surface	1-3%
Wind speed	Vector A100R 3-cup anemometer	~ 2 m above water surface	0.25ms^{-1}

Low river flow during February 2006, July and August 2003 and September 2004 resulted in extended periods of dewatering within the moorland reach and so these data were omitted from analysis. During 2006 sensors submerged within the water column and riverbed at the moorland reach were moved further into the channel to reduce potential for dewatering. Reach scale differences in surface water temperature within the Girnock catchment are insignificant (Imholt *et al.*, 2013a) and so fine scale (metres) relocation of the sensors was not considered to affect the homogeneity of observations. Datalogger failure caused a gap in observations for the moorland reach in March 2006, and so this month was omitted from analysis.

3.3.2 Estimation of stream energy balance components

The energy budget of a stream reach without tributary inflows may be quantified as (Webb and Zhang, 1997; Hannah *et al.*, 2008a):

$$Q_n = Q^* + Q_e + Q_h + Q_{bhf} \quad \text{(Equation 9)}$$

Where Q_n is total energy available to heat or cool the water column, Q^* is net radiation, Q_e is latent heat, Q_h is sensible heat and Q_{bhf} is bed heat flux. Since the focus of the paper is to understand inter-annual variability in vertical exchanges of energy between the stream and its environment, Equation (1) does not include the effects of advective heat transfers associated with groundwater discharge and hyporheic exchange and the divergence of the longitudinal advective heat flux (Q_a). Furthermore, energy derived from precipitation (after Evans *et al.*, 1998), biological and chemical processes (after Webb and Zhang, 1997) were assumed to be negligible. Following the method of Theurer *et al.* (1984), calculations for heat from fluid friction at the riverbed and banks indicated mean values in the range of 0.04- 0.81 $MJm^{-2}d^{-1}$ and 0.07- 1.4 $MJm^{-2}d^{-1}$ in the moorland and forest stream reaches, respectively. Thus,

frictional heating was considered to be negligible and omitted, as is in previous studies (e.g. Moore *et al.*, 2005b; Caissie *et al.*, 2007; Hannah *et al.*, 2008; Hebert *et al.*, 2011; Leach & Moore, 2011; MacDonald *et al.*, 2014b).

Latent (Q_e) and sensible (Q_h) heat were estimated and not measured (after Webb & Zhang, 1997). Latent heat (Wm^{-2}) was calculated using a Penman-style equation to derive heat lost by evaporation or gain by condensation (Equation 10).

$$Q_e = 285.9(0.132 + 0.143 * U)(e_a - e_w) \text{ (Equation 10)}$$

Where U is wind speed (ms^{-1}) and e_a and e_w are vapour pressures of air and water (kPa), respectively.

Vapour pressures were calculated as a function of air or water temperature (T) (K) after Stull (2000) (Equation 11).

$$e_{sat}(T) = 0.611 * \ exp\left[\frac{2.5*10^6}{461} * \left(\frac{1}{273.2} - \frac{1}{T}\right)\right] \text{ (Equation 11)}$$

Vapour pressure of water (e_w) was assumed to be equal to $e_{sat}(T_w)$. Vapour pressure of air was calculated using Equation 12.

$$e_a = \frac{RH}{100} e_{sat}(T_a) \text{ (Equation 12)}$$

Sensible heat (Wm^{-2}) was calculated as a function of Q_e (Equation 13) and Bowen ratio (β) (Equation 14), where P is air pressure (kPa).

$$Q_h = Q_e * \beta \text{ (Equation 13)}$$

$$\beta = 0.66 * \left(\frac{P}{1000}\right) * [(T_w - T_a)/(e_a - e_w)] \text{ (Equation 14)}$$

Herein, energy fluxes are considered positive (negative) when directed toward (away from) the water column and daily flux totals are reported in $MJm^{-2}d^{-1}$.

3.3.3 Data analysis

To place the current study in a broader climatic context, air temperature and precipitation during the seven year study-period are compared to 50 year means measured at the Balmoral monitoring station (<10 km from both reaches) (UK Meteorological Office, 2014).

For analyses of the AWS data, stream temperature and riparian microclimate, variables are presented as monthly means whilst energy fluxes are presented as monthly means of daily totals. Detailed methodologies appropriate to test the three hypotheses are provided in detail below.

Hypothesis 1

Mean monthly values were calculated for each site, month and year over the seven-year period in order to quantify inter-annual variability in stream temperature, microclimate and energy exchanges. An Ansari-Bradley test (Hollander and Wolfe, 1999) was used to investigate equality of variance between sites for each calendar month in order to test the null hypothesis that there was no significant difference in inter-annual variability between sites. *p* values were presented as false discovery rates (Benjamini and Hochberg, 1995) to account for multiple comparisons. The Ansari-Bradley test is a non-parametric test for differences in scale between two groups and makes no distributional assumptions. For each site and month, data were centred about the mean. Linear trends across years were removed prior to analysis to remove the variance associated with temporal trends.

Hypothesis 2

Difference plots (moorland minus forest) were used to illustrate the magnitude of between-reach differences in microclimate, net energy exchange and stream temperature. Positive (negative) observations indicated that moorland values were higher (lower) than those in the forest. Between reach differences (in any month) were considered significant where they exceeded the root of the sum of squares in the uncertainty of the accuracy of observations (uncertainty associated with each instrument is provided in Table 3) of each measurement in any calculation (Meyer, 1992). Difference plots also identified the nature of between-reach differences in each variable (i.e. moorland values typically greater than forest or *vice versa*). For months in which atypical between-reach differences occurred it was informative to attribute the cause to conditions in the moorland or forest. Thus, the difference was calculated between observations in these months and the seven-year mean for the reach and calendar month in which they occurred (long-term mean). The cause of atypical between-reach conditions was therefore attributed to the reach in which deviation from the long-term mean was greatest.

Hypothesis 3

The total energy available to heat or cool the stream was partitioned into heat sources and sinks (i.e. Q^*, Q_e, Q_h and Q_{bhf}) to identify the drivers of inter-annual variability in the energy budget of each reach. For months in which between-reach differences in net energy were atypical (see *Hypothesis 2*), the difference was calculated between observations of energy balance components in these months and the seven-year mean for the component, reach and calendar month in which they occurred (long-term mean). Significant differences were identified as described for *Hypothesis 2*. The drivers of atypical conditions were attributed to the energy flux in the reach in which deviation from the long-term mean was greatest.

3.4 RESULTS

Results are presented in three sections: (1) characterisation of the study period within a longer-term climatic context, (2) inter-annual variability in water column temperature, riparian microclimate and net energy exchange (sum of all fluxes in Equation 1) both at, and between, reaches (*Hypotheses 1* & *2*), and (3) hydrometeorological drivers of inter-annual variability in net energy exchange (*Hypothesis 3*).

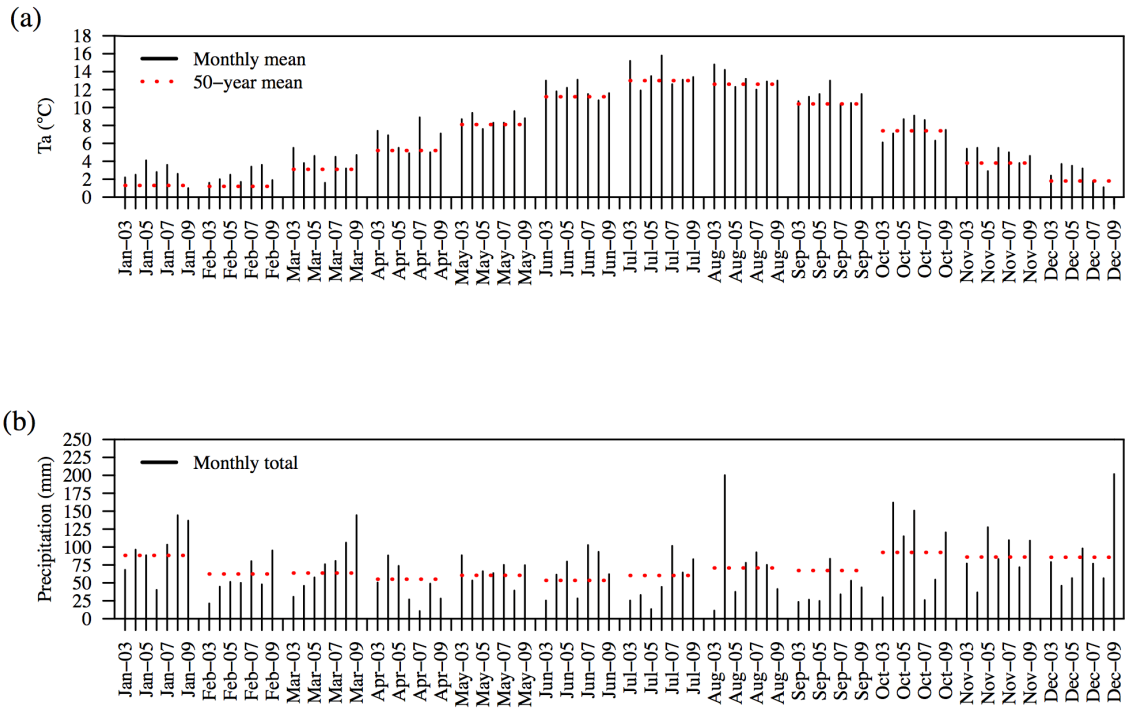

Figure 13. Monthly mean air temperature (a) and precipitation (b) at Balmoral compared to 50-year means

3.4.1 Climatic context

In comparison to the previous 50 years, the climate of the seven-year study-period was typically warm and dry. Air temperature was, on average, 1.2 °C greater than 50 year means in > 75 % of months studied. Precipitation totals were, on average, 27.6 mm less than the means of 50 year totals in > 50 % of months during the study period (Figure 13).

3.4.2 Quantification of inter-annual variability within and between reaches

Water column temperature

Variances of mean monthly water column temperatures (Table 4) were typically greater in the moorland reach than in the forest, indicating that water temperature in the moorland varied more between years than in the forest. Differences were significantly greater in the moorland between May and August, indicating that water temperature in the moorland varied more between years than in the forest. There was substantial within and between-year variability in the magnitude of differences in monthly mean water column temperature between the forest and moorland reaches (Figure 14). During spring and summer months, between-reach differences ranged from -2.0 °C to +3.2 °C, where positive numbers indicate the moorland was characterised by higher temperatures than the forest (Figure 14). Although there was considerable variability between months and years, differences were generally positive with the exception of April 2004, May, June, July and August 2005. During these months and years water temperature in the moorland was consistently less than the long-term means, while water temperature in the forest reach was more similar to long-term conditions (Figure 14).

Table 4. Variances of centred monthly means of water temperature and riparian microclimate variables for (a) moorland, (b) forest, and (c) *p* values as false discovery rates for Ansari-Bradley tests.

(a) Variable	Jan	Feb	Mar	Apr	May	Jun	Jul	Aug	Sep	Oct	Nov	Dec
Tw (°C)	0.29	0.23	2.58	1.62	0.93	0.85	2.57	1.43	0.64	2.27	0.36	0.27
Ta (°C)	0.80	0.60	2.88	1.50	0.63	0.63	2.05	0.46	0.65	2.04	0.56	2.22
e_a (mbar)	0.01	0.12	0.46	0.48	0.31	0.98	3.78	1.11	0.55	0.93	0.04	0.03
U (ms^{-1})	0.28	0.23	0.06	0.12	0.08	0.12	0.04	0.05	0.12	0.26	0.17	0.29

(b) Variable	Jan	Feb	Mar	Apr	May	Jun	Jul	Aug	Sep	Oct	Nov	Dec
Tw (°C)	0.37	0.30	1.09	1.42	0.39	0.23	1.04	0.28	0.44	1.55	0.28	0.23
Ta (°C)	1.07	0.40	1.67	1.95	0.54	0.63	1.71	0.40	0.53	1.39	0.62	1.64
e_a (mbar)	0.13	0.03	0.44	0.82	0.25	0.17	2.59	0.45	1.35	0.79	0.10	0.09
U (ms^{-1})	0.03	0.01	0.01	0.01	<0.01	<0.01	<0.01	<0.01	<0.01	0.01	0.01	0.01

(c) Variable	Jan	Feb	Mar	Apr	May	Jun	Jul	Aug	Sep	Oct	Nov	Dec
Tw (°C)	0.60	0.38	0.60	0.60	0.03	0.03	0.03	0.03	0.43	0.53	0.25	0.46
Ta (°C)	0.70	0.70	0.70	0.70	0.70	0.70	0.70	0.70	0.70	0.70	0.70	0.70
e_a (mbar)	0.94	0.12	0.60	0.67	0.60	0.60	0.60	0.46	0.60	0.60	0.89	0.96
U (ms^{-1})	0.03	0.02	0.06	0.03	0.02	0.03	0.03	0.03	0.03	0.03	0.06	0.02

Between-reach differences in monthly mean water column temperature were smaller in autumn and winter months (cf. spring and summer), ranging from -1.4 to +0.9 °C (Figure 14). Mean monthly water column temperature in the moorland reach exceeded water temperature in the forest during most months with the exception of October 2003 and 2005, November and December 2004. During these months, water temperatures in the moorland and forest reaches exhibited similar variability about long-term means (Figure 14). During October 2003 (2005) water temperature in both reaches was lower (higher) than the long-term mean. However, in November 2004 and 2005 the mean forest water temperature was greater than the long-term mean, while the moorland water temperature was closer to the long-term mean.

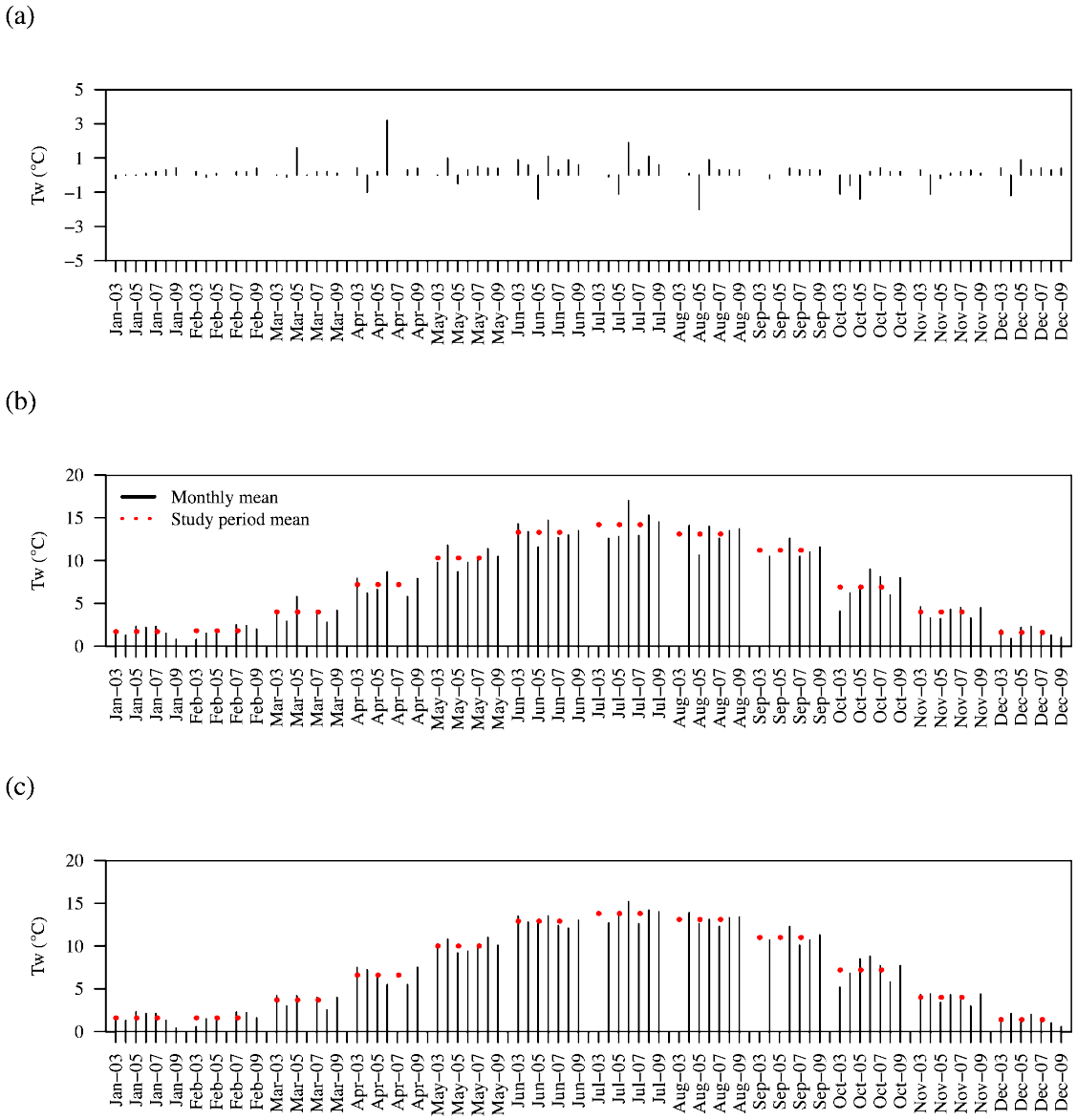

Figure 14. Monthly average water temperature: (a) moorland minus forest difference, (b) moorland, and (c) forest

Riparian microclimate

Mean monthly wind speed varied significantly more between years in the moorland than the forest. Mean monthly wind speed in the moorland was always greater than that in the forest, with moorland minus forest differences ranging from 0.96 ms^{-1} to 3.11 ms^{-1} (Figure 15).

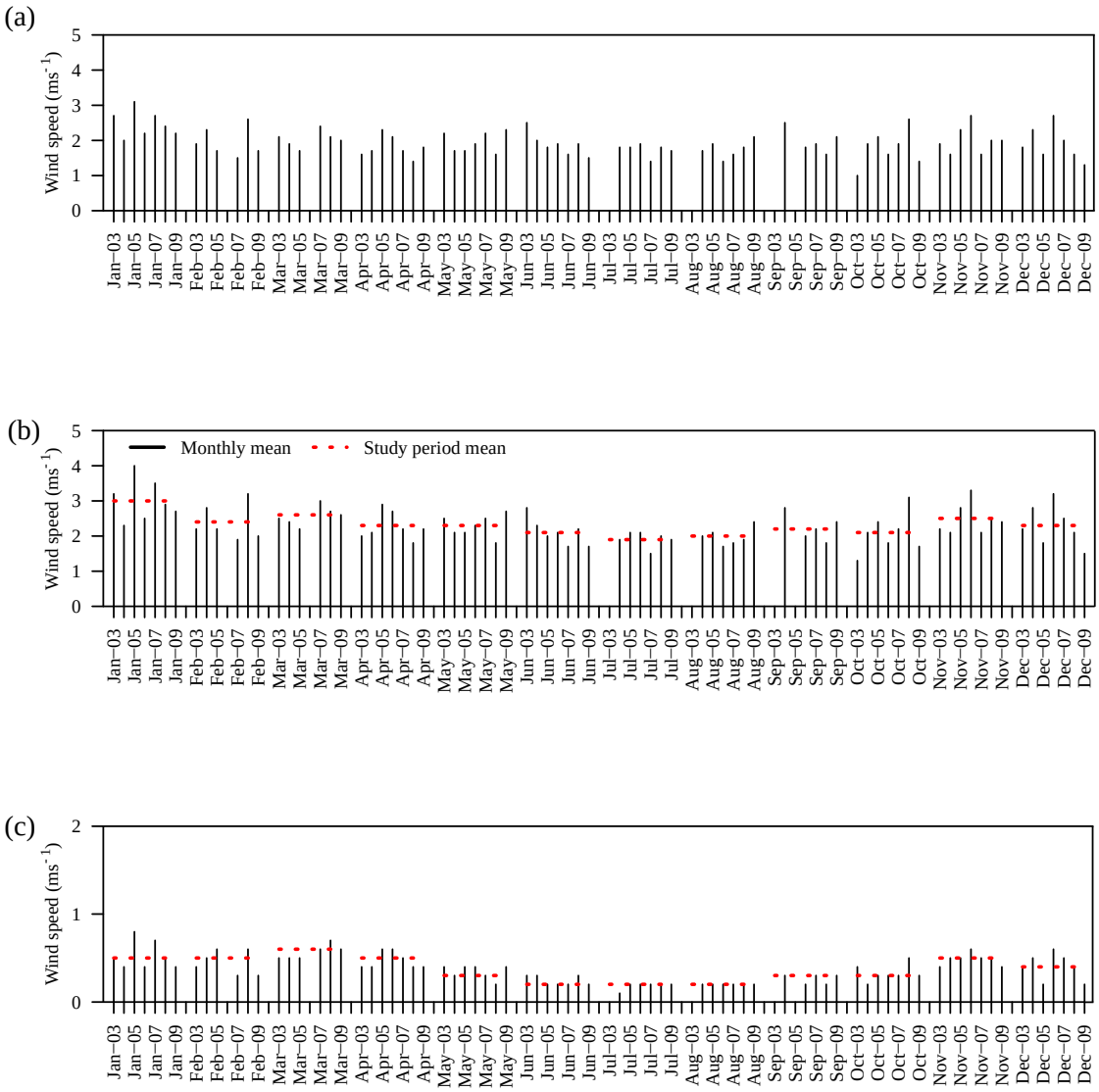

Figure 15. Monthly average wind speed: (a) moorland minus forest difference, (b) moorland, and (c) forest

Between reach differences in the variances mean monthly air temperature and vapour pressure (an absolute measure of moisture in the air; Hannah *et al.*, 2008) were insignificant, indicating that both reaches displayed similar inter-annual variability (Table 4). Mean monthly air

temperature (Figure 16) and vapour pressure (Figure 17) were generally greater in the forest reach with between-reach differences in air temperature and vapour pressure ranging from -1.67 °C to + 1.82 °C and 2.09 to 1.96 mbar, respectively.

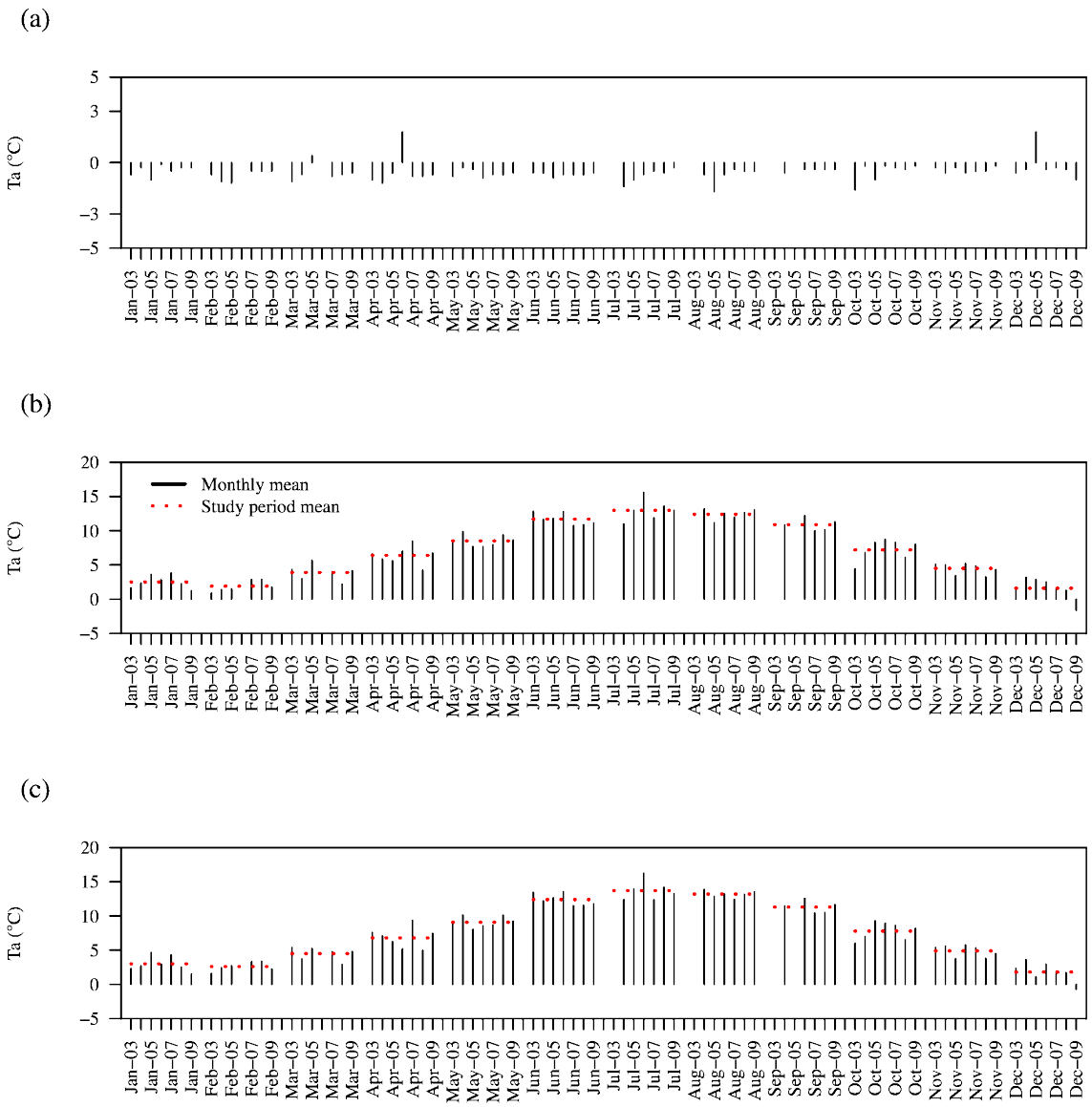

Figure 16. Monthly average air temperature: (a) moorland minus forest difference, (b) moorland, and (c) forest

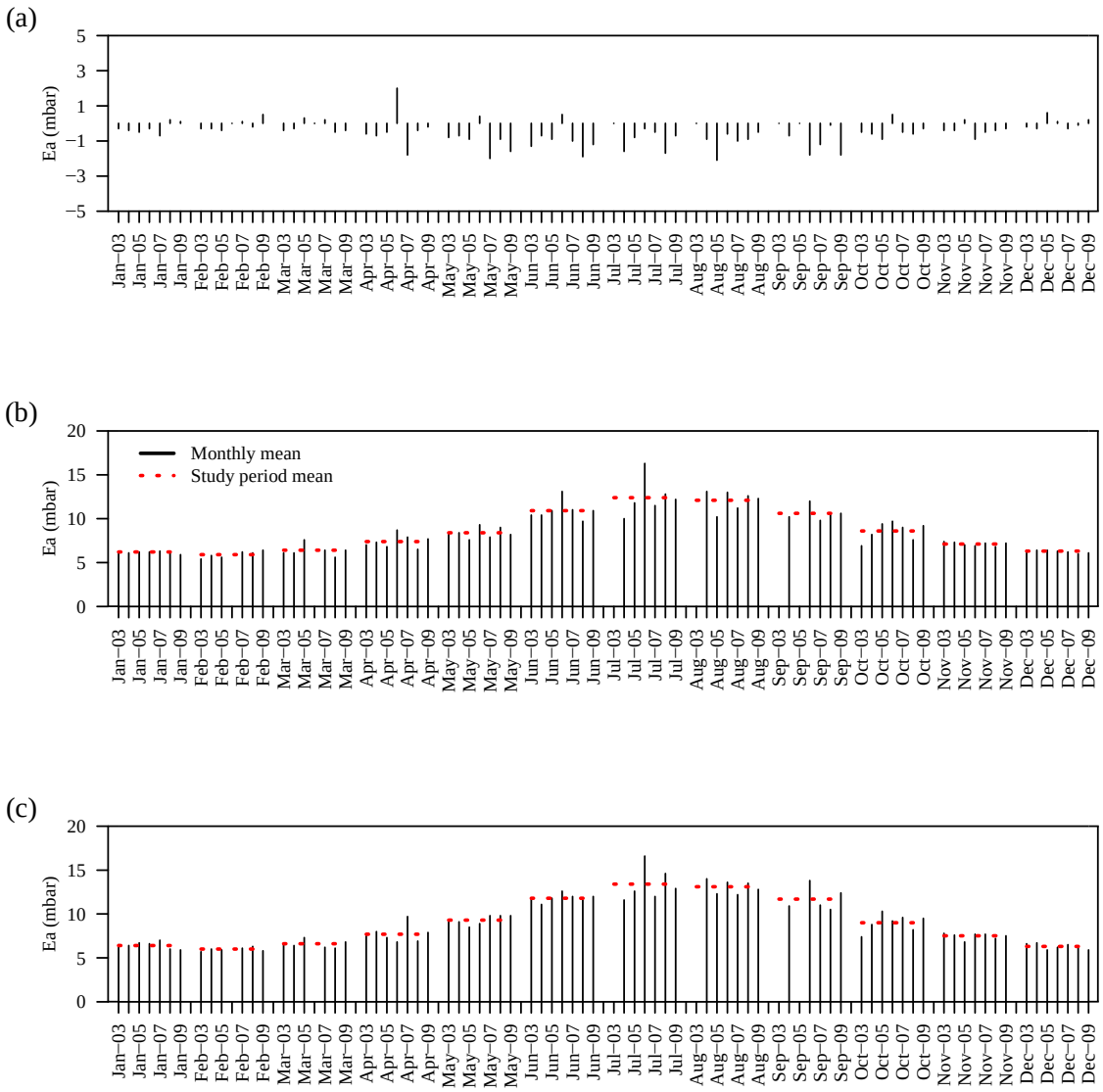

Figure 17. Monthly average vapour pressure: (a) moorland minus forest difference, (b) moorland, (c) forest

Net energy exchange

Net energy indicates the amount of energy available to heat or cool the water column at each reach (after Equation 9). Variances of monthly means of daily net energy totals were consistently greater in the moorland compared to in the forest, and significantly greater

between May and September (Table 5). Thus, net energy totals varied more between years in the moorland than the forest.

During spring and summer months, the water column received consistent net energy gains (Figure 18). Differences in monthly means of daily net energy totals ranged from -1.2 $MJm^{-2}d^{-1}$ to +3.1 $MJm^{-2}d^{-1}$ (moorland minus forest, Figure 18). Net energy in the forest reach only exceeded that in the moorland during May 2003, 2006 and 2007, and June 2003, 2004 and 2006. During these months (excluding June 2006) net energy gain in the moorland was considerably less than long-term means, while net energy gain in the forest was typically closer to long-term means.

Table 5. Variances of centred monthly means of daily total energy fluxes ($MJm^{-2}d^{-1}$) for (a) moorland and (b) forest, and (c) *p* values as false discovery rates for Ansari-Bradley tests.

(a) Variable	Jan	Feb	Mar	Apr	May	Jun	Jul	Aug	Sep	Oct	Nov	Dec
Tw (°C)	0.29	0.23	2.58	1.62	0.93	0.85	2.57	1.43	0.64	2.27	0.36	0.27
Ta (°C)	0.80	0.60	2.88	1.50	0.63	0.63	2.05	0.46	0.65	2.04	0.56	2.22
Ea (mbar)	0.01	0.12	0.46	0.48	0.31	0.98	3.78	1.11	0.55	0.93	0.04	0.03
WS (ms^{-1})	0.28	0.23	0.06	0.12	0.08	0.12	0.04	0.05	0.12	0.26	0.17	0.29

(b) Variable	Jan	Feb	Mar	Apr	May	Jun	Jul	Aug	Sep	Oct	Nov	Dec
Tw (°C)	0.37	0.30	1.09	1.42	0.39	0.23	1.04	0.28	0.44	1.55	0.28	0.23
Ta (°C)	1.07	0.40	1.67	1.95	0.54	0.63	1.71	0.40	0.53	1.39	0.62	1.64
Ea (mbar)	0.13	0.03	0.44	0.82	0.25	0.17	2.59	0.45	1.35	0.79	0.10	0.09
WS (ms^{-1})	0.03	0.01	0.01	0.01	<0.01	<0.01	<0.01	<0.01	<0.01	0.01	0.01	0.01

(c) Variable	Jan	Feb	Mar	Apr	May	Jun	Jul	Aug	Sep	Oct	Nov	Dec
Tw	0.60	0.38	0.60	0.60	0.03	0.03	0.03	0.03	0.43	0.53	0.25	0.46
Ta	0.70	0.70	0.70	0.70	0.70	0.70	0.70	0.70	0.70	0.70	0.70	0.70
Ea	0.94	0.12	0.60	0.67	0.60	0.60	0.60	0.46	0.60	0.60	0.89	0.96
WS	0.03	0.02	0.06	0.03	0.02	0.03	0.03	0.03	0.03	0.03	0.06	0.02

The water column typically received net energy gains during the early autumn (September), but net energy losses between October and February (Figure 18). Between-reach differences in autumn and winter months were smaller than those during spring and summer months, ranging from -1.3 $MJm^{-2}d^{-1}$ to +1.9 $MJm^{-2}d^{-1}$. The mean monthly net energy total in the moorland was generally less than in the forest, with the exceptions of February 2007 and 2008, October 2004, 2005 and 2006, November 2004 and 2005, and December 2004 and 2005. During these months, net energy loss in the moorland was typically considerably less than long-term means. In contrast, net energy loss in the forest was more comparable to the long-term means (Figure 18).

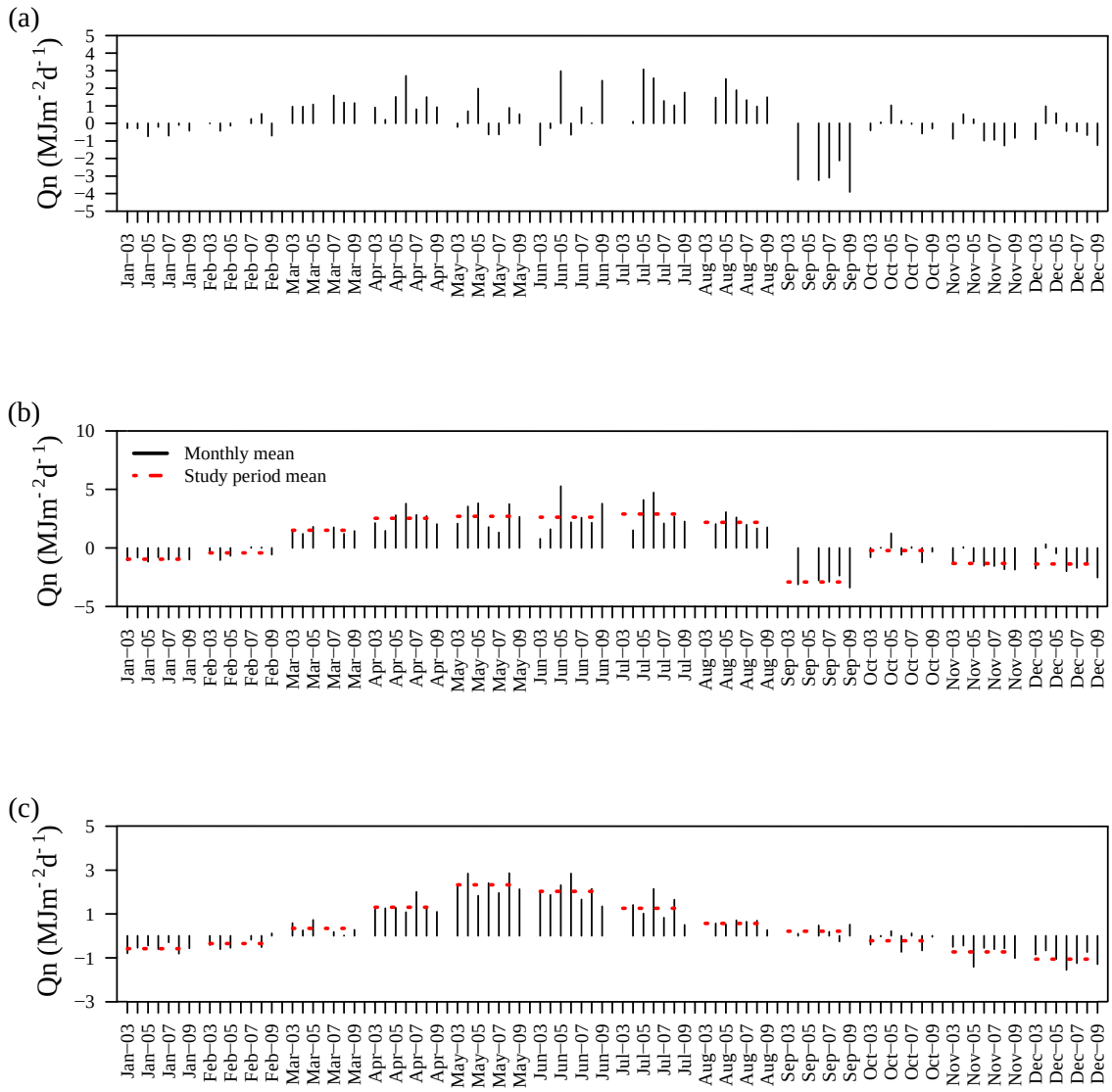

Figure 18. Monthly average net energy total: (a) moorland minus forest difference, (b) moorland, and (c) forest

3.4.3 Drivers of inter-annual variability in net energy exchange

Net energy totals were partitioned into energy sources and sinks in order to determine the energy exchange processes driving inter-annual variability in net energy exchange. Between March and September, net radiation was the predominant energy source and latent heat was

the predominant sink in both the moorland and forest reaches. Sensible heat and bed heat were very minor components of the energy budget in both reaches (Figure 19).

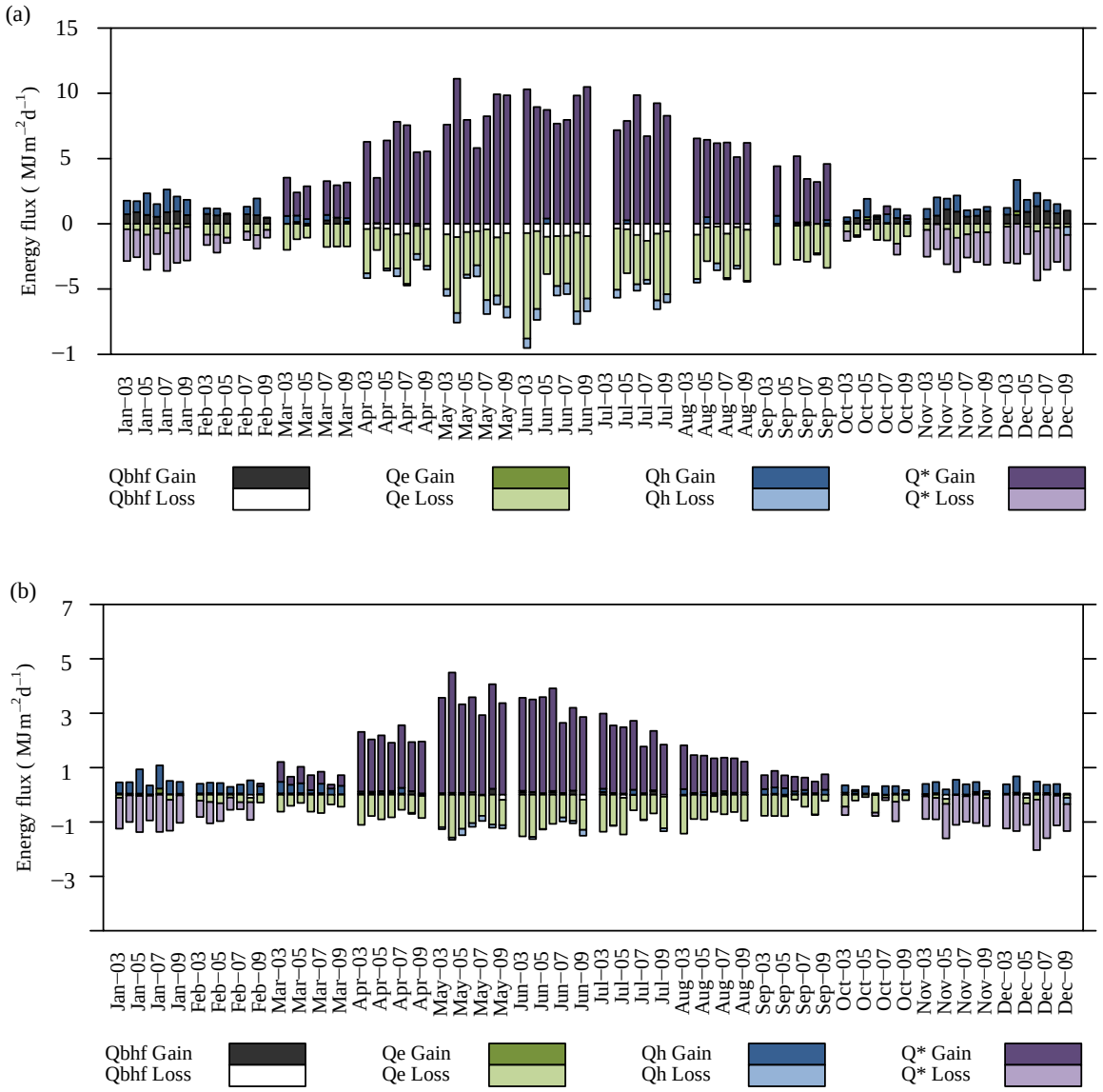

Figure 19. Monthly average daily total contributions of energy sources and sinks to energy gains and losses: (a) moorland and (b) forest

Net radiation and latent heat exhibited greater inter-annual variability in the moorland reach (Table 5). When net energy gain in the moorland reach was less than the forest, this was typically caused by two atypical scenarios: (1) net radiation receipt in the moorland was lower than the long-term mean (during May 2003, 2006 and June 2006; Figure 20) or (2) latent heat loss in the moorland was greater than long-term means (during May 2007, June 2003 and 2004; Figure 21). Net radiation and latent heat flux in the forest reach during these months was closer to long-term means (Figures 20 and 21, respectively).

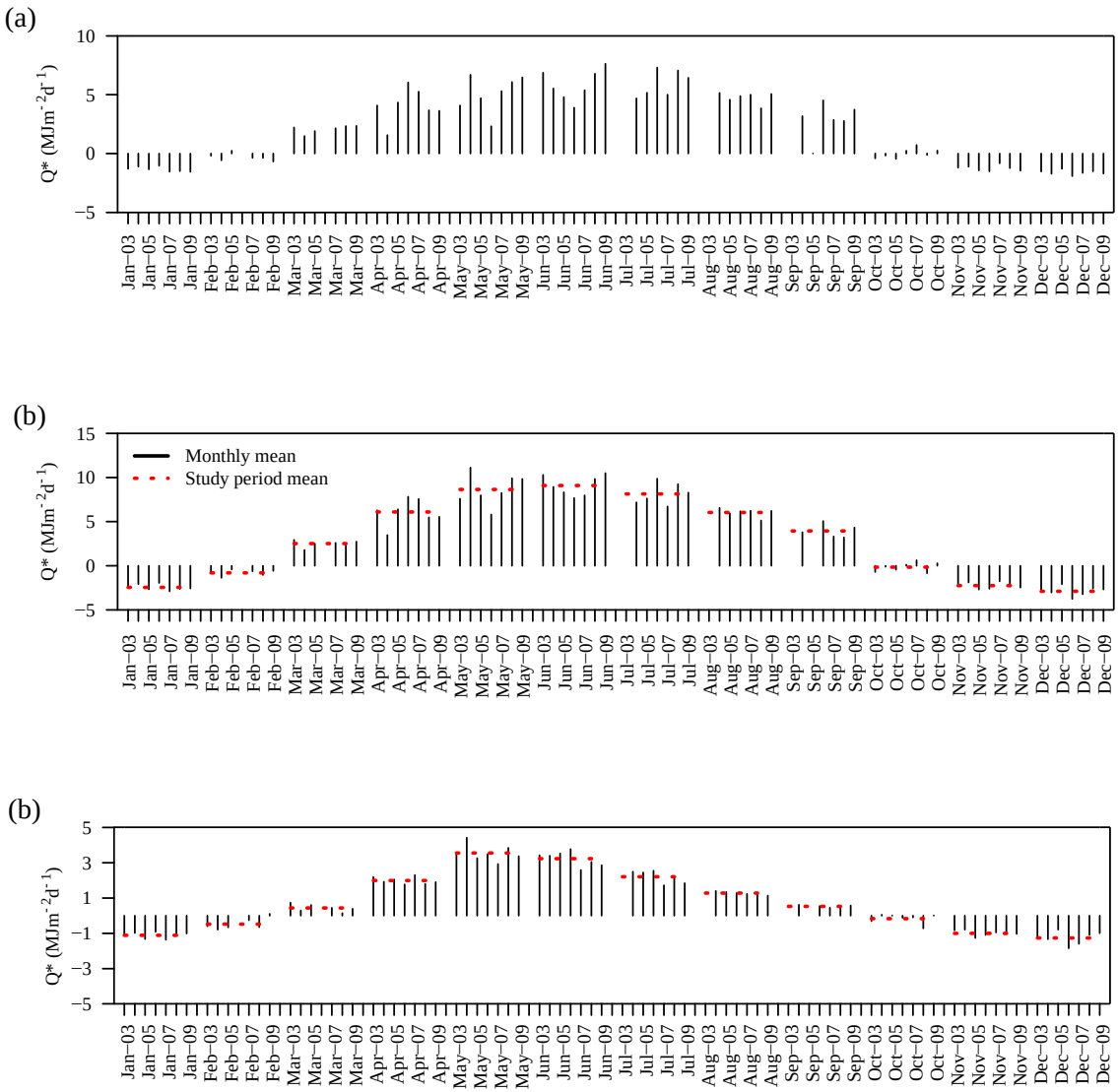

Figure 20. Monthly average net radiation total: (a) moorland minus forest difference, (b) moorland, and (c) forest

Energy sources and sinks shifted markedly between autumn and winter months. During September, net radiation was the predominant heat source and latent heat the predominant heat sink. However, in October, net radiation became a heat sink and sensible heat became a major heat source in both reaches, as did bed heat flux in the moorland. Latent heat was the predominant sink in both reaches during October and a minor sink between November and February (Figure 19). Sensible heat, latent heat and net radiation were more variable between years in the moorland reach (Table 5). Occasions when the moorland reach received more energy than the forested reach were associated with two atypical energy exchange conditions in the moorland: (1) net radiation gains occurred (during October 2004 and December 2005; Figure 20); (2) high sensible heat gains occurred (during February 2007 and 2008, October 2005, November 2004 and December 2004; Figure 21). During these months, net radiation and sensible heat fluxes in the forest were typically closer to long-term means and more variable about long-term means in the moorland (Figures 20 and 21, respectively). However, in contrast to the spring and summer months, atypical energy exchange conditions also occurred in the forest on two occasions, causing the reach to lose more energy than the moorland: (1) during December 2005 the forest received extremely low sensible heat gain and; (2) during October 2006 latent heat loss was unusually high for the forest (Figure 21).

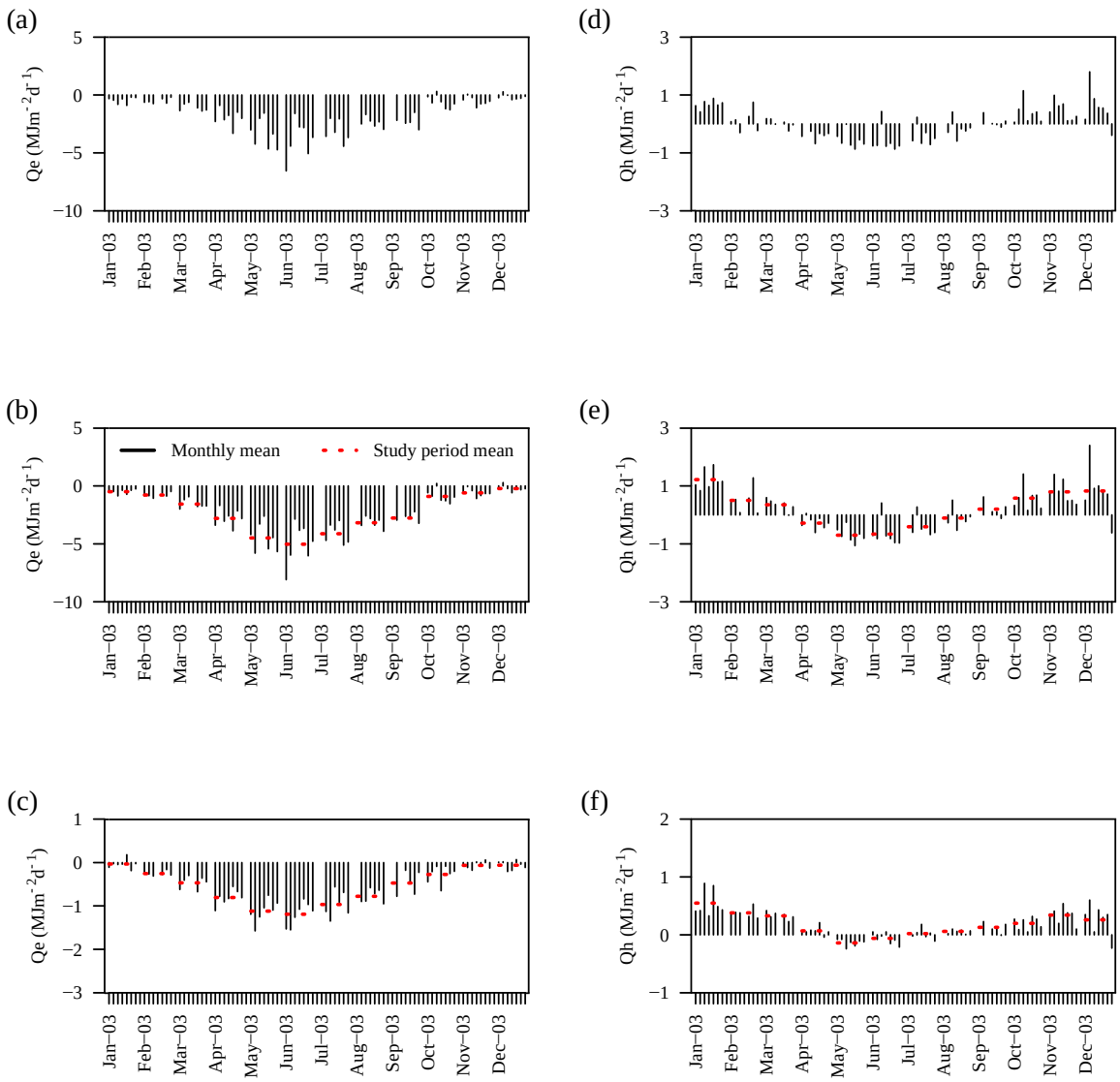

Figure 21. Monthly average daily total latent heat(a) moorland minus forest difference, (b) moorland, and (c) forest. Monthly average daily total sensible heat: (d) moorland minus forest difference, (e) moorland, and (f) forest

3.5 DISCUSSION

The seven year dataset presented here provides improved understanding of the effects of semi-natural riparian forest on riparian microclimate, energy exchange and stream temperature dynamics. Inter-annual variability in riparian microclimate, energy exchange and

stream temperature was typically greater in the moorland than the forest reach, especially during spring and summer. Marked inter-annual variability in moorland microclimate and energy exchange variables (cf. more stable forest environment) drove considerable inter-annual variability in the magnitude of temperature differences observed between reaches.

3.5.1 Effects of contrasting riparian landuse on inter-annual water temperature dynamics

Mean monthly water temperatures were up to 2.1 °C warmer in the moorland than the forest and thus the differences are comparable to those observed for conifer plantations and semi-natural forest in the UK (Webb and Crisp, 2006; Hannah *et al.*, 2008a; Brown *et al.*, 2010; Broadmeadow *et al.*, 2011). However, inter-comparisons between studies should be made with caution since the spatial configuration of the catchment in which a study is conducted may influence the magnitude of temperature differences observed (Gomi *et al.*, 2006). In the present study, the stream flowed through the moorland for ~ 2.5 km prior to flowing through ~ 1.5 km of forest. In pre- and post-harvesting approaches, the entire riparian corridor upstream of the monitoring site is forested. Thus in the present study, the relatively short distance the water flowed through the forest was likely to be associated with longitudinal advection of heat into the forested reach from the moorland, which may have influenced the magnitude of observed differences in water temperature between sites.

During spring and summer months, water temperature in the moorland varied considerably between years, compared to the relatively stable forest reach (Johnson and Jones, 2000). Consequently, the presence of riparian forest moderated inter-annual variability in water temperature and mitigated against the highest and lowest temperatures, which were observed only in the open, exposed moorland. The stream energy budgets calculated for the moorland and forest reaches during autumn and winter months suggest that water column temperatures

should have been cooler and more variable between years in the moorland. However, autumn and winter water temperatures in the moorland were actually warmer and as stable in the moorland reach. This is attributed to reach-scale contributions of heat from groundwater which enters the channel due to a valley constriction immediately upstream of the moorland site (Malcolm *et al.*, 2005b). These reach-scale contributions of groundwater are not thought to have been adequately characterised by the bed heat flux plate, which measured only point-scale heat exchanges between the streambed and water-column. The temperature of long-residence, well-mixed groundwater is generally stable and a few degrees above mean air temperature (Story *et al.*, 2003; O'Driscoll and DeWalle, 2006; Tague *et al.*, 2007; Herb and Stefan, 2011). For example, groundwater temperature in the upper levels of British aquifers is around 10- 11.5 °C year-round (Bloomfield *et al.*, 2013) compared to 10.5- 12.5 °C for mean annual air temperature (Garner *et al.*, 2013). Thus, groundwater discharge is thought to have provided inter-annual stability and warmer water temperatures in the moorland reach during the autumn and winter, an assertion partially supported by the available bed heat flux data and previous hydrological studies of the site (Malcolm *et al.*, 2004). In contrast, bed heat flux in the forested reach was an extremely minor driver of net energy. Groundwater inflows have confounded previous studies of the influence of riparian forest water temperatures (e.g. Story *et al.*, 2003; Moore *et al.*, 2005b; Leach and Moore, 2011). However this was only true for the autumn and winter temperatures in the present study where heat fluxes were generally small and as such bed heat flux could be proportionally large. Analysis of water temperatures was not confounded in spring and summer when energy exchange due to bed heat flux was estimated to be a very minor component of the energy budget in both reaches.

3.5.2 Drivers of inter-annual net energy exchange processes

In both the moorland and forest reaches, the stream energy budget was driven primarily by net radiation. This is consistent with previous studies (Brown, 1969; Webb and Zhang, 1997, 1999; Evans *et al.*, 1998; Hannah *et al.*, 2004, 2008a; Moore *et al.*, 2005; Leach and Moore, 2010, 2014; MacDonald *et al.*, 2014b). Latent heat was an important driver year-round, while sensible heat was important in autumn and winter months (Webb and Zhang, 1997; 1999; Hannah *et al.*, 2004; Hannah *et al.*, 2008a). Bed heat flux was an important energy source in the moorland reach in autumn and winter (see Discussion of *Effects of contrasting riparian landuse on inter-annual water temperature dynamics*).

The most extreme net energy gains and losses occurred in the moorland reach, whereas net energy exchanges in the forest were more stable between years. The moorland reach was not sheltered from variable meteorological conditions which varied substantially between years, most notably: (1) wind speed, which drove latent and sensible heat exchange (Hannah *et al.*, 2008a) and (2) cloud cover conditions, which drove net radiative exchange (Johnson and Jones; 2000, Hannah *et al.*, 2004). In contrast, the forest canopy during spring and summer and (to a lesser extent) tree trunks and crowns in autumn and winter shaded and sheltered the forest reach (Malcolm *et al.*, 2004) from prevailing wind and cloud cover conditions (Guenther *et al.*, 2012). Sheltering produced a more consistent microclimate, which produced more consistent turbulent and radiative heat flux between years.

The moorland reach typically gained more energy than the forest reach in spring and summer and lost more energy in autumn and winter (Hannah *et al.*, 2008a). However when atypical, low net energy gain occurred in the moorland reach due to: (1) high latent heat loss as a consequence of high wind speed or (2) low net radiation due to overcast daytime skies or clear nights (Johnson and Jones, 2000); the forested reach could experience greater energy

gain due to its greater relative stability. Similarly, when atypical low net energy loss occurred in the moorland during autumn and winter months due to high sensible heat gain due to low wind speed (Webb and Zhang, 1997; Hannah *et al.*, 2004; Hannah *et al.*, 2008a) or low net radiation loss due to clear sky days or cloudy nights, the forest reach lost relatively more energy.

3.6 SUMMARY

This study represents an important addition to the existing literature on the effects of riparian woodland on stream temperature. The data offers a unique long-term perspective on stream temperature, riparian microclimate and energy exchanges in semi-natural forest and moorland (no trees) reaches that has not been seen previously. The results provide new insights as to the potential of riparian vegetation to mitigate against stream water temperature extremes under present and future climates and, most importantly, the conditions under which smaller or larger forest effect sizes may be expected.

Water temperature, wind speed and energy exchange dynamics were typically more stable between years in the forest reach and more variable in the moorland (*Hypothesis 1*). Thus, the presence of riparian forest was associated with mitigating thermal and net energy flux variability. High inter-annual variability in the moorland reach caused considerable inter-annual variability in between-reach differences in water temperature, wind speed and net energy exchange (*Hypothesis 2*). Enhanced variability in the moorland reach was the consequence of riparian microclimate being strongly coupled to variable prevailing meteorological conditions, especially wind and cloud cover (driving radiative and turbulent heat exchanges, respectively). In contrast, the presence of riparian vegetation in the forest provided shelter from variable wind and cloud cover conditions and thus the microclimate and energy exchange processes were more stable between years (*Hypothesis 3*).

Planting of riparian vegetation is advocated as an effective way to mitigate stream water thermal extremes (Cole and Newton, 2000; Forestry Commission, 2011). Under present UK climate variability, and in reaches where water column-streambed exchanges are minor, riparian forest downstream of open moorland provides an environment for freshwater species that is typically cooler than moorland in spring and summer, when thermal extremes occur. However, this is not the case when: (1) net radiation gain is low in the moorland reach due to overcast skies during the day and/or clear skies at night; or (2) persistent strong winds enhance latent heat loss from moorland reaches; and consequently water temperatures are low in both reaches. Consequently, the effectiveness of riparian planting could vary depending on future climatological conditions associated with environmental change.

Future climate change is anticipated to include increased long wave radiation flux from the atmosphere (Ramanathan, 1981; Wild *et al.*, 1997; Andrews *et al.*, 2009); the effect of this on the energy balance, and consequently water temperature, would be similar to conditions observed at present under overcast skies. Future climate is also anticipated to be characterised by reduced summer rainfall. In catchments such as the Girnock Burn, where groundwater residence times and active storage contributions to streamflow are low, summer discharges are expected to decline (Cappel *et al.*, 2012) with consequences for maximum temperatures. To quantify the effects of riparian forest under climate change would require reliable information on the likely magnitude and variability of climate and hydrological processes in the future. Hydrological models coupled with process based stream temperature models (e.g. Moore *et al.*, 2005b; Caissie *et al.*, 2007; Leach & Moore, 2011) driven by downscaled probabilistic climate change projections offer considerable potential for such research.

CHAPTER FOUR: WHAT CAUSES COOLING WATER TEMPERATURE GRADIENTS IN FORESTED STREAM REACHES?

4.1 ABSTRACT

Previous studies have suggested that shading by riparian vegetation may reduce maximum water temperature and provide refugia for temperature sensitive aquatic organisms. Longitudinal cooling gradients have been observed during the daytime for stream reaches shaded by coniferous trees downstream of clear cuts, or deciduous woodland downstream of open moorland. However, little is known about the energy exchange processes that drive such gradients, especially in semi-natural woodland contexts, and in the absence of potentially confounding cool groundwater inflows. To address this gap, this study quantified and modelled variability in stream temperature and heat fluxes along an upland reach of the Girnock Burn (a tributary of the Aberdeenshire Dee, Scotland) where riparian landuse transitions from open moorland to semi-natural forest. Observations were made along a 1050 m reach using a spatially-distributed network of ten water temperature micro-loggers, three automatic weather stations and > 200 hemispherical photographs, which were used to estimate incoming solar radiation. These data parameterised a high-resolution energy flux model, incorporating flow-routing, which predicted spatio-temporal variability in stream temperature. Variability in stream temperature was controlled largely by energy fluxes at the water column-atmosphere interface. Predominantly net energy gains occurred along the reach during daylight hours, and heat exchange across the bed-water column interface accounted for < 1% of the net energy budget. For periods when daytime net radiation gains were high (under clear skies), differences between water temperature observations decreased in the streamwise direction; a maximum difference of 2.5 °C was observed between the upstream reach boundary and 1050 m downstream. Furthermore, daily maximum water temperature at 1050 m downstream was ≤ 1 °C cooler than at the upstream reach boundary and lagged the occurrence of daily maximum water temperature upstream by > 1 hour. Temperature

gradients were not generated by cooling of stream water, but rather by a combination of reduced rates of heating in the woodland reach and advection of cooler (overnight and early morning) water from the upstream moorland catchment. Longitudinal thermal gradients were indistinct at night and on days when net radiation gains were low (under over-cast skies), thus when changes in net energy gains or losses did not vary significantly in space and time, and heat advected into the reach was reasonably consistent. The findings of the study and the modelling approach employed are useful tools for assessing optimal planting strategies for mitigating against ecologically damaging stream temperature maxima.

4.2 INTRODUCTION

River temperature dynamics are of increasing interest to the scientific community, environment managers and regulators (Hannah *et al.*, 2008a), particularly given the contexts of a changing climate (e.g. van Vliet *et al.*, 2011, 2013a; Beechie *et al.*, 2013) and associated profound consequences of high water temperature for aquatic ecosystems (Poole and Berman, 2001; Caissie, 2006; Webb *et al.*, 2008; Wilby *et al.*, 2010; Leach *et al.*, 2012). Numerous studies have demonstrated that the presence of riparian woodland can decrease diurnal variability, mean and maximum stream temperatures (e.g. Malcolm *et al.*, 2008; Brown *et al.*, 2010; Imholt *et al.*, 2010, 2013b; Garner *et al.*, 2014), or conversely that forest removal results in temperature increases (e.g. Macdonald *et al.*, 2003; Danehy *et al.*, 2005; Moore *et al.*, 2005b; Gomi *et al.*, 2006). Consequently, there is substantial interest from researchers and stream managers in the potential of riparian vegetation cover to mitigate against climate change impacts (e.g. The River Dee Trust; Upper Dee Planting Scheme, 2011), especially in relation to thermal maxima.

Several studies have documented daytime cooling gradients (decreases in temperature in a streamwise direction measured at a single point in time) beneath forest canopies downstream

of open (no trees) landuse, although the magnitude of reported cooling effects varied between studies (e.g. Brown 1971; Rutherford *et al.*, 2004; McGurk *et al.*, 1988; Keith *et al.*, 1998; Torgersen *et al.*, 1999; Story *et al.*, 2003). For example, McGurck (1989), Keith *et al.* (1998) and Story *et al.* (2003) observed gradients of between 4.0 °C km^{-1} and 9.2 °C km^{-1}. However, little is known about the energy exchange processes that generate this apparent cooling effect (Story *et al.*, 2003). Studies conducted by Brown (1971) and Story *et al.* (2003) observed net energy gains to the water column measured predominantly across the air-water column interface. The presence of net energy gain conditions lead both Brown (1971) and Story *et al.* (2003) to attribute the generation of cooling gradients to reach-scale groundwater inputs that were underestimated by point-scale energy exchange measurements (e.g. Brown, 1971; Story *et al.*, 2003; Moore *et al.*, 2005b; Leach and Moore, 2011; Garner *et al.* 2014). Cooling gradients have also been observed in forested reaches downstream of open landuse in which groundwater inputs and hyporheic exchange are known to be minimal (e.g. Malcolm *et al.*, 2004; Imholt *et al.*, 2010; Imholt *et al.*, 2013b). However, a conceptualisation of the processes driving observed patterns of cooling in forested reaches without groundwater inputs is lacking; this is essential if stream managers are to plan future riparian planting strategies that maximise benefits at minimal cost.

This study aims to quantify and model spatio-temporal variability in stream water temperature and heat fluxes for an upland reach of the Girnock Burn (a tributary of the Aberdeenshire Dee, Scotland) where riparian landuse transitions from open moorland to semi-natural forest and stream temperature variability is driven largely by fluxes at the water column-atmosphere interface (i.e. not confounded by groundwater-surface water interactions). The specific objectives are:

1. To quantify the magnitude of longitudinal water temperature gradients within the reach and identify the meteorological conditions under which the strongest and weakest gradients instantaneous longitudinal gradients occur.
2. To explore the effect of changing riparian vegetation density on heat fluxes within the reach.
3. To understand, using a simple flow routing model in conjunction with a Lagrangian water temperature model, how water temperature changes as it travels through the forested reach and attribute this to underlying processes.

4.3 STUDY AREA

A 1050 m study reach with no tributary inputs was established within Glen Girnock, an upland basin that drains into the Aberdeenshire Dee, northeast Scotland (see Chapter 3 for a full description of the catchment). Upstream of the reach (~ 24 km^2), landuse is dominated by heather (*Calluna*) moorland. Within the reach landuse transitions from open moorland to semi-natural forest composed of birch (*Betula*), Scots pine (*Pinus*), alder (*Alnus*) and willow (*Salix*) (Imholt *et al.*, 2013b).

Previous work in the catchment suggests highly heterogeneous but spatially constrained groundwater discharge, with no significant groundwater inputs within the study reach (Malcolm *et al.*, 2005b). Hyporheic conditions within the study reach are characterised by very slight down-welling surface water (Malcolm *et al.*, 2005b). Thus contributions to streamflow are derived predominantly from surface water, and heat exchange within the reach was anticipated to be dominated predominantly by fluxes at the water column-atmosphere interface. The study reach flows in a mainly northerly direction and so experiences no significant changes in aspect that may influence solar radiation receipt along the reach (Figure

22). Maximum and minimum elevations of the reach are respectively 280 m and 255 m (Figure 22). Mean river width was 9.5 m during the study period.

4.4 METHODS

4.4.1 Experimental design

Ten water temperature loggers were deployed throughout a 1050 m reach of the Girnock where riparian landuse transitions from open moorland to semi-natural forest (Figure 22), and in which previous studies have identified measurable changes in stream temperature (e.g. Malcolm *et al.*, 2004; Malcolm *et al.*, 2008; Imholt *et al.*, 2010; Imholt *et al.*, 2013b). Three automatic weather stations (AWSs) were deployed along the reach to estimate spatio-temporal variability in energy fluxes: one in open moorland (AWS_{open}) and two in semi-natural forest (AWS_{FUS} followed by AWS_{FDS}). Instruments mounted on AWSs are described in Hannah *et al.* (2008) and in Table. The number and location of AWSs was limited by logistical and financial constraints. However, in excess of 200 hemispherical photographs were taken at 5 m intervals along the reach so that solar radiation measured at the open site AWS could be re-scaled to estimate radiative fluxes at a high spatial resolution. For locations where hemispherical images were taken, turbulent (i.e. latent and sensible heat) and bed heat fluxes were estimated by linearly interpolating between values at the two nearest AWSs. High resolution information on energy fluxes and stream temperature was combined with a flow-routing model to provide process-based understanding of spatio-temporal variability in stream temperature.

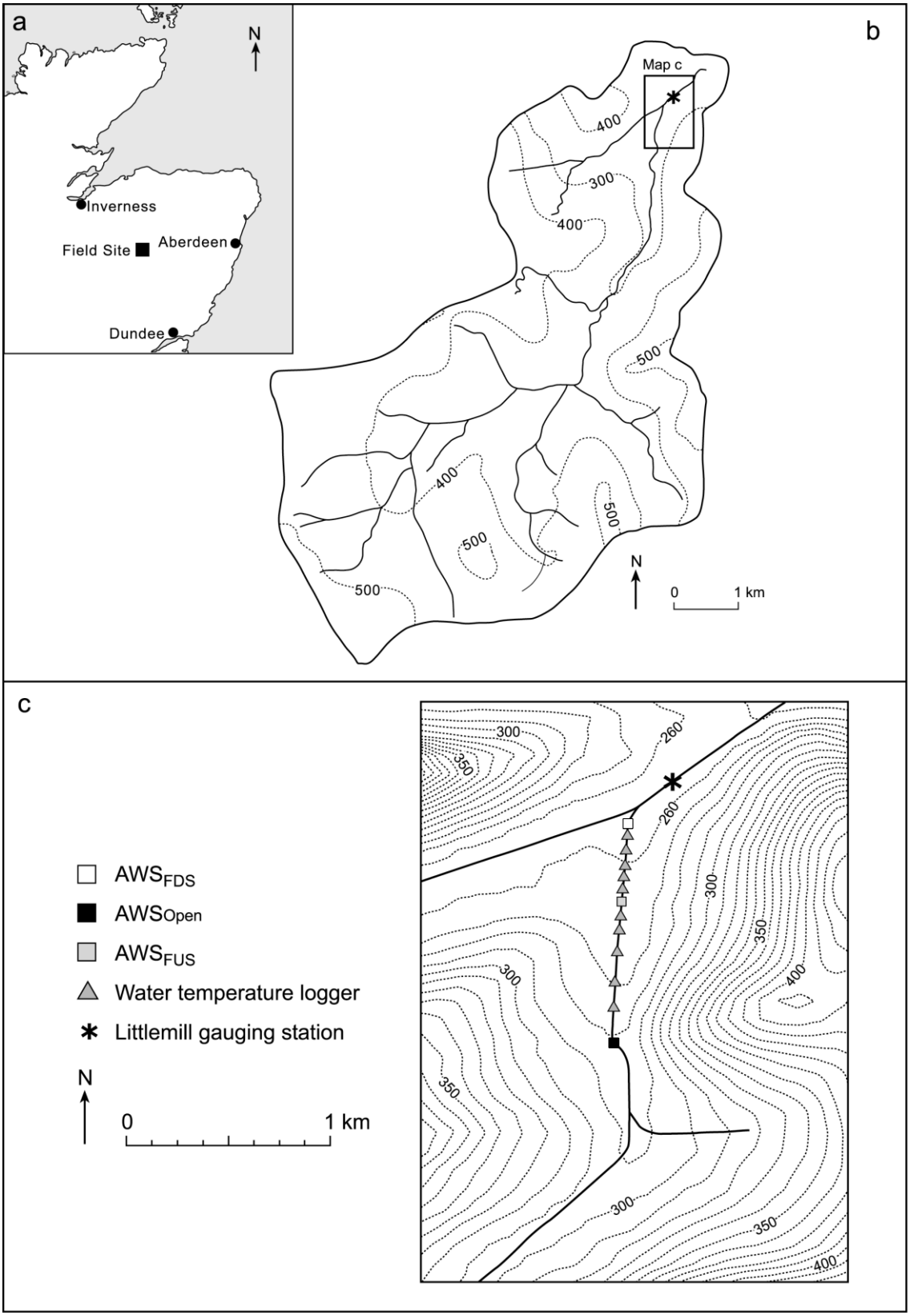

Figure 22. (a) Location map of the Girnock, (b) Girnock catchment, (c) locations of field data collection

4.4.2 Data Collection

Field data were collected between October 2011 and July 2013. A seven-day period comprising of 1 to 7 July 2013 was chosen to meet the aims of the present study because high air temperatures (i.e. > average air temperatures for this week in the preceding ten years) and extremely low flows (i.e. < average minimum flows for this week in the preceding ten years) occurred (Figure 23). High energy gains occurred on six days and relatively low energy gains occurred on one day. These data allowed assessment of: (1) potential mitigation of high temperatures by semi-natural forest under a 'worst case scenario' of high energy gains and low flows; and (2) the influence of contrasting prevailing meteorological conditions on longitudinal water temperature patterns.

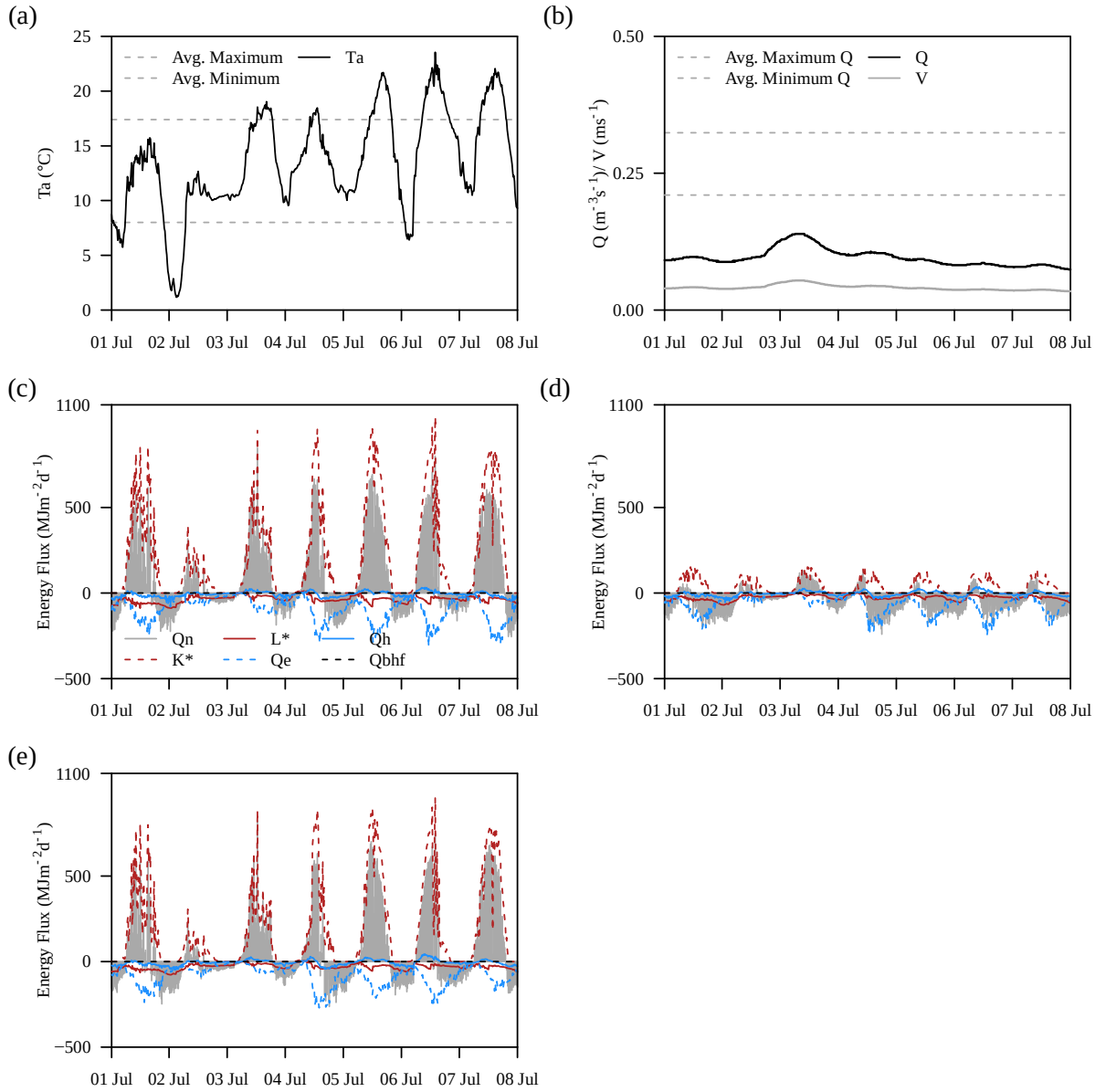

Figure 23. Study period (a) air temperature at AWS_{Open}, (b) discharge and velocity at Littlemill and energy fluxes at (c) AWS_{open}, (d) AWS_{FDS} and (e) AWS_{FUS}. Averages represent values for DOYs 183 to 189 in the 10 years preceding 2013

Stream temperature measurements

Stream temperature measurements were made at 15-minute intervals across a spatially-distributed network of ten water temperature TinyTag Aquatic 2 micro-loggers and three Campbell 107 thermistors connected to AWSs at 0 (AWS_{Open}), 190, 315, 460, 565, 630, 685

(AWS_{FUS}), 760, 815, 865, 940 1015 and 1050 (AWS_{FDS}) m downstream of the upstream reach boundary (Figure 22). The sensors were cross-calibrated (Hannah *et al.*, 2009) prior to installation and showed good agreement (i.e. < +/- 0.1 °C). Within the reach, sensors were housed in white plastic PVC tubes to shield them from direct solar radiation.

Hydrology and stream geometry

Flow accretion surveys (following the velocity-area method) were conducted at 200 m intervals along the reach to assess net flow gains and losses between the channel and subsurface (Leach and Moore 2011). No significant gains or losses were observed, with differences between gaugings consistently within +/- 10% of each other (i.e. within velocity – area measurement uncertainty; Leach and Moore, 2011). These gaugings upheld the assumption that groundwater gains and losses along the reach were negligible.

A Scottish Environmental Protection Agency (SEPA) gauging station at Littlemill (Figure 22) provided discharge data at 15-minute intervals. The discharge- mean velocity function for Littlemill presented in Tetzlaff *et al.*, (2005) was used to calculate water velocity and thus drive the flow-routing model. Good correspondence was observed between velocities (and discharge) measured during flow accretion surveys and those calculated from discharge (measured) at Littlemill. Stream surface width was measured at 50 m intervals along the reach.

Micrometeorological measurements

Three automatic weather stations (AWSs) were installed within the reach (Figure 22). The instruments deployed on AWSs are detailed in Table 3 (see Chapter 3) with the addition of a Skye SP1110 pyranometer on each that measured incoming solar radiation (Wm^{-2}). All sensors were cross-calibrated prior to installation and correction factors applied, if required.

Hydrometeorological variables measured included air temperature, relative humidity, wind speed, net shortwave radiation and bed heat flux. The sensors were sampled at 10-second intervals, with averages logged every 15-minutes.

Hemispherical images

Hemispherical images were taken at 5 m intervals along the stream centreline using a Canon EOS-10D 6.3 megapixel digital camera with Sigma 8 mm fisheye lens. Prior to taking each image the camera was orientated to north and levelled ~20 cm above the stream surface (Leach and Moore, 2010).

4.4.3 Estimation of stream energy balance components

Net energy

Net energy (Wm^{-2}) available to heat or cool the water column was calculated using Equation 9 (see Chapter 3). Heat from fluid friction was assumed to be negligible (see Chapter 3; Garner *et al.*, 2014) and was therefore omitted. Herein, energy fluxes are considered to be positive (negative) when directed toward (away from) the water column.

Net radiation

A deterministic radiation model developed by Moore *et al.* (2005) and evaluated by Leach and Moore (201) was used to compute net radiation (Q^*) at the location of each hemispherical image. At each location, net radiation was calculated as:

$$Q^* = K^* + L^* \quad \text{(Equation 15)}$$

Where K^* is net shortwave radiation (Equation 16) and L^* is net longwave radiation (Equation 17.

$$K^* = (1 - \alpha)[D(t)g(t) + s(t)f_v] \quad \text{(Equation 16)}$$

$$L^* = [f_v\varepsilon_a + (1 - f_v)\varepsilon_{vt}]\sigma(T_a + 273.2)^4 - \varepsilon_w\sigma(T_w + 273.2)^4 \quad \text{(Equation 17)}$$

Where α is the stream albedo, *D(t)* is the direct component of incident solar radiation at time t (Wm^{-2}), *g(t)* is the canopy gap fraction at the position of the sun in the sky at time *t*, *S(t)* is the diffuse component of solar radiation, f_v is the sky view factor, ε_a, ε_{vt} and ε_w are respectively the emissivity of the temperatures of the air, vegetation and water (°C), σ is the Stefan-Boltzmann constant (5.67 x 10^{-8} Wm^{-2} K^{-4}), and T_a and T_w are respectively air and water temperature (°C).

Values for atmospheric emissivity were calculated for clear-sky day and night conditions using the equation presented by Prata, 1996:

$$\varepsilon_0 = 1 - (1 + w)\exp\left[-(1.2 + 3.0)^{0.5}\right] \quad \text{(Equation 18)}$$

where ε_0 is emissivity for clear sky conditions and *w* is the perceptible water content of the atmosphere (cm) which is estimated as:

$$w = 465\left[\frac{\varepsilon_a}{T_a + 273.2}\right] \quad \text{(Equation 19)}$$

ε_0 was subsequently adjusted for cloud cover using the procedure demonstrated by Leach and Moore (2010), which relates the cloud fraction, *n*, to to the ratio of incoming solar radiation ($K\downarrow$) to the maximum incoming solar radiation ($K\downarrow_{max}$; equation) under clear skies.

$$K\downarrow_{max} = I_0\psi^{\left(\frac{P}{P_0}\right)}\cos\theta \quad \text{(Equation 20)}$$

where I_0 is the solar constant (1376 Wm^{-2}), Ψ is the transmisivity of clear skies (0.75), *P* is atmospheric pressure, P_0 is mean atmospheric pressure at sea level *(*101.3 kPa) and θ is the solar zenith angle. The transmisivity of non-clear (clouded) skies (ε_w) was calculated as:

$$\varepsilon_a = (1 + \kappa n)\varepsilon_0 \qquad \text{(Equation 21)}$$

where κ was a constant (0.26) representative of cloud the mean value for altocumulus, stratocumulus, stratus and cumulus cloud types, n was assumed to be 1.0 for $K\downarrow$: $K\downarrow_{max} \leq 0.2$ and to decrease linearly between 1.0 and 0.0 for $K\downarrow$: $K\downarrow_{max}$ between 0.2 and 1.0. Equation 21 could only be calculated for daylight hours; nocturnal values were calculated as the mean of n before and after the night of interest.

The emissivity and albedo were taken, respectively, to be 0.95 and 0.05 for water, and 0.97 and 0.03 for vegetation (Moore *et al.*, 2005b).

Gap fractions (g_*) were computed as a function of solar zenith angle (θ) and solar azimuth (ψ), $g_*(\theta\ \psi)$, which were derived from analysis of the hemispherical images with Gap Light Analyser software (Frazer *et al.*, 1999). Using equations in Iqbal (1983), the solar zenith and azimuth angles were computed as a function of time, *t*, so that the canopy gap at the location of the sun's disk could be derived from $g^*(\theta\ \psi)$ as a function of time, $g(t)$. View factor was computed as:

$$f_v = \frac{1}{\pi}\int_0^{2\pi}\int_0^{\pi/2} g^*(\theta,\psi)\cos\theta\sin\theta * d\theta * d\psi$$

(Equation 22)

The double integral was approximated by summation using an interval of 5° for both solar zenith and azimuth angles (after Leach and Moore, 2010). Solar radiation measurements made at AWS_{open} were used as input to the radiation models.

Latent and sensible heat fluxes

Latent heat was estimated using a Penman-style equation (after Webb and Zhang, 1997) to compute heat lost by evaporation or gain by condensation. Sensible heat was calculated as a function of Q_e and Bowen ratio (see Chapter 3, section *3.3.2 Estimation of energy balance components*).

4.4.4 Modelling approaches

Statistical models

Spatial (and temporal) variability in canopy density (and net energy flux) was extremely high. Therefore, generalised additive models (GAMs; Hastie and Tibshirani, 1986) were used to provide continuous smoothed estimates of the variability in each dataset so that broad patterns in space and time could be identified. GAMs were fitted in the MGCV package (Wood, 2006; version 1.7-13) for R (R Group for Statistical Computing; version 3.0.2). Degrees of freedom were estimated by MGCV but were limited (gamma= 1.4) to prevent over-fitting (Wood, 2006).

The GAM fitted to canopy density provided a continuous smoothed estimate of the spatial variability in density from discrete (5 m interval) point measurements determined from Gap Light Analyser outputs. Canopy density was calculated as the percentage of pixels representative of vegetation in each hemispherical image; this percentage was modelled as a smoothed function of distance downstream (i.e. from AWS_{Open}).

The second GAM provided a continuous smoothed estimate of the spatio-temporal variability in net energy flux estimated at 5 m intervals from the sum of scaled radiative flux (see Section 4.4.3), and turbulent and bed heat fluxes determined by linear interpolation between values calculated at the two nearest AWSs. Specifically, net energy was modelled as smoothed

functions of: (i) time of day, (ii) day of year, and (iii) distance downstream. The inclusion of three smoothed terms was validated by fitting models using each combination of the three terms and comparing using AIC (Akaike information criterion; Burnham and Anderson, 2002) score (a measure of model fit that balances fit and parsimony) between models.

Flow routing model

A flow routing model was used to predict the time taken by water parcels to travel through the reach. The model was based on a discharge- mean velocity function (Tetzlaff et al., 2005) and predicted the distance travelled by water parcels at 15-minute intervals. In combination with the dataset of spatio-temporally distributed water temperature observations, the model also identified the temperature of distinct water volumes at 15-minute intervals.

The model released water (*i*) from AWS_{open} at the start of every hour on each day of the study period. For each parcel of water, the distance travelled in 15 minutes from its initial location (*x*) to the next location (*x+1*) was calculated as the product of the length of the timestep (Δt, i.e. 900 seconds) and the average velocity at times *t* and t+Δt. The temperature of the parcel at location *x+1* and time t+Δt was determined by linear interpolation (to the nearest 1 m) between measurements at 15 minute intervals and between temperature loggers, respectively.

Lagrangian water temperature model

The Lagrangian modelling approach (after Rutherford *et al.*, 2004; Leach and Moore, 2011; MacDonald *et al.*, 2014a) divided the reach into a series of segments (s) bounded by nodes (indexed by *i*). For each time step, Δ_{900} (s), a water parcel (indexed by *j*) was released from the upstream boundary; its initial temperature was an observed value. As the water parcel travelled downstream from *i* towards *i*+1 the model computed the heat exchange and the net

change in stream temperature over each segment as the mean of net energy flux within the segment at time *t* and time *t+Δt*:

$$\frac{dT_w}{dx} = \frac{[[w_{(s)}(K^*_{(s,t)}+L^*_{(s,t)}+Q_{h(s,t)}+Q_{e\,(s,t)}+Q_{bhf\,(s,t)})+w_{(s)}(K^*_{(s,t+\Delta t)}+L^*_{(s,t+\Delta t)}+Q_{h(s,t+\Delta t)}+Q_{e\,(s,t+\Delta t)}+Q_{bhf\,(s,t+\Delta t)})]/2]}{C\,[(F_{(s,t)}+F_{(s,t+\Delta t)})/2]}$$

(Equation 23)

Where $W_{(s)}$ is the mean width of the stream surface (m), $K^*_{(s,t/\ t+\Delta t)}$, $L^*_{(s,t/\ t+\Delta t)}$, $Q_{e\,(s,t/\ t+\Delta t)}$, $Q_{h\,(s,t/\ t+\Delta t)}$ and $Q_{bhf\,(s,t/\ t+\Delta t)}$ are the mean net shortwave, net longwave, latent, sensible and bed heat fluxes at within segment *s* at time *t* or *t+Δt* (Wm^{-2}). C is the specific heat capacity of water (4.18×10^6 Jm^{-3} $°C^{-1}$) and $F_{(s,t/\ t+\Delta t)}$ is the discharge (m^3s^{-1}; scaled by catchment area) within segment *s* at time *t* or *t+Δt*.

Water temperature was calculated at 1 m intervals along the reach by integration of Equation 23 in the deSolve package (Soetaert *et al*., 2010) for R (Version 3.0.2, R Group for Statistical Computing, 2013).

Unsmoothed energy flux data was used for numerical modelling. Incident solar radiation was modelled at 5 m intervals (see section 4.4.3, *Net radiation*); values at 1 m intervals were interpolated linearly. Emitted longwave radiation, latent and sensible heat fluxes were dependent on water temperature. Therefore, these fluxes were calculated at each time step within Equation 23 using values for air temperature, humidity and wind speed calculated by linear interpolation between the two AWSs nearest to the upstream boundary of the segment.

4.5 RESULTS

Results are presented in four sections: (1) prevailing weather conditions; (2) observed spatio-temporal water temperature patterns; (3) riparian canopy density and net energy flux patterns, and (4) modelled spatio-temporal water temperature patterns.

4.5.1 Prevailing hydrological and weather conditions

Stream discharge measured at Littlemill was very low, reasonably stable, and exhibited no sudden changes throughout the study period (Figure 23). The 1st, 3rd, 4th, 5th, 6th and 7th days of the study period were characterised by high net energy gains to the water column during daylight hours, driven by clear-skies and consequently high solar radiation receipt (Figure 23). On the 2nd day, net energy gains were markedly lower, due to overcast skies and associated low solar radiation receipt (Figure 23). This data window permitted consideration of the influence of contrasting energy gain conditions (i.e. low versus high net energy gain) on the spatio-temporal variability of water temperature and energy flux.

4.5.2 Observed spatio-temporal water temperature patterns

Minimum daily water temperature was the same at both AWS_{Open} and AWS_{FDS} (9.8 °C) but maximum temperature was higher at AWS_{Open} than at $AWS_{FDS,}$ with observed temperatures of 23.0 °C and 22.0 °C (both occurring on the 6th day), respectively. Minimum temperatures occurred synchronously across all locations. Maximum temperatures at AWS_{FDS} lagged those at AWS_{Open} by between 1 hour and 1.75 hours on all days except the 2nd (which was overcast, and the water column received lower solar receipt), when maximum temperatures occurred synchronously across all locations.

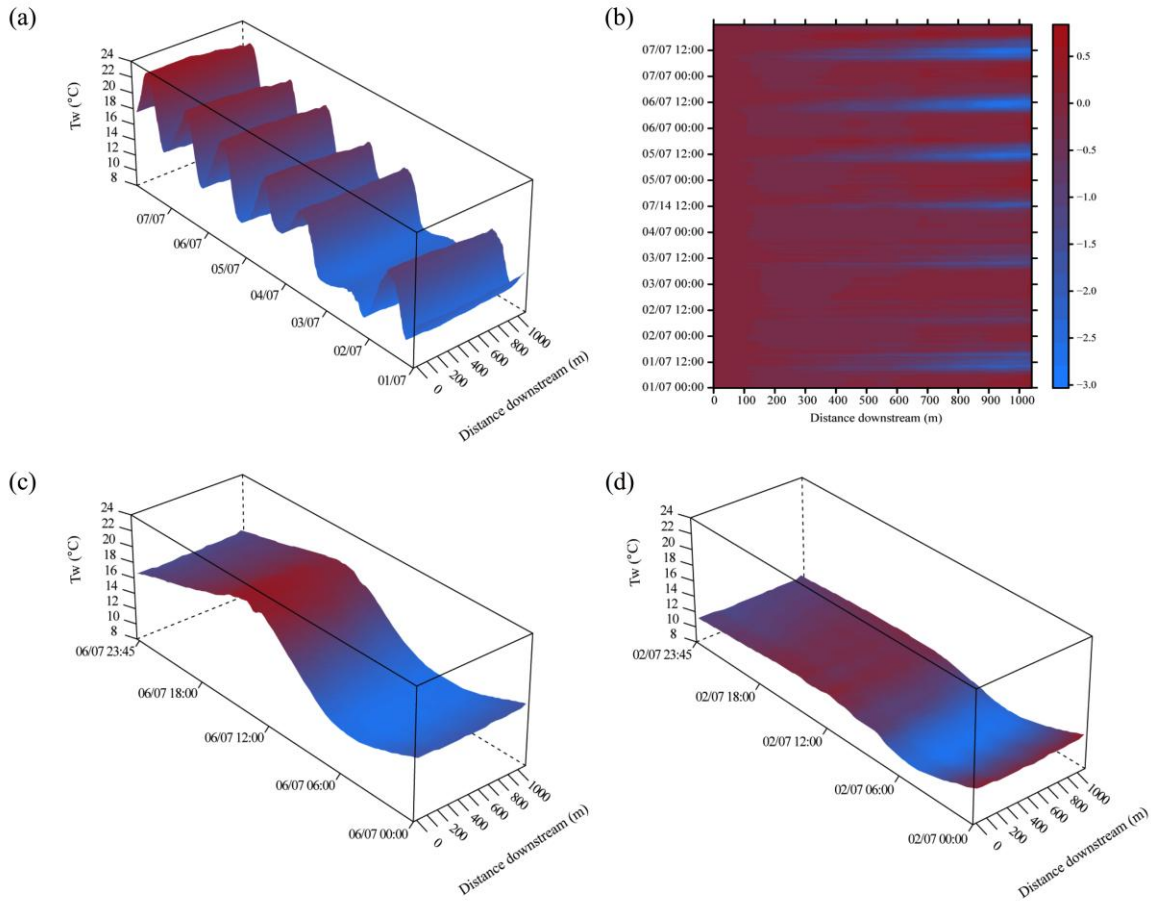

Figure 24. Spatial patterns in instantaneous water temperature measurements, (a) entire study period (b) , differences between AWS_{open} and each monitoring location, (c) 2nd day and (d) 6th day

Longitudinal gradients in instantaneous water temperature measurements (at a particular point in time across the entire reach) were observed during daylight hours on each day of the study period. Instantaneous water temperature was greatest at AWS_{Open} and decreased downstream towards AWS_{FDS}. Large daily temperature amplitudes (Figure 24a) and distinct downstream gradients of > 1 °C (Figure 24b) were observed on the 1st, 3rd, 4th, 5th, 6th and 7th days between 11:00 and 16:00.

The greatest instantaneous temperature gradient was 2.5 °C in magnitude, observed on the 6th day at 12:00 (Figures 24b and 24d). On the 2nd day, the diurnal water temperature cycle was greatly reduced and longitudinal water temperature gradients were small (Figures 24c and 24d) with the greatest gradient (0.6 °C) observed at 08:00, and smaller gradients (< 0.2 °C i.e. below measurement accuracy of the sensors) observed between 11:00 and 15:00.

Overnight, longitudinal gradients were reversed (*cf.* daylight hours); instantaneous water temperature was lowest at AWS_{Open} and increased downstream towards AWS_{FDS} (Figure 24b). However, the difference in temperature between these two sites was consistently < 0.5 °C in magnitude.

4.5.3 Riparian canopy density and energy flux patterns

Between AWS_{Open} (0m) and 400 m patchy forest cover (e.g. Figures 25a and 25b) generated canopy density ranging from 0.0 % to 70.3 % (Figure 26a). Between 400 m and 1050 m (AWS_{FDS}) continuous riparian forest of variable density (e.g. Figures 25c and 25d) produced typically lower, but more variable gap fractions ranging from 22.5 to 92 % (Figure 26a). The forest canopy was densest between 400 m and 800 m and decreased in density between 800 m and 1050 Figure 26a).

The spatial variability in net energy corresponded broadly inversely to canopy density. Net energy gains during daylight hours decreased gradually from AWS_{Open} to 400 m before declining sharply between 400 m and 800 m. Between 800 m and 1050 m (AWS_{FDS}), net energy flux increased markedly. Strong diurnal signals and distinct spatial patterns were observed during daylight hours on the 1st, 3rd, 4th, 5th, 6th and 7th days, with spatial patterns especially clear around solar noon (Figure 26b). On the 2nd day, the spatial and temporal variability of net energy fluxes was much subdued. Around solar noon on the 2nd day, net

energy flux was slightly lower at 800 m but differences within the reach were otherwise indistinguishable (Figure 26c), driven by smaller differences (relative to clear sky conditions) in solar radiation gain between open and forested sites (Figure 23c to 23e).

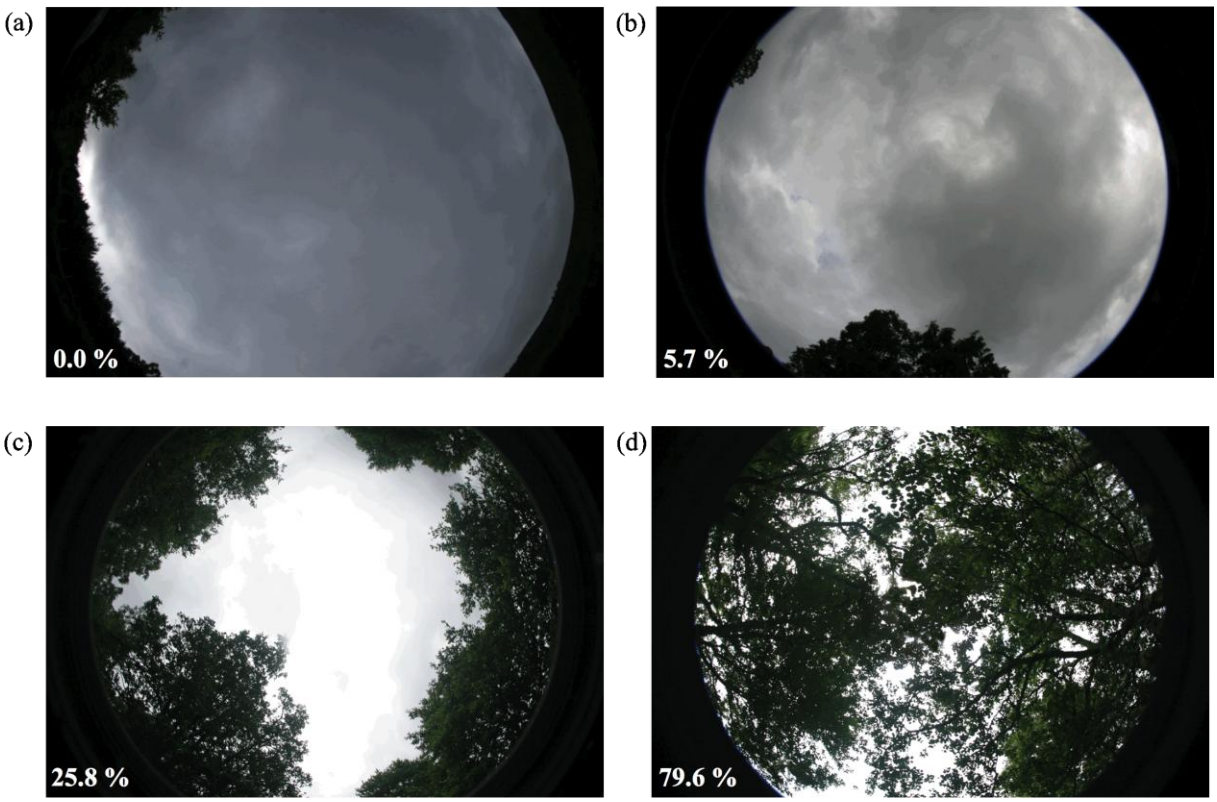

Figure 25. Hemispherical photographs representative of (a) clear sky view, (b) low density, patchy riparian forest (c) low density, continuous riparian forest, (d) high density, continuous riparian forest.

Nocturnally, small and temporally consistent differences in net energy occurred within the reach (Figure 26). Net energy losses were greatest at AWS_{Open} and declined up until 400 m before stabilising and increasing again between 800 m and 1050 m, yet spatial variability was reduced drastically in comparison to daytime conditions on the 1st, and 3rd through 7th days.

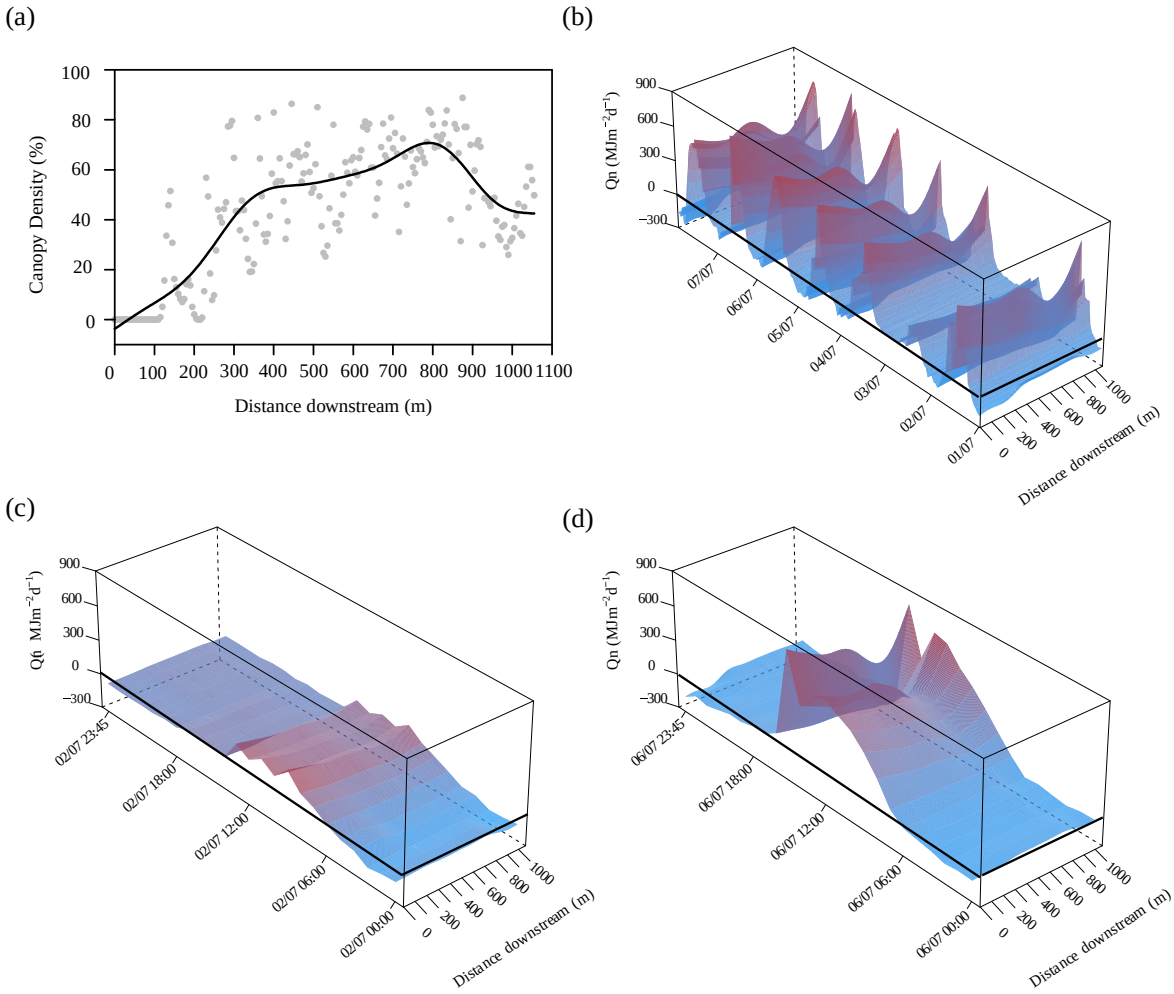

Figure 26. Spatial patterns within the reach in (a) canopy density and net energy flux (b) throughout the study period (c) n day two (d) on day six.

4.5.4 Modelled spatio-temporal water temperature patterns

The flow routing model was evaluated by predicting the change in temperature of water parcels (using the water temperature model). Observed temperature changes over the reach were compared with those predicted for water leaving AWS_{open} (0 m, the upstream boundary of the reach) at 06:00, 07:00, 08:00 and 09:00 (i.e. when the greatest temperature increases were observed). Predictions of downstream water temperature change were typically good (Figure 27).

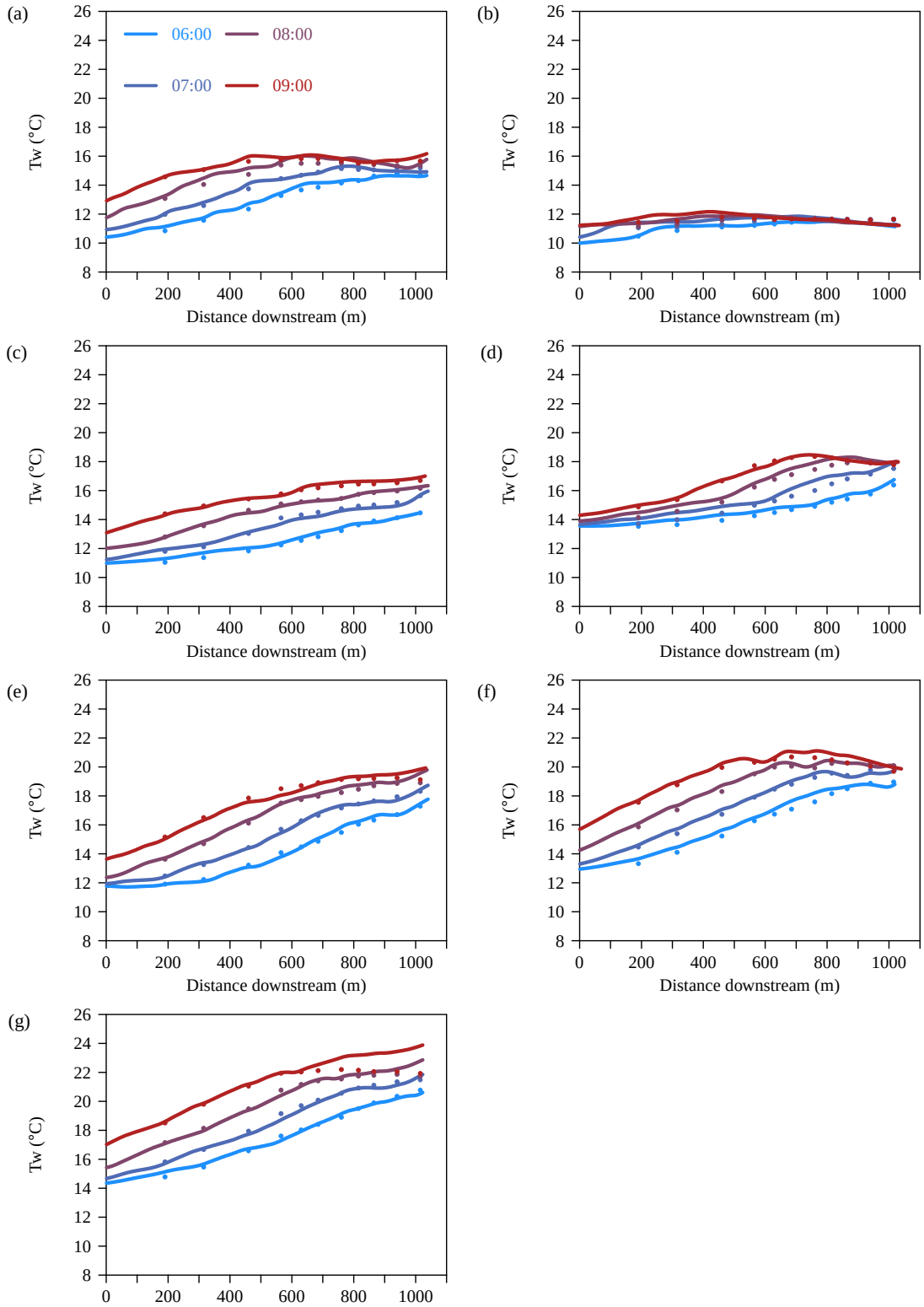

Figure 27. Modelled (solid lines) and observed (points) water temperature of water parcels released at 06:00, 07:00, 08:00 and 09:00 on (a) day one, (b) day two, (c) day three, (d) day four, (e) day five, (f) day six, (f) day seven.

Using the simple flow routing model, the time taken for water to travel 1050 m through the reach from AWS_{Open} to AWS_{FDS} averaged 7.5 hours. Typically, water travelling from the upstream boundary of the reach between 01:00 and 12:00 warmed as it travelled through the reach while water beginning its journey through the reach between 13:00 and 00:00 cooled (Figure 28).

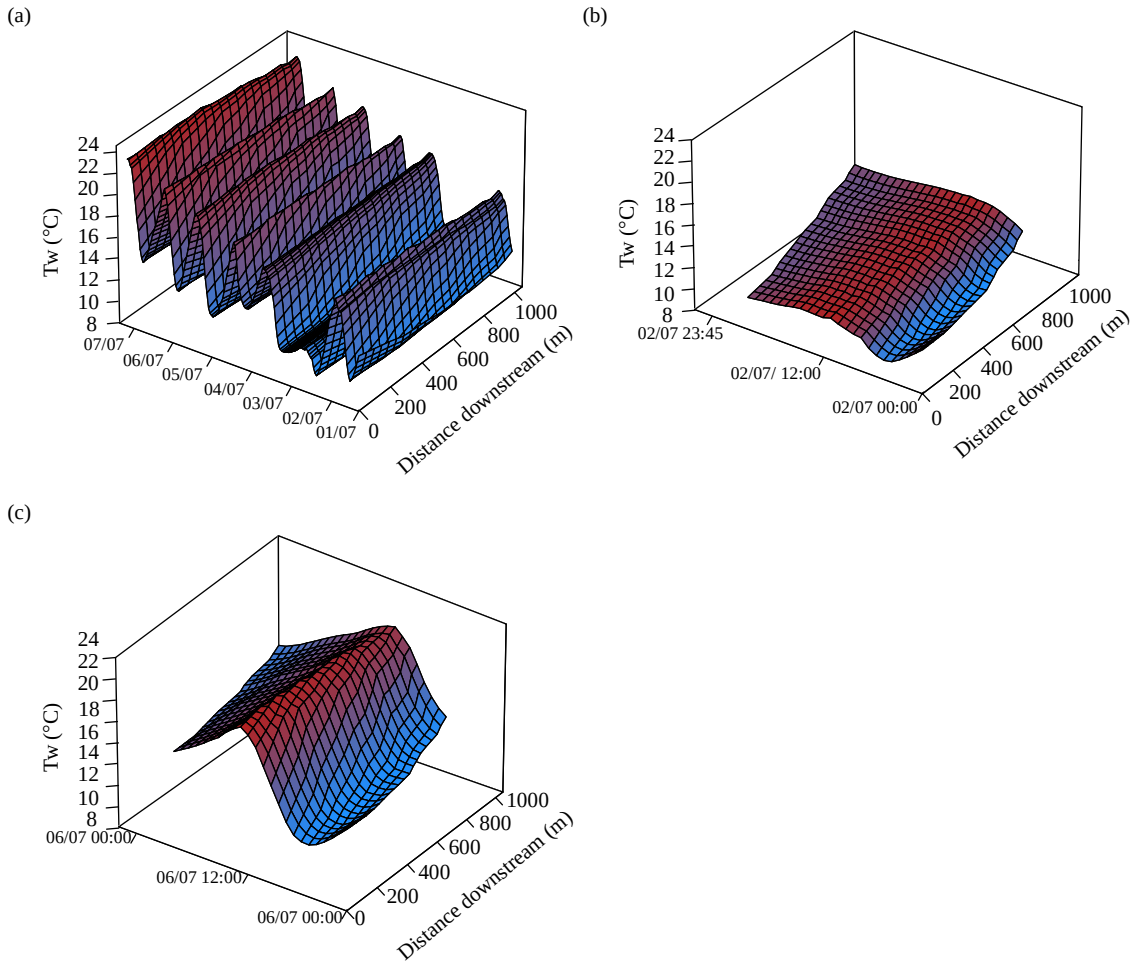

Figure 28. Temperature of water parcels (black lines on the date and time axis) routed through the reach from AWS_{open} at hourly intervals (a) on every day of the study period, (b) on day two, (c) on day six.

On the 1st, 3rd, 4th, 5th, 6th and 7th days water warmed between 4.2 °C and 6.9 °C while travelling through the reach; but, at the time of arrival at AWS_{FDS}, it was cooler than the water temperature observed at AWS_{open} at the same time (Figure 28a and 28b). For example, on the 6th day water leaving AWS_{open} at 08:00 was 14.3 °C. This water passed through the reach and arrived at AWS_{FDS} at 15:30, by which time its temperature had risen to 19.9 °C. The water leaving AWSopen at 15:30 had a temperature of 21.4 °C (Figure 28c). Thus at 15:30, the water at AWS_{FDS} was 1.5 °C cooler than that at AWS_{Open}.

Distinct instantaneous cooling gradients were not observed on the 2nd day, when water warmed < 1.5 °C while travelling through the reach. The water travelling from AWS_{open} on day two at 07:00 had a temperature of 10.4 °C and reached AWS_{FDS} at 14:15 attaining a temperature of 11.8 °C. Water travelling downstream from AWS_{open} at 14:15 also had a temperature of 11.8 °C and thus no cooling gradient was observed (Figure 28b).

4.6 DISCUSSION

This study has quantified longitudinal water temperature patterns in a stream reach where landuse transitions from open moorland to semi-natural forest. Furthermore, the riparian landuse controls plus associated energy exchange and water transport processes that generate water temperature patterns have been identified. Significant groundwater inflows do not occur within the reach and thus energy exchange was dominated by fluxes at the air-water column interface, allowing clearer conceptual understanding of the processes of longitudinal stream water cooling gradients under forest canopies. The following discussion identifies the key drivers and processes, and their space-time dynamics.

4.6.1 Micrometeorological and landuse controls on energy exchange and water temperature

During daylight hours net energy gains modelled at 5 m resolution throughout the reach, corroborating the observations of Brown *et al.* (1971) and Story *et al.* (2003) for shaded streams downstream of clearings. Distinctive longitudinal patterns in net energy within the reach were observed on clear skies days when solar radiation, and net energy gains were greatest; whereas net energy varied little within the reach on overcast days indicating that meteorological conditions were a first-order control on patterns of net energy flux (Rutherford *et al.*, 1997; 2004). The density of the semi-natural riparian forest canopy was a second order control on net energy flux. On clear-sky days, net energy gain was greatest where trees were absent (Moore *et al.*, 2005b) or the canopy was sparse, and least where the canopy was densest (Leach and Moore, 2010), owing to the canopy providing shading from solar radiation (Macdonald *et al.*, 2003; Malcolm *et al.*, 2004; Moore *et al.*, 2005b; Hannah *et al.*, 2008; Imholt *et al.* 2010; 2013b*).*

Contrasting meteorological conditions, and thus net energy gain conditions within the study period drove differences in the timing and magnitude of water temperature dynamics (Malcolm *et al.*, 2004) and gradients observed within the reach. On overcast days, within-reach differences in the magnitude (Johnson and Jones, 2000) and timing of maximum daily temperatures, and longitudinal water temperature gradients were indistinguishable. However, on clear sky days, maximum daily temperatures decreased between the upstream and downstream reach boundary by up to 1 °C, locations further downstream experienced maximum temperatures later in the day and instantaneous cooling gradients of up to 2.5 °C (equivalent to 2.4 °C km^{-1}) were observed. These decreases in temperature were much less than those observed by McGurck (1989), Keith *et al.* (1998) and Story *et al.* (2003) and, who

observed instantaneous cooling gradients of between 4.0 °C km^{-1} and 9.2 °C km^{-1}. Variability in cooling gradients at and between sites may be attributed to differing climatic zones, prevailing weather conditions (Rutherford *et al.*, 2004), riparian vegetation density and orientation, channel orientation and subsurface hydrology which all control the magnitude of energy exchange processes and consequently water temperature (Poole and Berman, 2001; Webb and Zhang, 1997).

4.6.2 Re- conceptualisation of processes generating longitudinal water temperature gradients

The water temperature model reproduced downstream temperature patterns with a high level of accuracy using physically realistic parameters scaled from local micrometeorological and river flow measurements. This suggests that the energy balance was near closed. Previous studies (e.g. Story *et al.*, 2003) have stated that cool groundwater inputs are necessary for longitudinal cooling gradients to occur. This study has demonstrated how cooling gradients can be produced in the absence of groundwater inputs in a shaded stream reach downstream of open landuse. It is now possible to conceptualise, for the first time, the processes that may generate spatio-temporal water temperature patterns on: (i) a clear sky day and (ii) an overcast sky day. On clear sky days, net energy fluxes increase reasonably consistently between sunrise and solar noon, driven by increasing solar radiation receipt. Consequently, the temperature of water crossing the upstream boundary and into the forest of the study reach between sunrise and solar noon increases continually (i.e. more heat is advected into the reach). On entering the forest, water temperature continues to increase but at a much reduced rate (Rutherford *et al.*, 2004), as solar radiation and thus net energy are reduced considerably. Consequently, when net energy gains occur, water flowing through the forest is consistently cooler than water travelling through the upper reach and moorland during the same time.

On overcast days, net energy gains increase little between sunrise and solar noon and differences in net energy gains between moorland and and forested sites are thus minimal. Therefore, the temperature of water crossing the upstream reach boundary changes little over the day (i.e. heat advected into the reach is reasonably constant) and water temperature changes at similar rates whether flowing through forest or moorland. Consequently, minor differences in water temperature are observed throughout the reach.

4.7 SUMMARY

The findings of the study have a number of important implications for researchers and river managers who may wish to assess the potential to mitigate water temperature extremes using riparian shading (e.g. afforestation). The key finding is that water does not cool as it flows downstream under a semi-natural forest canopy. Instead, energy gains to the water column are reduced dramatically in comparison to open landuse, which reduces the rate at which water temperature increases. Thus, observed temperatures are controlled by a combination of lagged temperatures from upstream open reaches and lower rates of temperature increase within the forest. For reaches such as the Girnock Burn, where upstream landuse does not shade the channel, instantaneous longitudinal cooling gradients are generated when the temperature of water advected into the reach increases over the day, while temperature increases are minimal for the stream flowing underneath the forest canopy. This study was conducted under a 'worst case' scenario of low flows and high energy gains; thus under these extreme conditions, cooler stream habitats are anticipated to be present under forest canopies during daylight hours, but warming of the water column upstream of the forest will control absolute water temperatures. Therefore shading headwater reaches, where water is not in dynamic equilibrium with the atmosphere (e.g. Erdinger *et al.*, 1968; Hrachowitz *et al.*, 2010; Kelleher *et al.*, 2012; Garner *et al.*, 2013) and is thus cooler than the majority of locations lower in the

basin (Poole and Berman, 2001), is anticipated to provide cool water habitats for temperature sensitive species and reduce temperatures further downstream.

Under future climates, surface energy balances are anticipated to change (Ramanathan, 1981; Wild *et al.*, 1997; Andrews et al., 2009) and flow volume in catchments such as the Girnock, which have little storage and low groundwater residence time, is anticipated to be more variable/ extreme (Cappel *et al.*, 2013). The water temperature modelling approach used in this study allows researchers and stream managers to explore the effects of variable prevailing weather and hydraulic conditions on stream temperatures, and identify optimal locations for the generation of cooling gradients under different shading regimes under present and future climates. Future research should utilise tools such as those presented herein to understand the effects of climate, hydraulic conditions, channel orientation and shading scenarios on water temperature for which observational datasets are unavailable.

CHAPTER FIVE: THE ROLE OF RIPARIAN VEGETATION DENSITY, CHANNEL ORIENTATION AND WATER VELOCITY IN DETERMINING RIVER WATER TEMPERATURE DYNAMICS

5.1 ABSTRACT

There is substantial scientific and practical interest in the potential of riparian shading to mitigate climate change impacts on river temperature extremes. However, there is limited process-based evidence to determine the density and spatial extent of riparian tree planting required to obtain temperature targets under differing environmental conditions. This paper demonstrates the importance of riparian vegetation density, channel orientation and flow velocity in determining river temperature dynamics using a process based stream temperature model. Water temperature measurements, energy exchange observations and hemispherical photographs were taken along a ~1050 m reach of the Girnock Burn (a tributary of the Aberdeenshire Dee, Scotland), where riparian landuse transitions from open moorland to semi-natural woodland. Field data were used to underpin a simulation experiment that investigated the effects of: (1) channel shading, (2) channel orientation, and (3) water velocity on heat exchange patterns and water temperature dynamics. Nine hemispherical images, each representing increasing degrees of shading (10-90%) were used to parameterise a deterministic net radiation model and simulate radiative fluxes associated with reforestation of the reach. The effects of channel orientation were investigated for each scenario by changing the location of north in each image at 45-degree intervals. Simulated radiative fluxes plus scaled measurements of sensible and latent fluxes drove a Lagrangian water temperature model that predicted spatio-temporal variability in stream temperature throughout the reach at a 50 m resolution. Water temperature simulations were performed under a low and a high flow velocity scenario. Under both low and high velocity scenarios, clear increases in mean (up to 6.1 °C) and maximum (up to 8.8 °C) temperatures were observed as canopy density decreased. Water velocity controlled the residence time of water in the reach, and thus heat accumulation and dissipation; consequently slow-flowing water was associated with higher

maximum temperatures and lower minimum temperatures (*cf.* fast-flowing water) for any given time and location within the transect. When the reach was either very densely vegetated (canopy density 80-90 %) or very sparsely vegetated (canopy density < 30%) the orientation of the channel had little effect on radiative fluxes and water temperature dynamics. Intermediate levels of shade (canopy density 30-60 %) produced highly variable radiative flux and water temperature dynamics due to variability in the time of day the vegetation shaded the stream. Critically, the study demonstrates that in many reaches relatively sparsely vegetated canopies are able to substantially reduce daytime temperature maxima relative to unshaded channels. Thus, the findings and modelling approach may be used to inform optimal tree planting strategies to mitigate increasing stream temperature maxima in a changing climate.

5.2 INTRODUCTION

Climate warming is anticipated to alter river and stream temperature regimes, with elevated temperatures expected for most watercourses (e.g. Beechie *et al.*, 2013; van Vliet *et al.*, 2013a; MacDonald *et al.*, 2014b; Garner *et al.*, 2013). Such changes, particularly increased maxima, are expected to diminish the spatial and temporal extent of suitable cool-water habitat for temperature sensitive organisms with potential impacts on the composition and productivity of aquatic ecosystems (Wilby *et al.*, 2010; Leach *et al.*, 2012). Consequently, there is substantial interest in adaptation strategies that may ameliorate the effects of climate warming including: riparian planting (e.g. Hannah *et al.*, 2008a; Brown *et al.*, 2010; Imholt *et al.*, 2013b; Ryan et al., 2013), reconnecting rivers to their floodplains (e.g. Poole et al., 2008; Opperman et al., 2010), reducing and retaining urban runoff (e.g. Booth and Leavitt, 1999) and reducing rates of abstraction (Poole and Berman, 2001).

In upland streams, where catchment hydrology and geomorphology have not been altered significantly by human activities, few options exist for protecting aquatic ecosystems from thermal extremes (Beschta, 1997; Poole and Berman, 2001). Observational datasets, often in combination with deterministic modelling approaches, have demonstrated that water temperature is controlled by a combination of: (1) advected heat from upstream, and (2) heat exchange at the air-water column interface (e.g. Westhoff *et al.*, 2011; Leach and Moore, 2014; MacDonald *et al.*, 2014b; Chapter 4), which is dominated in summer by solar radiation gains (Hannah *et al.*, 2008; Leach and Moore, 2010; MacDonald *et al.*, 2014b.). Recognising this, river managers (e.g. The River Dee Trust, 2011) are increasingly interested in using shade provided by riparian vegetation to reduce total energy inputs to the water column, which has been demonstrated to reduce thermal variability and extremes (e.g. Gomi *et al.*, 2006; Johnson and Jones, 2000; Hannah *et al.*, 2008; Imholt *et al.* 2010; 2013b; Garner *et al.*, 2014).

Few studies have simulated water temperature continuously within stream reaches and incorporated the effects of riparian landuse change (e.g. Watanabe *et al.*, 2005; Hrachowitz *et al.*, 2010; Roth *et al.*, 2010; Malcolm *et al.*, 2008; Brown *et al.*, 2010; Imholt *et al.*, 2010, 2013Lee *et al.*, 2012). Previous studies demonstrate that: (1) water temperatures are lower when vegetation is present (*cf.* absent) (e.g. Hrachowitz *et al.*, 2010), (2) narrow vegetated buffers can be as effective as wide buffers (e.g. Watanbe *et al.*, 2005), (3) longitudinal extent of riparian vegetation is important (e.g. Watanbe *et al.*, 2005) and (4) the location of vegetation relative to the path of the sun is important (Lee *et al.*, 2007). Furthermore, observational studies demonstrate that stream temperature reductions are greatest at sites under the densest canopies (e.g. Broadmeadow *et al.*, 2011; Groom *et al.*, 2011; Cross *et al.*, 2013; Imholt *et al.*, 2013b); and longitudinal temperature gradients are less within steeper,

and thus faster flowing, reaches compared with shallower, slower flowing reaches (e.g. Danehy *et al.*, 2005; Subehi *et al.*, 2009; Groom *et al.*, 2011).

However, no process-based, systematically-derived information exists on the effects of channel shading, orientation and water velocity on river temperature. Knowledge of these controls and their interactions is important to inform optimal tree planting strategies. In this context, this study aims to simulate the effects of varying riparian vegetation density and channel orientation on the stream energy budget and quantify the influence of these riparian vegetation scenarios on water temperature dynamics under scenarios of high and low water velocity.

5.3 STUDY AREA

Data were collected along a 1050 m study reach with no tributary inputs within Glen Girnock, an upland basin that drains into the Aberdeenshire Dee, northeast Scotland (Figure 22). Upstream of the reach (~ 24 km^2), landuse was dominated by heather (*Calluna*) moorland. Within the reach, landuse transitions from open moorland to semi-natural forest composed of birch (*Betula*), Scots pine (*Pinus*), alder (*Alnus*) and willow (*Salix*).

Detailed descriptions of the Girnock catchment and the study reach are found in Chapters Three and Four, respectively. Heat exchange within the study reach is driven almost exclusively by energy fluxes at the water column-atmosphere interface (Chapter 4). Thus, the influence of riparian canopy density, channel orientation and flow velocity was investigated in a reach without significant groundwater inflows. Groundwater inflows have been a confounding factor in understanding the 'cooling effect' of riparian shading in other river temperature studies (e.g. Story *et al.*, 2003), so our research was designed to exclude this potential control.

5.4 DATA AND METHODS

5.4.1 Experimental design

Field data were used as model inputs to a simulation experiment that investigated the influence of: (1) riparian vegetation density, (2) channel orientation (and thus vegetation orientation relative to the sun's path), and (3) water velocity (and thus stream gradient) on heat exchange patterns and water temperature dynamics within a 1050 m reach.

Nine hemispherical images (Figure 29; termed 'vegetation scenarios' herein), each representing increasing canopy density (i.e. 10- 90 %), were used to parameterise a deterministic net radiation model (Leach and Moore, 2010) and simulate net solar radiation fluxes at 1 m intervals associated with reforestation of the entire reach. The effect of channel orientation on energy exchanges and water temperature was investigated for each scenario by changing the orientation of hemispheric images at 45-degree intervals. Air temperature, relative humidity and wind speed were also scaled to represent conditions under each vegetation scenario in order to calculate longwave radiation, sensible and latent heat fluxes t 1 m intervals. Modelled energy exchanges were used to drive a Lagrangian water temperature model (after Rutherford *et al.*, 2004; Leach and Moore, 2011; MacDonald *et al.*, 2014b) that predicted spatio-temporal variability in stream temperature along the reach at 50 m resolution. Water temperature simulations were performed for each vegetation scenario and channel orientation under a low water velocity (associated with Q_{90}) and a high water velocity (associated with Q_{10}) scenario (Figure 30h). Changing the water velocity, but not discharge, simulated the effects of each vegetation scenario and channel orientation on water temperature in a low gradient (i.e. slow flowing) versus a high gradient (i.e. fast flowing) stream.

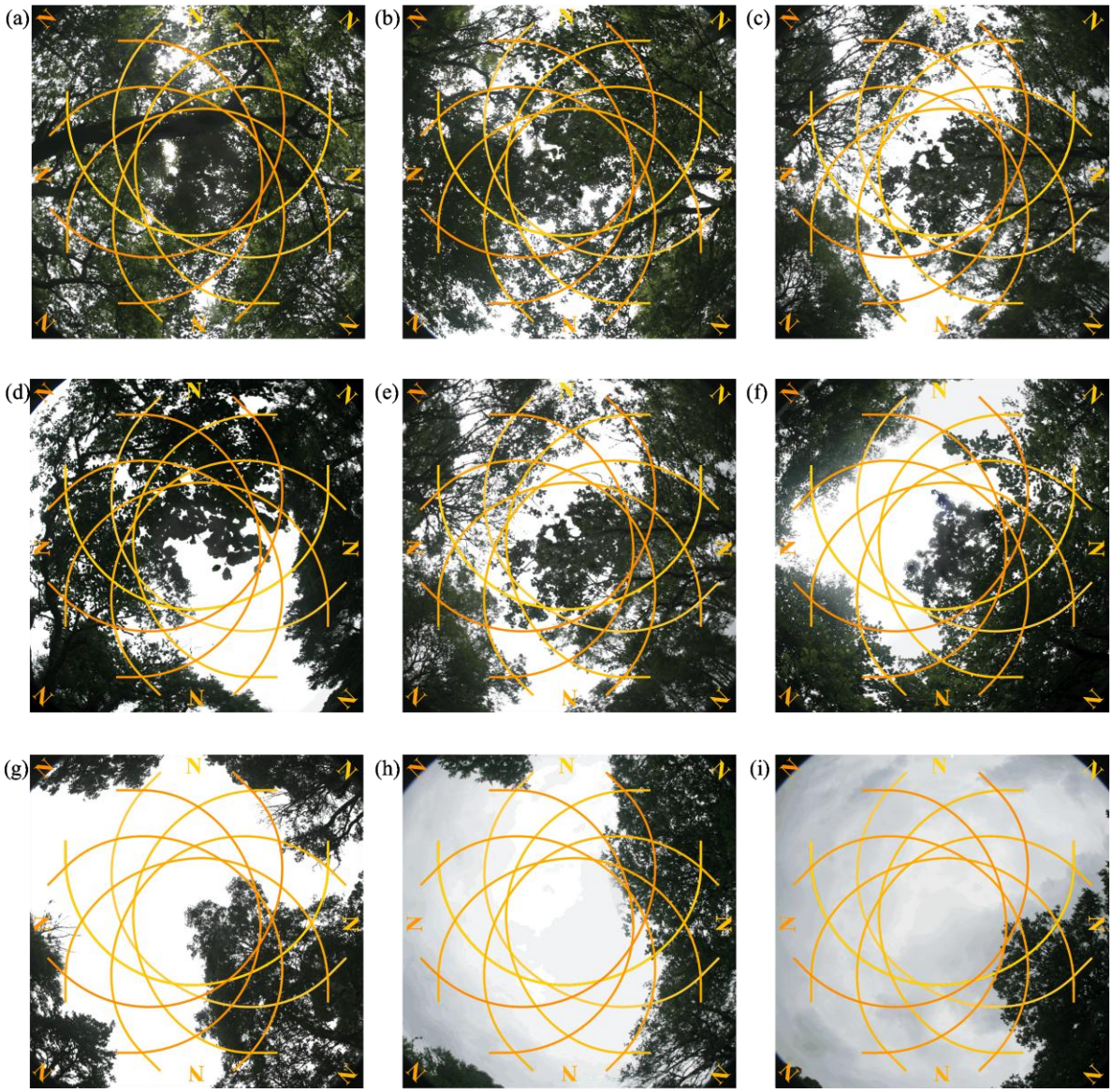

Figure 29. Hemispherical images used to represent (a) 90% (b) 80% (c) 70% (d) 60% (e) 50% (f) 40% (g) 30% (h) 20% (i) 10% riparian vegetation density scenarios. Eight coloured lines on each image represent the path of the sun across the sky relative to changing the channel orientation at 45-degree intervals

5.4.2 Data

Field data collection is described in detail in Chapter 4. In brief, stream temperature measurements were made at 15-minute intervals along a spatially distributed network of ten standalone, miniature water temperature loggers plus three Campbell 107 thermistors

connected to automatic weather stations (AWSs: AWS_{Open}, AWS_{FUS} and AWS_{FDS}) (Figure 22). In addition, each AWS measured: air temperature, relative humidity, wind speed, shortwave radiation and bed heat flux every 10-seconds and recorded averages at 15-minute intervals (details of instruments are found in Chapters 3 and 4). A Scottish Environmental Protection Agency (SEPA) gauging station at Littlemill provided discharge data at 15-minute intervals (Figure 22). A discharge-mean velocity function for Littlemill (derived by Tetzlaff *et al.*, 2005) was used to estimate water velocity. Velocity was assumed to be uniform throughout the reach. Hemispherical photographs were taken on the stream centreline using a Canon EOS-10D 6.3 megapixel digital camera with Sigma 8 mm fisheye lens.

Hydrometeorological data collected on 7 July 2013 (Figure 30) were chosen to meet the aims of the present study. On this day, measured water temperatures (Figure 30a) and shortwave (solar) radiation gains to the water column at AWS_{open} were high (Figure 30b) and discharge measured at Littlemill was very low (Figure 30h and 30i). Consequently, the effects of vegetation density, channel orientation and flow velocity on water temperature were evaluated under a 'worst-case scenario' of high energy inputs and low flows.

5.4.3 Estimation of stream energy balance components

Net energy

Net energy (Qn) available to heat or cool the water column was calculated as the sum of net solar radiation (K^*), net longwave radiation (L^*), sensible (Q_h) and latent heat (Q_e) fluxes (all Wm^{-2}):

$$Qn = K^* + L^* + Q_h + Q_e \qquad \text{Equation 24}$$

In some reaches significant groundwater in/ outflows and hyporheic exchanges occur and bed heat flux (Q_{bhf}) is therefore a significant component of the stream energy balance. It was excluded in this study because the research was designed to exclude these potential controls. As previously, heat from fluid friction was omitted (Chapters 3 and 4; Garner *et al.*, 2014) and energy fluxes were considered to be positive (negative) when directed toward (away from) the water column.

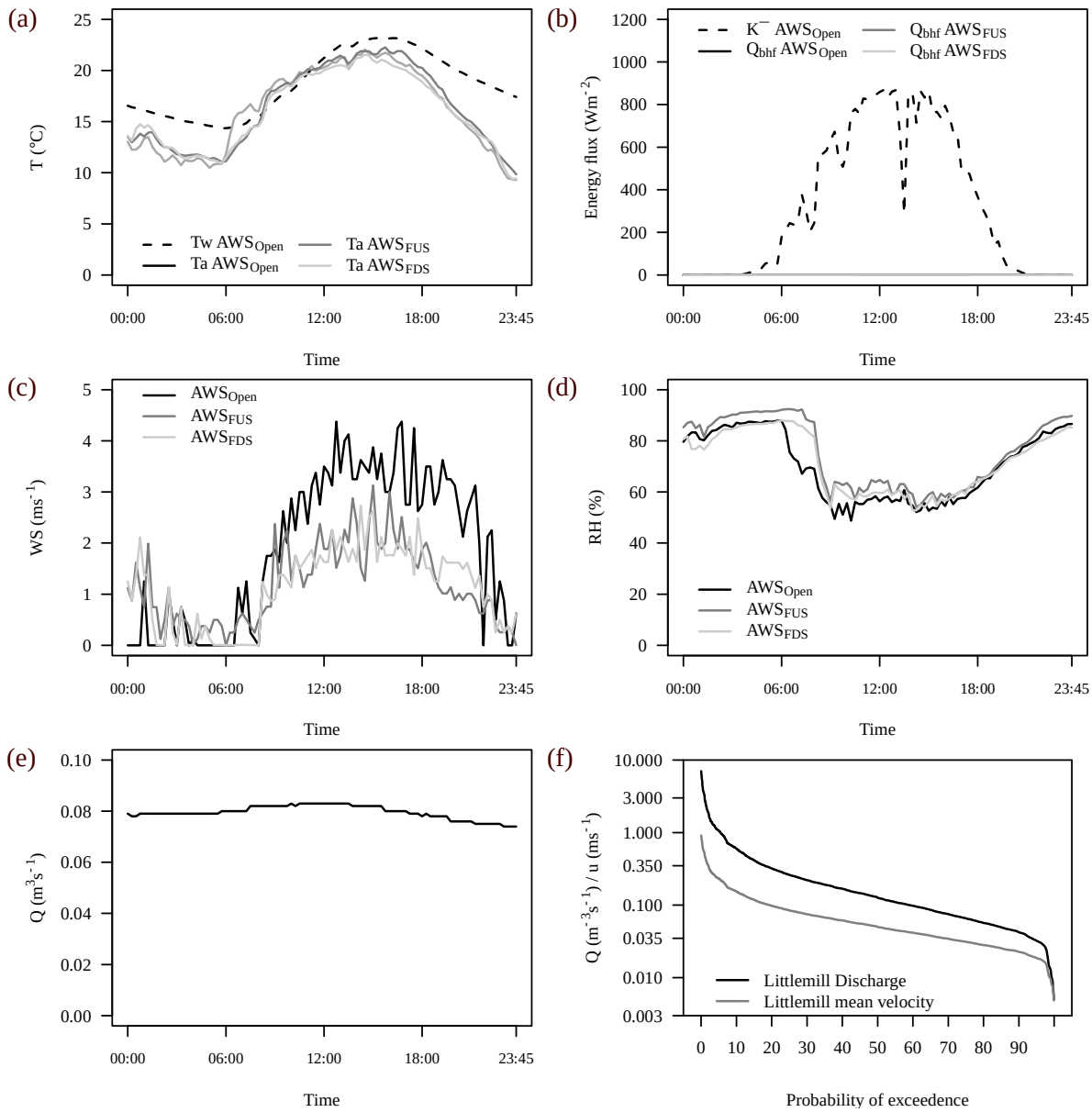

Figure 30. Model input data for 7 July 2013 (a) air and water temperatures (b) solar radiation (c) wind speed (d) relative humidity (e) discharge, and (f) discharge and water velocity duration curves at Littlemill for 1987- 2013.

Net radiation

A deterministic net radiation model developed by Moore *et al.* (2005b) and then extended and evaluated by Leach & Moore (2010) was used to simulate net solar radiation and net longwave radiation. The model is described in detail in Chapter 4 (see section *4.4.4 Modelling Approaches*)

Solar radiation measured at AWS_{open} was used to drive the solar radiation model under each scenario and simulate this flux at 1 m intervals. For each vegetation scenario, meteorological air temperature data used to calculate net longwave radiation was scaled by linear interpolation between the two nearest AWSs to the point along the stream centreline at which the hemispherical image representative of the scenario was taken. At the upstream boundary, net longwave radiation was calculated from water temperatures observed at AWS_{open}, however, modelled water temperatures were used throughout the rest of the reach.

Latent and sensible heat fluxes

Latent heat was estimated using a Penman-style equation (after Webb and Zhang, 1997) to compute heat lost by evaporation or gain by condensation (see Chapter 3, section *3.3.2 Estimation of stream energy balance components*).

Sensible heat was calculated as a function of Q_e and Bowen ratio (β) (see Chapter 3, section *3.3.2 Estimation of stream energy balance components*).

Turbulent fluxes at the upstream boundary were calculated using meteorological data (i.e. air temperature, wind speed and relative humidity) scaled to represent conditions under each vegetation scenario as described above for net longwave radiation. Observed water

temperatures at AWS_{open} were used at the upstream boundary and modelled temperatures were used throughout the remainder of the reach.

5.4.4 Modelling approach

Lagrangian water temperature model

The Lagrangian modelling approach (after Rutherford *et al.*, 2004; Leach and Moore, 2011; MacDonald *et al.*, 2014) was used to simulate the temperature of discrete parcels of water released from the upstream reach boundary. Parcels were released each hour and their temperature simulated at 50 m intervals driven by hydrometeorological data for 07 July 2013. Full details of the model are provided in Chapter 4 (see section *4.4.4 Modelling Approaches*), in this instance (i.e. in the absence of bed heat flux) it was expressed as:

$$\frac{dT_w}{dx} = \frac{[[w_{(s)}(K^*_{(s,t)}+L^*_{(s,t)}+Q_{h(s,t)}+Q_{e\,(s,t)})+w_{(s)}(K^*_{(s,t+\Delta t)}+L^*_{(s,t+\Delta t)}+Q_{h(s,t+\Delta t)}+Q_{e\,(s,t+\Delta t)})]/2]}{C\,[(F_{(s,t)}+F_{(s,t+\Delta t)})/2]}$$

Equation 25

5.5 RESULTS

5.5.1 Stream energy balance

Net solar radiation

Net solar radiation gains to the water column increased as vegetation density decreased (Figure 31). The orientation of the channel influenced net solar radiation gains substantially under scenarios of 30-60% canopy density (i.e. sky view; Figure 31d- 31g). Under these scenarios, large portions of the sky remained unshaded (Figure 29d- 29f). Consequently, low net solar radiation gains were simulated when the channel was orientated so that it was shaded while the sun was in south-east, south and south-westerly sky-positions (i.e. when potential gains were greatest) and high net solar radiation gains were simulated when the water column

remained exposed to the sun at these times. The orientation of the channel had little impact on net solar radiation gains under: (1) the densest canopies (i.e. 70-90 % density; Figure 31a-c), when limited portions of the stream remained unshaded (Figure 29a- 29c) and (2) under the sparsest canopies (i.e. ≤ 20%; Figure 31h and 31i), when vegetation had a minimal shading effect regardless of channel orientation (Figure 29h and 29i).

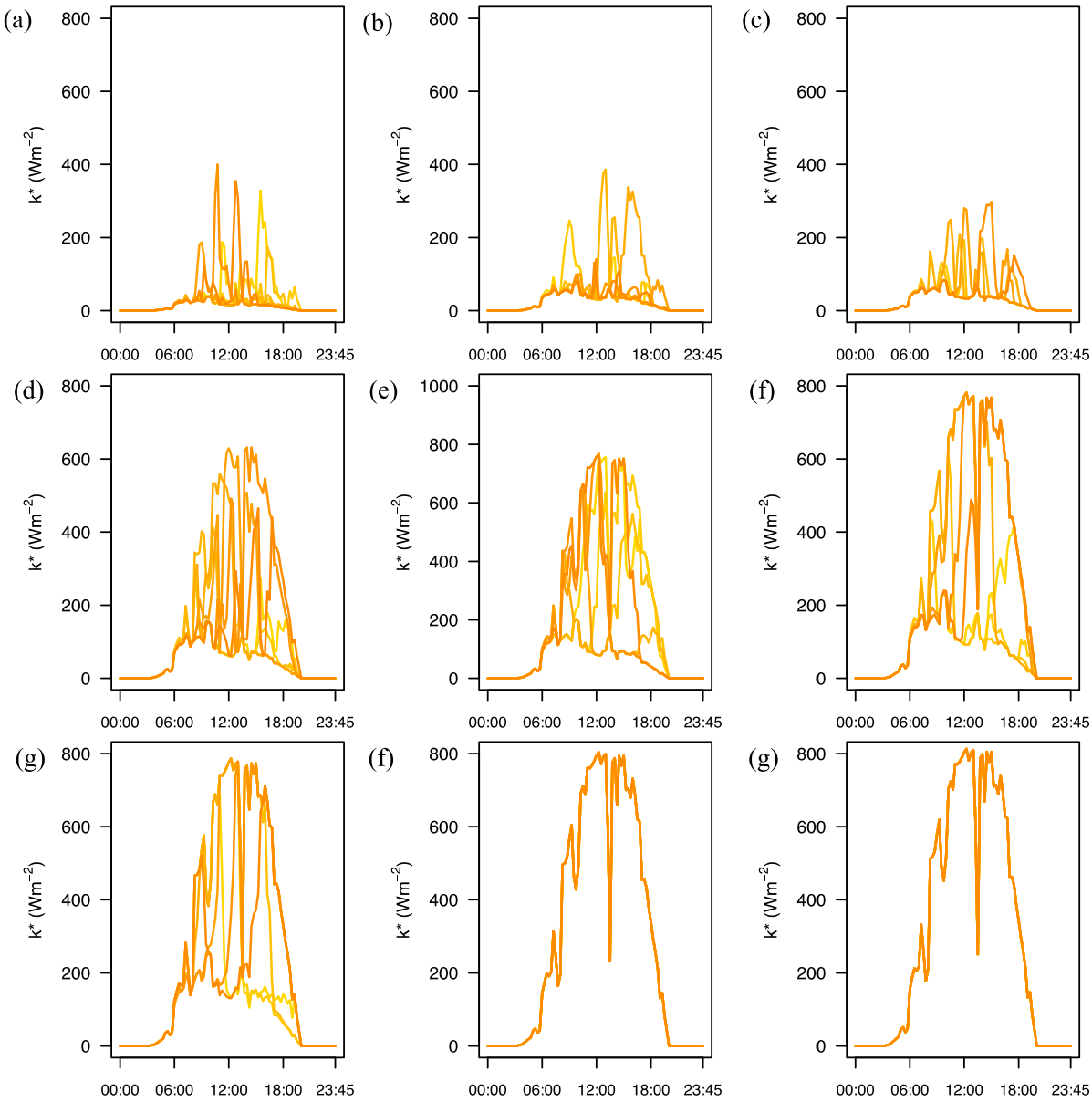

Figure 31. Simulated net solar radiation for scenarios of (a) 90% (b) 80% (c) 70% (d) 60% (e) 50% (f) 40% (g) 30% (h) 20% (i) 10% vegetation density. Eight coloured lines in each plot represent changing the channel orientation at 45-degree intervals. Note that net solar radiation was uniform throughout the reach under each scenario.

Net energy

Net energy flux was calculated in part as the sum net longwave radiation, latent, and sensible heat fluxes, which are dependent on water temperature. Consequently, net energy flux was not uniform throughout the reach under each scenario. Therefore modelled net energy at the upstream reach boundary is described in order to compare the differences in energy loss from and gain to the water column between vegetation scenarios. Beneath the densest riparian canopies (70-90% density), net energy losses dominated most of the day and night and thus heat was almost always lost from the stream (Figure 32a- 32c). For scenarios of between 40-60 % canopy density was highly variable, the magnitude of energy gains or losses depended on channel orientation (Figure 32d- 32g). Small losses or gains were simulated during daylight hours when channel orientation provided shading near to mid-day and conversely, large net energy gains were simulated when the channel was orientated so that the water column was exposed at these times. Beneath the sparsest canopies (i.e. 10-20 % density), the water column received consistently high net energy gains during daylight hours, regardless of channel orientation (Figure 32h and 32i).

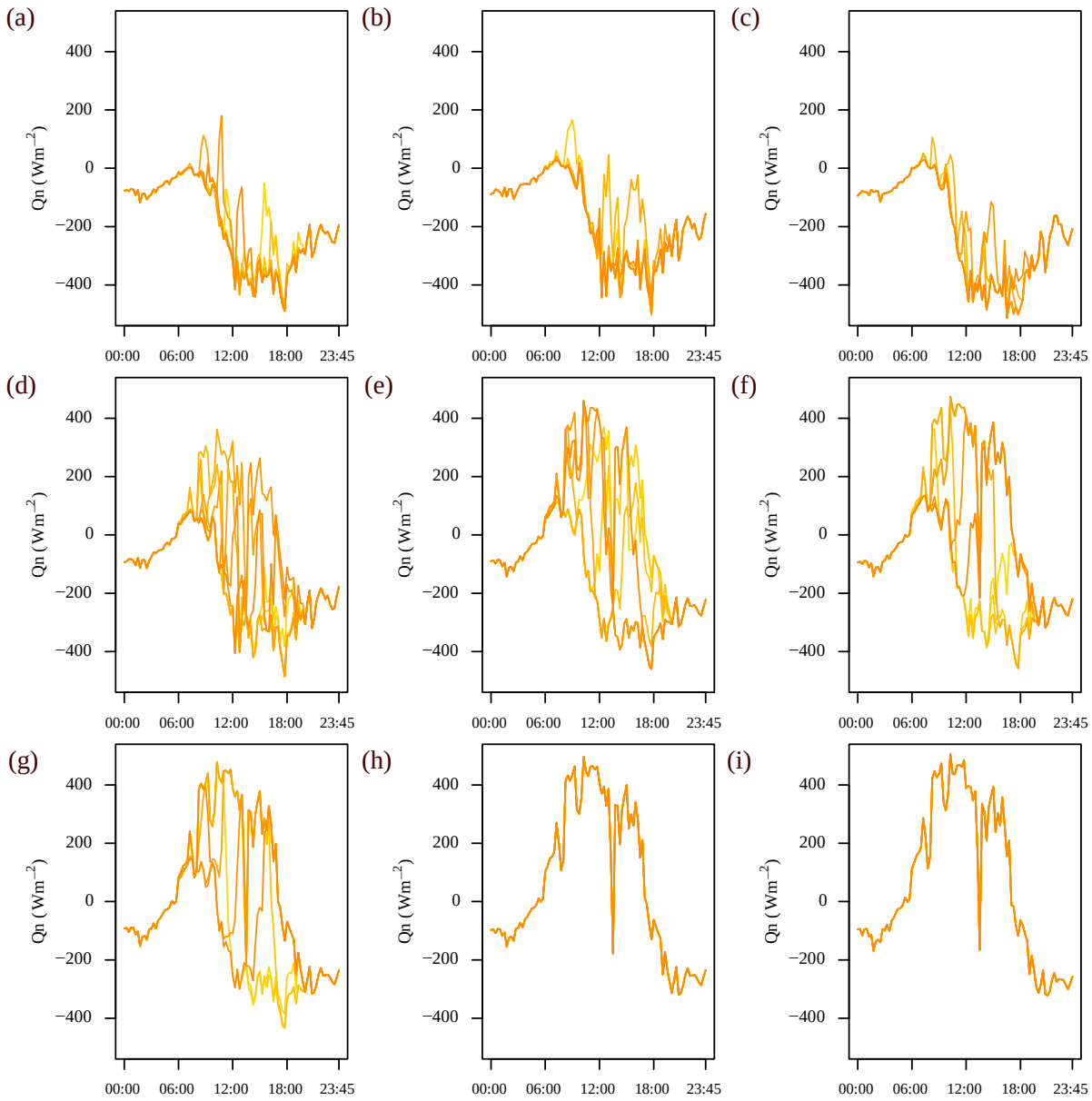

Figure 32. Simulated net energy for scenarios at the upstream reach boundary under (a) 90% (b) 80% (c) 70% (d) 60% (e) 50% (f) 40% (g) 30% (h) 20% (i) 10% vegetation density. Eight coloured lines in each plot represent changing the channel orientation at 45-degree intervals. Net energy was dependent on water temperature at was therefore not uniform throughout the reach. Net energy at the upstream reach boundary is plotted.

5.5.2 Water temperature

Water temperature model evaluation

Field data collected for existing riparian vegetation conditions within the study reach (see Chapter 4) were used to evaluate the performance of the water temperature model driven by data collected on 7 July 2013. Water 'parcels' were released from the upstream boundary (AWS_{open}) at hourly intervals and their temperature simulated at 50 m intervals. The temperature of water parcels released from the upstream boundary during the mid- and late afternoon were increasingly overestimated, especially while travelling through the lower reach (Figure 33). Otherwise, model performance was generally good and evaluation statistics (i.e. Nash-Sutcliffe estimator, R^2, percent-bias, root mean square error and mean error; Table 6) were well within limits proposed for watershed simulations by Moriasi *et al.* (2007). Furthermore, daily maximum, mean and minimum water temperatures that occurred throughout the reach (i.e. of all 483 modelled temperatures) were reproduced with good accuracy (Table 6).

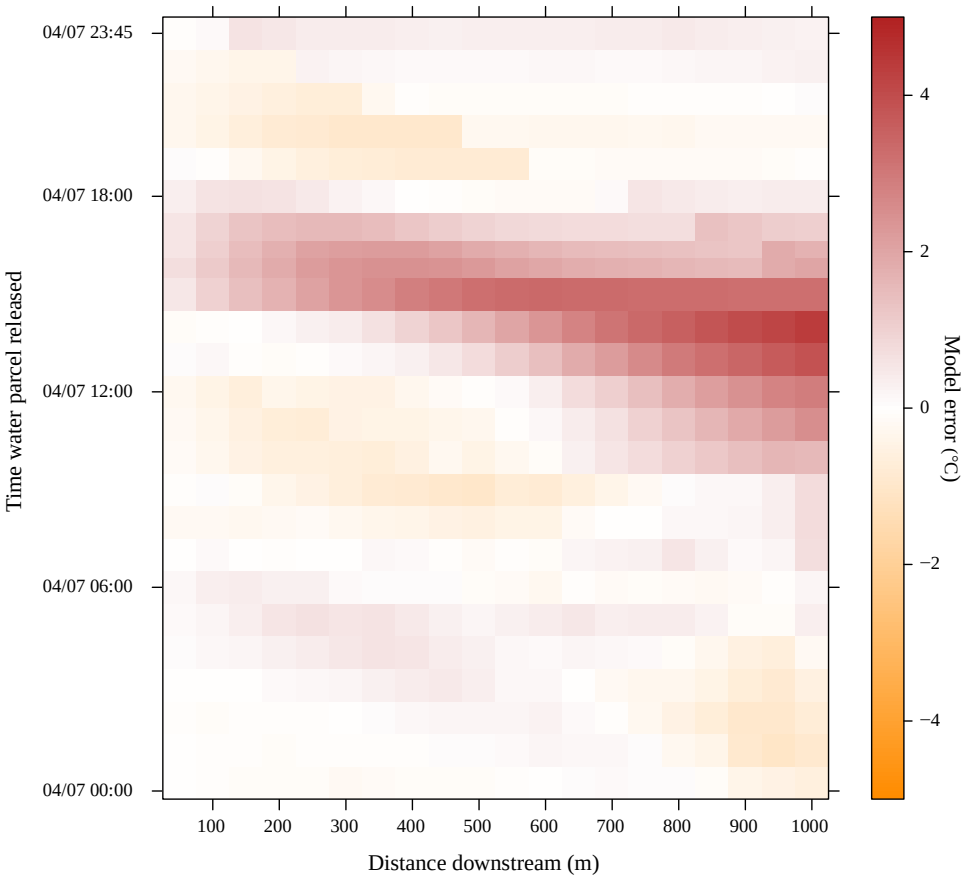

Figure 33. Model error (modelled minus observed water temperature) across space and time

Table 6. Water temperature model evaluation statistics for 7 July 2013

Nash-Sutcliffe efficiency	R^2	Bias (%)	Root mean square error (°C)	Mean Error (°C)	Error in max. Tw (°C)	Error in mean. Tw (°C)	Error in min. Tw (°C)
0.86	0.91	2.4	1.1	0.4	0.2	0.4	0.2

Simulated water temperature dynamics

Water temperature metrics were calculated and duration curves constructed from water temperatures simulated throughout the reach (n= 483 temperatures). Channel orientation had little effect on simulated water temperature dynamics under the sparsest (i.e. ≤ 20 %) and densest (i.e. ≥ 70%) canopy scenarios (Figure 34). Under intermediate canopies (i.e. between 30- 60 %), varying channel orientation was associated with large variability in maximum (up to 8.5 °C) and mean (up to 5.0 °C) temperatures, although there was no discernable effect on minimum temperatures (Figure 34). Temperature duration curves for vegetation density scenarios of 30-60 % (Figure 35) demonstrate that only the highest simulated temperatures (top 40 %) were influenced by channel orientation. Furthermore, under these intermediate vegetation scenarios channel orientation influenced the location of maximum temperature observations within the reach. For example, under 40 % canopy density and when the stream was orientated so that vegetation shaded the water column from the strongest (around noon) solar radiation gains, maximum temperatures occurred close to the upstream boundary (Figures 36b and 36e). Conversely, when the channel was orientated so that the water column was exposed to the greatest solar radiation gains, high temperatures persisted throughout the reach but the highest temperatures occurred closer to the downstream reach boundary (Figures 36a and 36c).

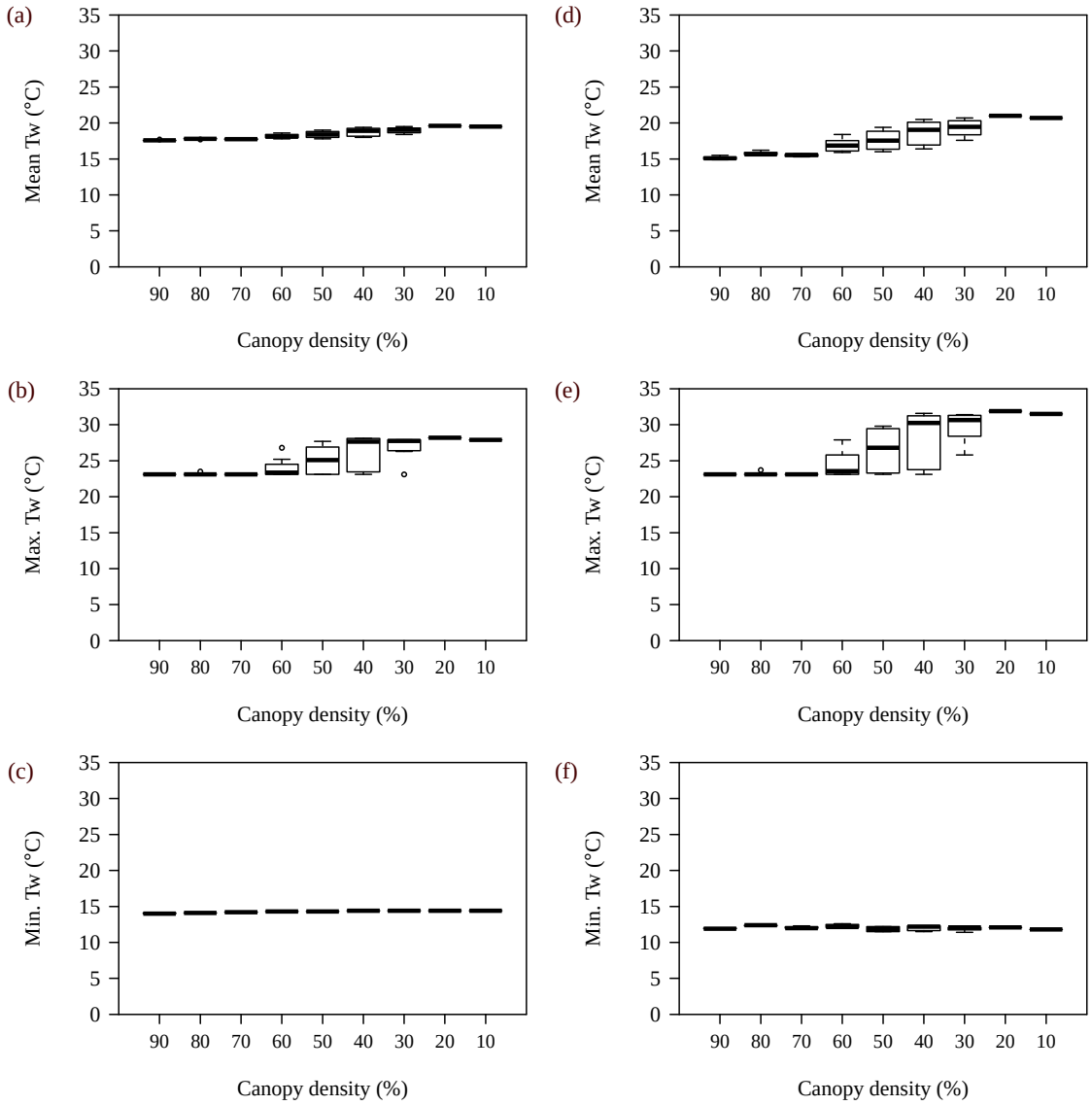

Figure 34. Simulated water temperature dynamics (a-c) high flow velocity scenario (d-f) low flow velocity scenario. Metrics for each scenario were calculated from simulated water temperature dynamics throughout the entire reach (n= 483)

Increasing vegetation density from 10- 90% for both low and high velocity scenarios decreased mean temperatures by 6.1°C and 2.1 °C, maximum temperatures by 8.8°C and 5.1 °C, and minimum temperatures by 1.2°C and 0.4 °C, respectively (Figure 34). Differences in simulated stream temperature between vegetation and channel orientation simulations were greater for the low velocity scenario (Figure 35). Low velocities increased residence times

within the reach resulting in greater heating and cooling over the reach (Figure 36a, 36b, 36d, 36e, 36g, and 36h). For example, with < 40% canopy density, changing the channel orientation caused a reduction in maximum (mean) temperatures by up to 8.5 °C (4.1 °C) under the low flow velocity scenario compared to 5.0 °C (1.4 °C) under the high velocity scenario (Figure 34).

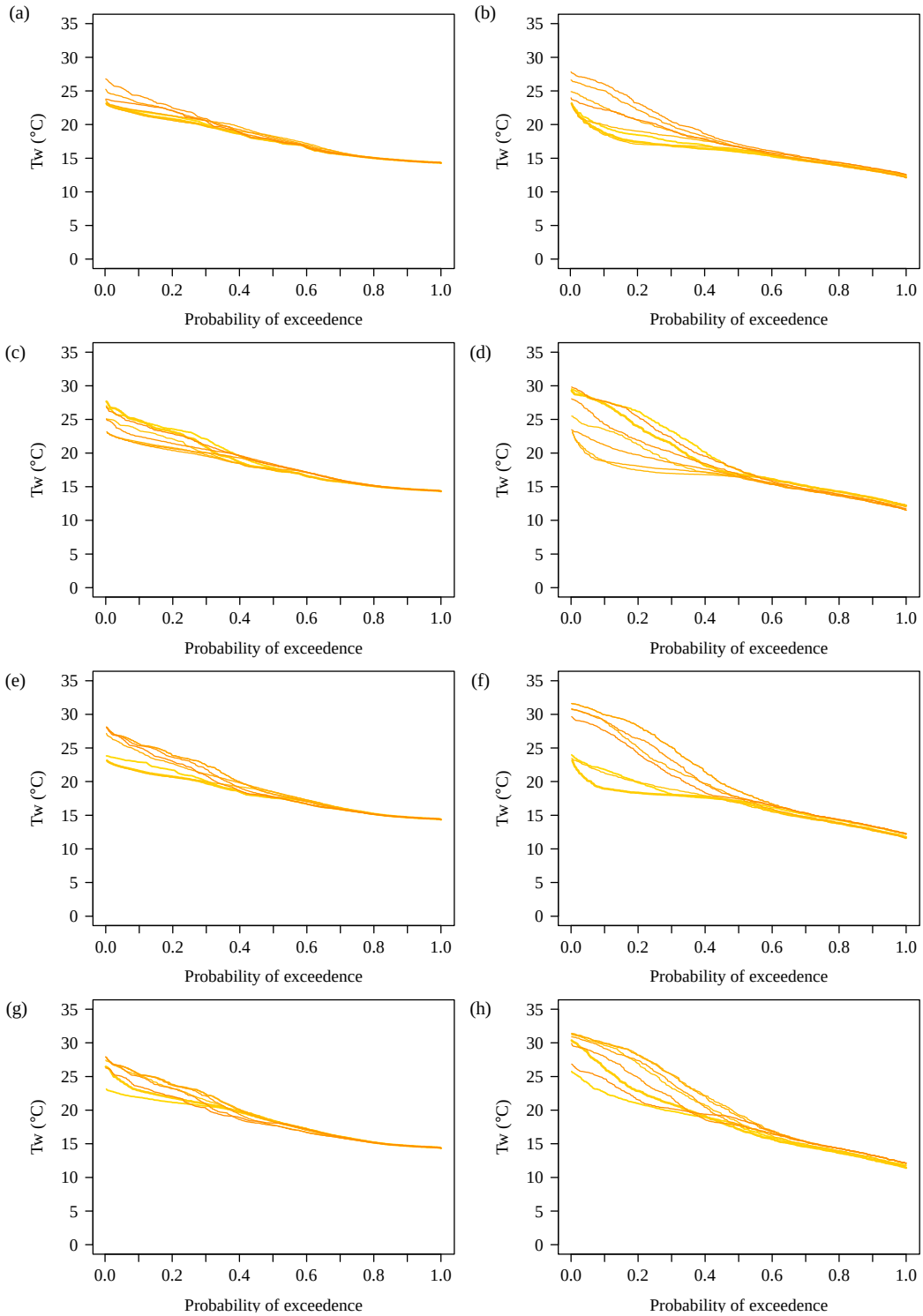

Figure 35. Duration curves for water temperatures simulated throughout the reach (n= 483) under the high flow velocity scenario: (a) 60% (b) 50% (c) 40% (d) 30% canopy density and under the low flow velocity scenario: (e) 60% (f) 50% (g) 40% (h) 30% canopy density. Eight coloured lines in each plot represent changing the channel orientation at 45-degree intervals. Each curve is constructed of 483 values modelled throughout the reach

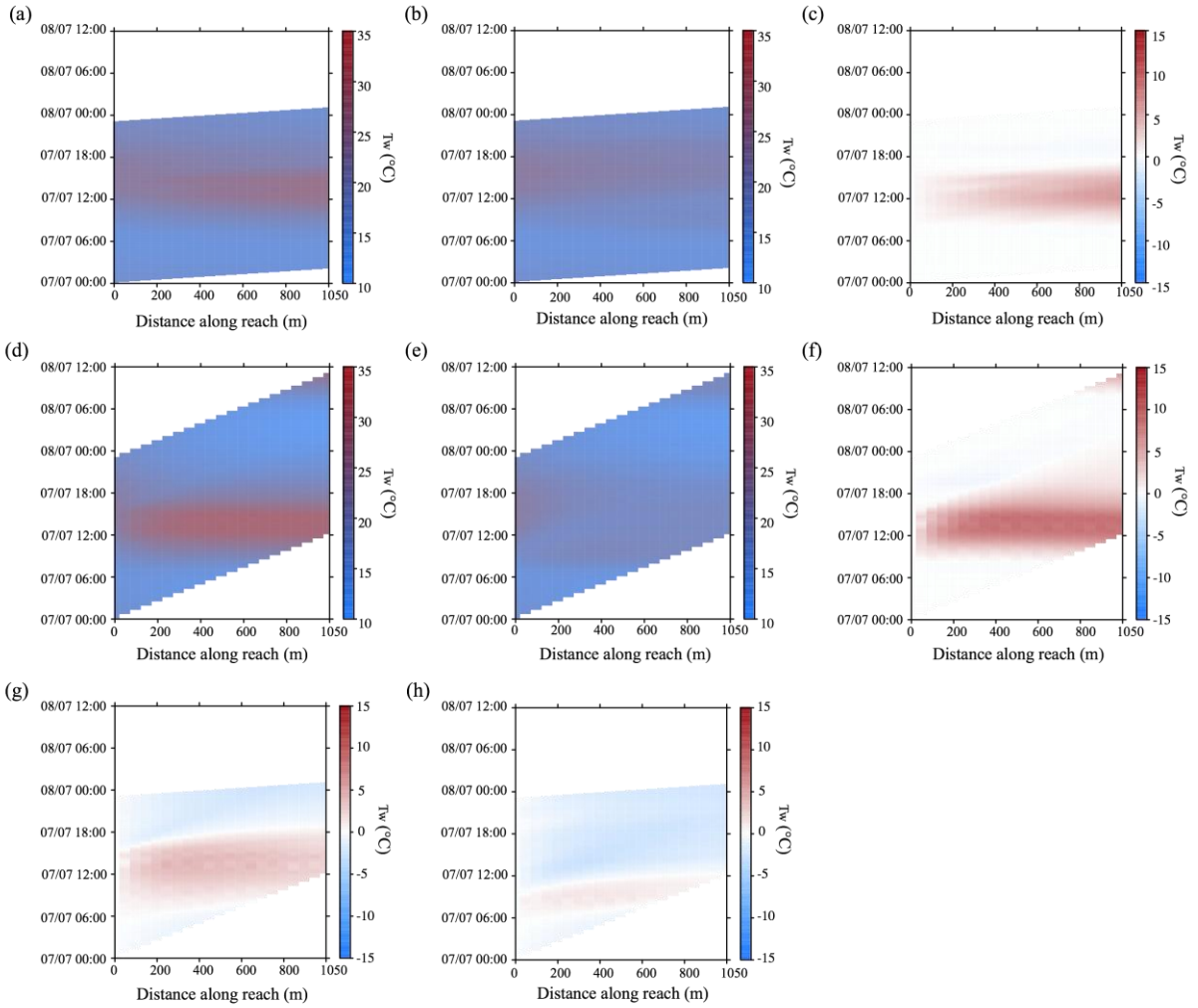

Figure 36. Water temperatures simulated throughout the reach under the scenario of 40 % canopy density under (a) channel orientation under which southerly sky-positions are not shaded and high flow velocity (b) channel orientation under which southerly sky-positions are shaded and high flow velocity (c) difference between a and b (d) channel orientation under which southerly sky-positions are shaded and low flow velocity (e) channel orientation under which southerly sky-positions are shaded and high flow velocity (f) difference between d and e (g) difference between a and d (h) difference between b and e.

5.6 DISCUSSION

This study has quantified the influence of riparian vegetation density on energy exchange and water temperature dynamics in channels of varying orientation and water velocity. The latter is a surrogate variable for hydraulic retention time, which increases for lower gradient streams

(if other channel dimensions do not change). The following discussion considers the effects of: (1) interactions between vegetation density and channel orientation, and (2) water velocity on stream heating and cooling processes. The implications of these findings are assessed in each section with respect to their utility to inform optimal tree planting strategies for mitigation of potentially ecologically-damaging river temperature extremes.

5.6.1 Vegetation density, channel orientation and effects on stream heating and cooling

In stream reaches shaded by riparian vegetation the riparian canopy reduces solar radiation inputs and consequently net energy available to heat the water column (Hannah *et al.*, 2004; 2008b; Leach and Moore, 2010; Garner *et al.*, 2014). Where solar radiation is not sufficiently reduced to produce net energy losses (i.e. where energy gains occur), downstream reductions in instantaneous temperatures are generated when cool water that flows through exposed reaches overnight and during the early morning is advected through a forested reach and warms slowly due to greatly reduced net energy gains (*cf.* open reaches upstream) (Chapter 4). The present study supports these observations; significant reductions in maximum and mean temperatures were simulated where riparian vegetation shaded the water column when it was subject to net energy gains. Further to this, the present study contributes new knowledge on cooling processes below forest canopies. Net energy losses were simulated under the densest canopies (i.e. 70– 90 %) and maximum water temperatures within the reach did not exceeded those at the upstream reach boundary. Therefore, under very dense riparian canopies solar radiation is blocked to such an extent that net energy losses occur and so water cools as it travels downstream.

Previous studies have demonstrated that greater riparian vegetation density is associated with decreased water temperatures, especially maxima (Broadmeadow *et al.*, 2011; Groom *et al.*, 2011; Imholt *et al.*, 2013; Cross *et al.*, 2014) and that the orientation of vegetation relative to

the path of the sun is also important (Lee *et al.*, 2012). This study demonstrated that for intermediate canopy densities, the effect of riparian vegetation on maximum and mean temperatures was strongly dependent on channel orientation and thus location of vegetation relative to the path of the sun. A canopy cover of 40 % density could be as effective as 60% density, provided that it shaded the water column when potential solar radiation gains were greatest (i.e. when the sun was between south-westerly and south-easterly sky positions in the Northern Hemisphere), while a canopy cover of up to 60% could have little effect in reducing maximum temperatures if it did not shade the channel at these times.

When planning riparian planting strategies, stream managers must decide whether their goal is to: (1) cool water, or (2) reduce warming of water as it flows downstream. The channel must be shaded almost entirely to generate cooling, so this is an 'expensive' way to create thermal refugia. However, cooling may be required where temperatures are near, or anticipated to exceed, lethal or sub-lethal thresholds for an organism of interest (Beechie *et al.*, 2014). Where stream managers wish to use riparian vegetation to reduce further warming of water as it flows downstream then the orientation of the channel should inform the location and density of planting. Critically, vegetation must be positioned so that it overhangs the stream centreline and so that it shades the stream when solar radiation gains are greatest, thus between southwest and southeast for streams in the Northern Hemisphere. Based on these results, streams flowing east-west, northeast-southwest, or northwest-southeast, and *vice versa*, can be vegetated with relatively sparse vegetation on their most southerly bank to achieve large reductions in mean and maximum temperatures at minimal cost. Streams that flow north-south, and *vice versa*, do not have a southerly bank that can be afforested and will require more dense, over-hanging vegetation on their west and east banks to shade the water

column from the highest solar radiation gains and to yield significant reductions in water temperature.

5.6.2 Effects of water velocity on stream heating and cooling

Water temperature mean and maxima were increased and minima decreased when water travelled at low velocity (*cf.* high velocity) due to longer residence time within the reach and thus greater accumulation (dissipation) of heat (Subehi *et al.*, 2009; Danehy *et al.*, 2005; Groom *et al.*, 2011) under net energy gain (loss) conditions. Under real-world conditions the temperature of water entering the reach would likely be different in a steep, fast-flowing stream in comparison to a gentle, slow-flowing stream, whereas in these simulations the same time-series of data were input for each scenario. Notwithstanding this, novel insights gained into heating and cooling processes in fast- *versus* slow-flowing streams allow recommendations for stream management to be made. In fast-flowing streams where net energy losses occur (or are desired), longer stretches of riparian vegetation are required to produce the magnitude of cooling possible in a shorter stretch in a slower-flowing stream. Conversely, where energy exchange conditions do not allow cooling (i.e. net energy gains occur) then greater lengths of vegetation should be provided in slow-flowing streams to reduce accumulation of heat when retention times are longer.

5.7 SUMMARY

This study used field data from an upland Scottish stream to underpin simulation experiments and provide systematic, mechanistic understanding of the effects of riparian shading scenarios, channel orientation and hydraulic conditions on water temperature dynamics. The knowledge yielded, and modelling approach employed, allow scientists and catchment managers to make better-informed decisions on the: (1) optimal reaches in which to implement riparian tree planting strategies, and (2) density and longitudinal extent of

vegetation required to maximise the availability of cool water habitats. The specific magnitude of reduction in water temperature under a given canopy density will be dependent on local conditions (Ryan *et al.*, 2013) as determined by magnitude of net energy exchange (linked to vegetation cover density and channel orientation), water velocity and hydrology. The experiments presented here demonstrate that where southerly banks may be afforested, then relatively sparse, overhanging vegetation is able to produce spatially and temporally extensive cool-water refugia when thermal extremes occur. Only in reaches where a southerly bank cannot be afforested is dense, overhanging vegetation required. Furthermore, longer reaches should be afforested in slower-flowing streams to minimise the amount of time water spends accumulating heat in high energy open environments. Shorter lengths may be afforested in fast-moving streams where water transit times are quicker and less heat is accumulated.

Researchers and river managers can use models such as those presented here to quantify potential changes in river thermal conditions associated with riparian planting schemes under both present and future climates. However, these models require large observational datasets that are rarely available, and logistically and financially unfeasible to collect in many circumstances. Consequently, future research should seek to upscale the information yielded in this study to identify the locations most sensitive to a changing climate across large geographical areas (e.g. Garner *et al.*, 2013) and to identify reaches most suitable for afforestation. This could be achieved, for example, by linking the outputs of rapid riparian canopy density assessments (e.g. Imholt *et al.*, 2013a) with radiation estimates in combination with statistical models capable of water temperature prediction in a spatially distributed manner (e.g. Hrachowitz *et al.*, 2010).

CHAPTER SIX:
SYNTHESIS, IMPLICATIONS AND FUTURE DIRECTIONS

6.1 INTRODUCTION

The research presented in this thesis was motivated by the anticipation amongst scientists, environment managers and regulators that water thermal regimes have been (e.g. Langan *et al.*, 2001; Durance and Ormerod, 2007; Kaushal *et al.*, 2010; Orr *et al.*, 2013) and will continue to be (e.g. van Vliet *et al.*, 2011; MacDonald *et al.*, 2014a) highly sensitive to changing climatological and hydrological processes, with associated profound potential impacts on freshwater ecosystems as a whole (Ormerord, 2009). So that we may make well-informed decisions regarding river thermal regimes in a changing climate and consequently protect freshwater ecosystems, the research yielded new process-based knowledge on the rivers most sensitive to a changing climate and the potential of riparian forest to mitigate these damaging effects.

The thesis adopted a multi-scale research design and addressed four research objectives in four interlinked, key sub-themes. In Chapter 2 (objective 1), spatial patterns and inter-annual variability in the shape and magnitude of annual river temperature regimes were identified across England and Wales, and regime sensitivity to air temperature and river basin properties elucidated. In Chapter 3 (objective 2), for a Scottish upland stream (the Girnock Burn) the prevailing hydrometeorological conditions were identified under which shading by riparian vegetation may be effective in mitigating river thermal variability and extremes. In Chapter 4 (objective 3), a high-resolution water temperature model was applied to a 1000 m reach of the Girnock Burn to identify the processes driving cooling water temperature gradients in forested stream reaches. In Chapter 5 (objective 4), the water temperature model was used to quantify the effects of riparian shading scenarios, channel orientation and water velocity on reach-scale stream temperatures dynamics. In this Chapter, the key findings of the research are identified and synthesised, and future research prospects proposed.

6.2 KEY RESEARCH FINDNGS

The research presented was unique in: (1) presenting the first assessment of large-scale spatial and temporal variability of the shape and magnitude of annual river temperature regimes within England and Wales, a quantification of their associations with air temperature regimes, and the identification of basin controls that modified the strength of air-river temperature links, (2) providing the first long-term perspective on stream temperature, riparian microclimate and energy exchanges in semi-natural forest and moorland reaches, (3) demonstrating that cooling water temperature gradients beneath forest canopies may be generated in the presence of net energy gains and in the absence of cool groundwater inflows, and (4) presenting the first systematically derived, process-based evidence to inform specific guidelines on the density and extent of riparian tree planting required to produce cool water habitats. Major research outcomes are as follows:

1. River temperature regime shape (timing of response/ seasonality) may be anticipated to be most sensitive to a changing climate than regime magnitude (size of response) in the largest and least permeable basins. Regime magnitude in the headwaters and most permeable basins is anticipated to be least sensitive (Chapter 2).
2. Shading headwater streams with semi-natural riparian vegetation is effective in mitigating thermal variability and extremes under high energy input. Thus, riparian shade provides a habitat for freshwater species that is typically cooler than moorland environments when thermal maxima occur (Chapter 3).
3. Shading headwater streams reduces the rate at which water warms as it flows downstream (Chapter 3). Cool water refugia develop beneath forest canopies due to a combination of advection of cool overnight and early morning water and reduced rates

of warming beneath the canopy. Only under the densest canopies does water cool as it moves downstream (Channel 4).

4. Where southerly riverbanks may be afforested then relatively sparse, overhanging vegetation is able to produce spatially and temporally extensive cool-water refugia when thermal extremes occur. Longer reaches should be afforested in slower-flowing streams to minimise the time water spends accumulating heat in high energy exposed environments. Shorter reaches may be afforested in fast-moving streams where water is washed out of catchments more quickly having accumulated less heat (Chapter 5).

6.3 SYNTHESIS

This section synthesises the new knowledge yielded in the thesis to identify the processes and controls that influence the sensitivity of water temperature to climate at multiple spatial scales.

Rivers are hierarchical systems (Montgomery, 1998), and thus for a specific point on a river, water column temperature is determined: (1) initially by the mix of water source contributions and (2) subsequently by the energy gained or lost across the water surface and riverbed interfaces as water flows downstream. The research presented within this thesis suggests that this process cascade also controls the sensitivity of river waters to climate. The source of most headwater streams in temperate regions (such as the UK) is groundwater (spring-head) discharge. During summer months, when ecologically damaging thermal maxima occur, the temperature of this cool and (relatively) diurnally stable (Chapter 4) water is the temperature from which streams warm (Chapter 4) due to accumulation of heat within the water column (Chapter 3 and 4) as they flow through the river network (Poole and Berman, 2001). In basins underlain by productive regional aquifers (e.g. the Chalk in central southern England, Chapter 2), groundwater contributions to streamflow throughout river networks reduce downstream

warming. Thus, the magnitude of the river thermal regime is dampened; and they are less sensitive to climate variability than rivers fed by a grater proportion of surface-water (Garner *et al.*, 2013; Chapter 2). Rivers that are underlain by less permeable geologies warm faster towards dynamic equilibrium with the atmosphere, maximum temperatures are higher, minimum temperatures are lower, and they are more sensitive to climatic variability (Garner *et al.*, 2013; Chapter 2).

Downstream warming trends (Poole and Berman, 2001; Cox and Bolte, 2007) can be reduced (Chapter 4) or reversed (Chapter 5) temporarily by localised processes (Poole and Berman, 2001; Moore *et al.*, 2005; Gomi *et al.*, 2006; Roth *et al*, 2010; Leach *et al.*, 2011: Westhoff et al., 2011). For example where reach-scale contributions of groundwater occur, effects are as described above (Leach *et al.*, 2011; Westhoff *et al.*, 2011; Garner *et al.*, 2014; Chapter 3), where riparian vegetation shades the water column from solar radiation gains (Moore *et al.*, 2005; Gomi *et al*., 2006; Rutherford *et al.*, 2004; Garner *et al.*, 2014; Chapters 3, 4 and 5), or where channel gradient and thus flow velocity increases (Chapter 5). Beneath riparian vegetation the effects of variable prevailing weather conditions on microclimate are reduced, solar radiation receipt is reduced greatly and net energy inputs and variability are also reduced (Chapter 3). Consequently, water temperature beneath forest canopies is less variable in response to climate (Guenther *et al.*, 2012) and thermal extremes are dampened (Garner *et al.*, 2014; Chapter 3) due to cooling or reduced warming as the river flows downstream (Chapters 4 and 5). The largest reductions in river thermal extremes and dampened responses to climate variability may occur where riparian vegetation overhangs the channel and shelters the stream while solar radiation gains are greatest i.e. on southerly banks in the Northern Hemisphere (Chapter 5). In faster flowing reaches water runs-off more quickly and therefore accumulates less heat (*cf.* at low velocity) (Chapter 5). Consequently, lower river temperatures may be

anticipated where water flows faster, thus longer lengths of river may be anticipated to be less sensitive to climate since water temperature will equilibrate with the atmosphere farther downstream (*cf.* slow flowing streams).

To summarise, river temperature may be anticipated to warm more slowly towards atmospheric equilibrium, and thus be least sensitive to climate and thus cooler throughout catchments where runoff is sourced predominantly from productive aquifers, where frequent localised groundwater upwelling occurs, where large proportions of southerly banks are shaded or where channel gradient is steep.

6.4 IMPLICATIONS FOR RIVER MANAGEMENT

The spatial extent of water temperature monitoring networks is sparse throughout the UK (Orr *et al.*, 2010; Orr *et al.*, 2013; Chapter 2), but limited high-resolution monitoring demonstrates that under present climatic conditions instantaneous maximum temperatures approach lethal-limits for sensitive species (e.g. Malcolm *et al.*, 2008). It is essential that freshwater ecosystems are protected from potentially damaging thermal maxima and so river managers must identify urgently the river waters most at risk so that mitigation measures may be implemented as a priority. The research presented within this thesis has a number of important implications for this.

Research herein suggests that river managers should anticipate lowland rivers sourced from surface water dominated runoff and shaded minimally throughout the river network to be most vulnerable to the highest temperatures (see *6.3 Synthesis*). Thus, river managers should seek strategies to reduce temperatures in these reaches as a priority. Strategies postulated to ameliorate, or mitigate against, the effects of a changing climate on water temperature include: providing shade using riparian vegetation (e.g. Hannah *et al.*, 2008; Brown *et al.*,

2010; Imholt *et al.*, 2013b; Ryan *et al.*, 2013), reconnecting rivers to their floodplains (e.g. Poole *et al.*, 2008; Opperman, 2010), reducing and retaining urban runoff (e.g. Booth and Leavitt, 1999) and lowering abstraction (Poole and Berman, 2001). This thesis was concerned primarily with semi-natural environments (i.e. Chapters 3- 5) in which catchment hydrology and geomorphology have not been altered significantly by human activities. Thus, in such catchments, riparian planting is one of the only feasible options for reducing high temperatures and thus protecting aquatic ecosystems (Beschta, 1997; Poole and Berman, 2001) and were a main focus of this research. Although Chapter 1 suggests that surface water dominated and minimally shaded lowland rivers to be most vulnerable to the highest temperatures (see *6.3 Synthesis*), paradoxically, the greatest benefits to lowlands and throughout river systems are unlikely to be achieved by riparian planting schemes in these reaches. Instead, headwaters should be afforested, firstly because riparian vegetation must overhang the water-column to be effective (Chapter 5); this is possible in headwater reaches where streams are narrow (Chapters 4 and 5) but will become more difficult and eventually impossible as a stream widens through the basin. Secondly, shading headwater reaches maintains or reduces (Chapters 4 and 5) already lower headwater temperatures; thus reducing the maximum temperature the river will warm to downstream. Consequently, it is hypothesised that concentrating management efforts in the headwaters, for example by shading with riparian vegetation will yield water temperature reductions in these streams and also throughout river basins.

In the absence of a strong knowledge base on which to make decisions, riparian planting schemes to date have focussed on afforesting open reaches without considering the density or longitudinal extent of shade required to meet temperature targets (e.g. Upper Dee Riparian Planting Scheme, 2011). In many cases this has likely caused planting schemes to be more

‘expensive’ than necessary, since the density and extent of riparian planting in headwaters should be informed by channel orientation and water velocity (Chapter 5). This research suggests that targeted afforestation on southerly banks with relatively sparse, overhanging vegetation will yield substantial reductions in maximum temperatures (Chapter Five). Consequently, planting a mosaic of forested and open landuse should be hypothesised to reduce maximum temperatures at minimal cost.

6.8 FUTURE RESEARCH PROSPECTS

Decisions regarding river catchment management are made increasingly in unmonitored basins (Soulsby *et al.*, 2006) and at large spatial scales (Soulsby *et al.*, 2006; Bachmair and Weiler, 2014). Consequently, future research should yield process-based information that is transferable between sites and scales. To achieve this, Researchers may wish to address the following fundamental research gaps as priorities:

- Work presented herein and elsewhere (e.g. Chu *et al.*, 2010; Kelleher *et al.*, 2012; Johnson *et al.*, 2014) has yielded considerable knowledge on the influence of static basin properties (e.g. geology and landuse). However, significant gaps remain in our knowledge concerning the role of dynamic basin processes, especially discharge regimes, on river temperature.
- Deterministic river temperature models driven by local micrometeorological data perform better than those driven by remote climate data (Benyahya *et al.*, 2010). The value of existing long-term microclimatic datasets (e.g. Chapter 3) should be leveraged by identifying transfer functions for predicting hydrometeorological variables and consequently water temperature at unmonitored sites from more common atmospheric observations (e.g. air temperature and atmospheric pressure).

- The effects of localised, small-scale (i.e. reach) processes such as those demonstrated herein (e.g. shaded reaches, localised groundwater upwelling and changing flow velocity) on temperature response at larger scales (i.e. throughout river basins) remains unknown. Thus, investigation of these integrated catchment-scale responses and identification of laws of transferability between scales should be a priority for future research.

In addition, future research should seek to inform river temperature management under future climates, and quantify the efficacy of potential mitigation measures. For example:

- For the UK, there are very few predictive modelling studies of river temperature under climate or hydrological change (i.e. Webb and Walling, 1992; Webb and Walsh, 2004). These studies used statistical methods that predict river temperature responses at coarse spatial (individual sites) and temporal resolution (i.e. weeks or months) and the climate projections which drove them have since been superseded. Consequently, improved future projections for river temperature at wider spatial (e.g. van Vliet et al., 2013) and finer temporal scales are required (e.g. van Vliet *et al*., 2013a; MacDonald *et al.*, 2014a).
- Worldwide, the efficacy of potential mitigation scenarios (e.g. riparian afforestation) requires assessment under scenarios of future climate and hydrological change.

6.9 FINAL REMARKS

The research presented in this thesis has improved our understanding of the influences of hydrometeorology, and riparian landuse controls on stream temperature dynamics and associated processes at a number of key spatial and temporal scales. As such, it contributes significant new knowledge that may be used by environment managers and regulators in

decision making regarding identification of the river waters throughout the UK that are most sensitive to a changing climate. The research also contributes significantly towards informing where and how riparian vegetation may be used to successfully mitigate these damaging thermal maxima.

REFERENCES

Alvarez D, Nicieza AG. 2005. Compensatory response "defends" energy levels but not growth trajectories in brown trout, Salmo trutta L. Proceedings. *Biological sciences / The Royal Society*. **272**: 601–607. DOI: 10.1098/rspb.2004.2991

Andrews T, Forster PM, Gregory JM. 2009. A Surface Energy Perspective on Climate Change. *Journal of Climate*. **22**: 2557–2570. DOI: 10.1175/2008JCLI2759.1

Arismendi I, Johnson SL, Dunham JB, Haggerty R. 2013. Descriptors of natural thermal regimes in streams and their responsiveness to change in the Pacific Northwest of North America. *Freshwater Biology*. **58**: 880–894. DOI: 10.1111/fwb.12094

Arismendi I, Johnson SL, Dunham JB, Haggerty R, Hockman-Wert D. 2012. The paradox of cooling streams in a warming world: Regional climate trends do not parallel variable local trends in stream temperature in the Pacific continental United States. *Geophysical Research Letters*. **39**: L10401. DOI: 10.1029/2012GL051448

Beechie T et al. 2013. Restoring Salmon Habitat for a Changing Climate. *River Research and Applications*. **29**: 939–960. DOI: 10.1002/rra.2590

Benjamini Y, Hochberg Y. 1995. Controlling the False Discovery Rate: A Practical and Powerful Approach to Multiple Testing. *Journal of the Royal Statistical Society. Series B (Methodological)*. **57**: 289–300. DOI: 10.2307/2346101

Beschta RL, Taylor RL. 1988. Stream temperature increases and land use in a forested Oregon watershed. *Journal of the American Water Resources Association*. **25**: 19-25. DOI: 10.1111/j.1752-1688.1988.tb00875.x

Blaen PJ, Hannah DM, Brown LE, Milner AM. 2013. Water temperature dynamics in High Arctic river basins. *Hydrological Processes*. **27**: 2958–2972. DOI: 10.1002/hyp.9431

Bloomfield JP, Jackson CR, Stuart ME. 2013. Changes in groundwater levels, temperature and quality in the UK over the 20thCentury: an assessment. *LWEC Working Paper*. Available from: http://www.lwec.org.uk/publications/water-climate-change-impacts-report-card/1-groundwater-temperature-quality

Boisneau C, Moatar F, Bodin M, Boisneau P. 2008. Does global warming impact on migration patterns and recruitment of Allis shad (Alosa alosa L.) young of the year in the Loire River, France? *Hydrobiologia*. **602**: 179–186. DOI: 10.1007/s10750-008-9291-6

Booth DB, Leavitt J. 1999. Field evaluation of permeable pavement systems for improved stormwater management. *Journal of the American Planning Association*. **65** : 314–325. DOI: 10.1080/01944369908976060

Boscarino BT, Rudstam LG, Mata S, Gal G, Johannsson OE, Mills EL. 2007. The effects of temperature and predator-prey interactions on the migration behavior and vertical distribution of Mysis relicta. *Limnology and Oceanography*. **52**: 1599–1613. DOI: 10.4319/lo.2007.52.4.1599

Bower D, Hannah DM, McGregor GR. 2004. Techniques for assessing the climatic sensitivity of river flow regimes. *Hydrological Processes*. **18**: 2515–2543. DOI: 10.1002/hyp.1479

Broadmeadow SB, Jones JG, Langford TEL, Shaw PJ, Nisbet TR. 2011. The influence of riparian shade on lowland stream water temperatures in southern England and their viability for brown trout. *River Research and Applications*. **27**: 226–237. DOI: 10.1002/rra.1354

Brown GW. 1969. Predicting Temperatures of Small Streams. *Water Resources Research*. **5**: 68–75. DOI: 10.1029/WR005i001p00068

Brown GW, Swank GW, Rothacher JND. 1971. Water temperature in the steamboat drainage. *USDA Forest Service Research Paper*. PNW-119. [online] Available from: http://www.treesearch.fs.fed.us/pubs/26238 (Accessed 22 June 2014)

Brown LE, Cooper L, Holden J, Ramchunder SJ. 2010. A comparison of stream water temperature regimes from open and afforested moorland, Yorkshire Dales, northern England. *Hydrological Processes*. **24**: 3206–3218. DOI: 10.1002/hyp.7746

Burnham KP, Anderson DR. 2002. Model Selection and Multimodel Inference: A Practical Information Theoretic Approach. Springer, New York. 480 pp.

Caissie D. 2006. The thermal regime of rivers: a review. *Freshwater Biology*. **51**: 1389–1406. DOI: 10.1111/j.1365-2427.2006.01597.x

Caissie D, Satish MG, El-Jabi N. 2007. Predicting water temperatures using a deterministic model: Application on Miramichi River catchments (New Brunswick, Canada). *Journal of Hydrology*. **336**: 303–315. DOI: 10.1016/j.jhydrol.2007.01.008

Capell R, Tetzlaff D, Soulsby C. 2013. Will catchment characteristics moderate the projected effects of climate change on flow regimes in the Scottish Highlands? *Hydrological Processes*. **27**: 687–699. DOI: 10.1002/hyp.9626

Carling PA, Orr HG, Glaister MS. 1994. Preliminary observations and significance of dead zone flow structure for solute and fine particle dynamics. In: *Mixing and Transport in the Environment*, Beven KJ, Chatwin PC, Millbank JH (eds). John Wiley & Sons: Chichester, 139-157.

Casado A, Hannah DM, Peiry J-L, Campo AM. 2013. Influence of dam-induced hydrological regulation on summer water temperature: Sauce Grande River, Argentina. *Ecohydrology*. **6**: 523–535. DOI: 10.1002/eco.1375

Chu C, Jones NE, Allin L. 2010. Linking the Thermal Regimes of Streams in the Great Lakes Basin, Ontario, to Landscape and Climate Variables. *River Research and Applications*. **26**: 221–241. DOI: 10.1002/rra.1259

Clark E, Webb BW, Ladle M. 1999. Microthermal gradients and ecological implications in Dorset rivers. *Hydrological Processes*. **13**: 423–438. DOI: 10.1002/(SICI)1099-1085(19990228)13:3<423::AID-HYP747>3.0.CO;2-#

Cole E, Newton M. 2000. Influence of streamside buffers on stream temperature response following clear-cut harvesting in western Oregon. *Canadian Journal of Forest Research*. **43**: 993–1005. DOI: 10.1139/cjfr-2013-0138

Crisp DT. 1999. Water temperature of Plynlimon streams. *Hydrology and Earth System Sciences*. **1**: 535–540. DOI: 10.5194/hess-1-535-1997

Crisp DT, Matthews AM, Westlake DF. 1982. The temperatures of nine flowing waters in southern England. *Hydrobiologia* **89**: 193–204. DOI: 10.1007/BF00005705

Cross BK, Bozek MA, Mitro MG. 2013. Influences of Riparian Vegetation on Trout Stream Temperatures in Central Wisconsin. *North American Journal of Fisheries Management*. **33**: 682–692. DOI: 10.1080/02755947.2013.785989

Danehy RJ, Colson CG, Parrett KB, Duke SD. 2005. Patterns and sources of thermal heterogeneity in small mountain streams within a forested setting. *Forest Ecology and Management*. **208**: 287–302. DOI: 10.1016/j.foreco.2004.12.006

Durance I, Ormerod SJ. 2007. Climate change effects on upland stream macroinvertebrates over a 25-year period. *Global Change Biology*. **13**: 942–957. DOI: 10.1111/j.1365-2486.2007.01340.x

Edinger JE, Duttweiler DW, Geyer JC. 1968. The Response of Water Temperatures to Meteorological Conditions. *Water Resources Research*. **4**: 1137–1143. DOI: 10.1029/WR004i005p01137

Erickson TR, Stefan HG. 2000. Linear Air/Water Temperature Correlations for Streams During Open Water Periods. *Journal of Hydrologic Engineering*. **5**: 317–321. DOI: 10.1061/(ASCE)1084-0699(2000)5:3(317)

Evans EC, McGregor GR, Petts GE. 1998. River energy budgets with special reference to river bed processes. *Hydrological Processes*. **12**: 575–595. DOI: 10.1002/(SICI)1099-1085(19980330)12:4<575::AID-HYP595>3.0.CO;2-Y

Frazer GW, Canham CD, Lertzman KP. 1999. *Gap Light Analyzer (GLA), Version 2: Imaging Software to Extract Canopy Structure and Light Transmission Indices from True-Colour Fisheye Photographs, User's Manual and Program Documentation*, Simon Frazer University and Institute of Ecosystem Studies, Millbrook, NY, 36 pp.

Forestry Commission. 2011. *Forests and Water Guidelines*, 5th edn. Forestry Commission: Edinburgh; 80, ISBN 978-0-85538-837-9.

Garner G, Hannah DM, Sadler JP, Orr HG. 2013. River temperature regimes of England and Wales: spatial patterns, inter-annual variability and climatic sensitivity. *Hydrological Processes*. DOI: 10.1002/hyp.9992

Garner G, Malcolm IA, Sadler JP, Hannah DM. 2014. Inter-annual variability in the effects of riparian microclimate, energy exchanges and water temperature of an upland Scottish stream. *Hydrological Processes*. DOI: 10.1002/ hyp.10223.

Groom JD, Dent L, Madsen LJ, Fleuret J. 2011. Response of western Oregon (USA) stream temperatures to contemporary forest management. *Forest Ecology and Management*. **262**: 1618–1629. DOI: 10.1016/j.foreco.2011.07.012

Gu RR, Li Y. 2002. River temperature sensitivity to hydraulic and meteorological parameters. *Journal of Environmental Management*. **66**: 43–56.

Guenther SM, Moore RD, Gomi T. 2012. Riparian microclimate and evaporation from a coastal headwater stream, and their response to partial-retention forest harvesting. *Agricultural and Forest Meteorology*. **164**: 1–9. DOI: 10.1016/j.agrformet.2012.05.003

Hannah DM, Malcolm IA, Bradley C. 2009. Seasonal hyporheic temperature dynamics over riffle bedforms. *Hydrological Processes*. **23**: 2178–2194. DOI: 10.1002/hyp.7256

Hannah DM, Malcolm IA, Soulsby C, Youngson AF. 2004. Heat exchanges and temperatures within a salmon spawning stream in the Cairngorms, Scotland: seasonal and sub-seasonal dynamics. *River Research and Applications*. **20**: 635–652. DOI: 10.1002/rra.771

Hannah DM, Malcolm IA, Soulsby C, Youngson AF. 2008a. A comparison of forest and moorland stream microclimate, heat exchanges and thermal dynamics. *Hydrological Processes*. **22**: 919–940. DOI: 10.1002/hyp.7003

Hannah DM, Smith BPG, Gurnell AM, McGregor GR. 2000. An approach to hydrograph classification. *Hydrological Processes*. **14**: 317–338. DOI: 10.1002/(SICI)1099-1085(20000215)14:2<317::AID-HYP929>3.0.CO;2-T

Hannah DM, Webb BW, Nobilis F. 2008b. River and stream temperature: dynamics, processes, models and implications - Preface. *Hydrological Processes*. **22**: 899–901. DOI: 10.1002/hyp.6997

Hari RE, Livingstone DM, Siber R, Burkhardt-Holm P, Güttinger H. 2006. Consequences of climatic change for water temperature and brown trout populations in Alpine rivers and streams. *Global Change Biology*. **12**: 10–26. DOI: 10.1111/j.1365-2486.2005.001051.x

Harper MP, Peckarsky BL. 2006. Emergence cues of a mayfly in a high-altitude stream ecosystem: Potential response to climate change. *Ecological Applications*. **16**: 612–621. DOI: 10.1890/1051-0761(2006)016[0612:ECOAMI]2.0.CO;2

Harris NM, Gurnell AM, Hannah DM, Petts GE. 2000. Classification of river regimes: a context for hydroecology. *Hydrological Processes*. **14**: 2831–2848. DOI: 10.1002/1099-1085(200011/12)14:16/17<2831::AID-HYP122>3.0.CO;2-O

Hastie T, Tibshirani R. 1987. Generalized Additive-Models - Some Applications. *Journal of the American Statistical Association*. **82**: 371–386. DOI: 10.2307/2289439

Hebert C, Caissie D, Satish MG, El-Jabi N. 2011. Study of stream temperature dynamics and corresponding heat fluxes within Miramichi River catchments (New Brunswick, Canada). *Hydrological Processes*. **25**: 2439–2455. DOI: 10.1002/hyp.8021

Herb WR, Janke B, Mohseni O, Stefan HG. 2008. Thermal pollution of streams by runoff from paved surfaces. *Hydrological Processes*. **22**: 987–999. DOI: 10.1002/hyp.6986

Herb WR, Stefan HG. 2011. Modified equilibrium temperature models for cold-water streams. *Water Resources Research*. **47**: W06519. DOI: 10.1029/2010WR009586

Hester ET, Bauman KS. 2013. Stream and Retention Pond Thermal Response to Heated Summer Runoff From Urban Impervious Surfaces. *Journal of the American Water Resources Association*. **49**: 328–342. DOI: 10.1111/jawr.12019

Hollander M, Wolfe DA. 1999. *Nonparametric Statistical Methods*. 2nd Edition. Wiley-Interscience: New York

Hrachowitz M, Soulsby C, Imholt C, Malcolm IA, Tetzlaff D. 2010. Thermal regimes in a large upland salmon river: a simple model to identify the influence of landscape controls and climate change on maximum temperatures. *Hydrological Processes*. **24**: 3374–3391. DOI: 10.1002/hyp.7756

Huguet F, Parey S, Dacunha-Castelle D, Malek F. 2008. Is there a trend in extremely high river temperature for the next decades? A case study for France. *Natural Hazards and Earth System Sciences*. **8**: 67–79.

Imholt C, Gibbins CN, Malcolm IA, Langan S, Soulsby C. 2010. Influence of riparian cover on stream temperatures and the growth of the mayfly Baetis rhodani in an upland stream. *Aquatic Ecology*. **44**: 669–678. DOI: 10.1007/s10452-009-9305-0

Imholt C, Malcolm IA, Bacon PJ, Gibbins CN, Soulsby C, Miles M, Fryer RJ. 2011. Does diurnal temperature variability affect growth in juvenile Atlantic salmon Salmo salar? *Journal of Fish Biology*. **78**: 436–448. DOI: 10.1111/j.1095-8649.2010.02838.x

Imholt C, Soulsby C, Malcolm I a., Gibbins C n. 2013a. Influence of contrasting riparian forest cover on stream temperature dynamics in salmonid spawning and nursery streams. *Ecohydrology*. **6**: 380–392. DOI: 10.1002/eco.1291

Imholt C, Soulsby C, Malcolm IA, Hrachowitz M, Gibbins CN, Langan S, Tetzlaff D. 2013b. Influence of Scale on Thermal Characteristics in a Large Montane River Basin. *River Research and Applications*. **29**: 403–419. DOI: 10.1002/rra.1608

Isaak DJ, Hubert WA. 2001. A hypothesis about factors that affect maximum summer stream temperatures across montane landscapes. *Journal of the American Water Resources Association*. **37**: 351–366. DOI: 10.1111/j.1752-1688.2001.tb00974.x

Isaak DJ, Wollrab S, Horan D, Chandler G. 2012. Climate change effects on stream and river temperatures across the northwest US from 1980-2009 and implications for salmonid fishes. *Climatic Change*. **113**: 499–524. DOI: 10.1007/s10584-011-0326-z

Iqbal M. 1983. *An Introduction to Solar Radiation*. Academic Press, Toronto. 360 pp.

Jensen AJ. 2003. Atlantic salmon (Salmo salar) in the regulated River Alta: Effects of altered water temperature on parr growth. *River Research and Applications*. **19**: 733–747. DOI: 10.1002/rra.710

Johnson MF, Wilby RL, Toone JA. 2014. Inferring air- water temperature relationships from river and catchment properties. *Hydrological Processes*. **28**: 2912–2928. DOI: 10.1002/hyp.9842

Johnson SL, Jones JA. 2000. Stream temperature responses to forest harvest and debris flows in western Cascades, Oregon. *Canadian Journal of Fisheries and Aquatic Sciences*. **57** : 30–39. DOI: 10.1139/f00-109

Kalkstein LS, Tain G, Skindlov JA. 1987. An evaluation of three clustering procedures for use in synoptic climatological classifications. *Journal of Applied Meteorology* **26**(6): 717–730.

Kaushal SS, Likens GE, Jaworski NA, Pace ML, Sides AM, Seekell D, Belt KT, Secor DH, Wingate RL. 2010. Rising stream and river temperatures in the United States. *Frontiers in Ecology and the Environment*. **8**: 461–466. DOI: 10.1890/090037

Keith RM, Bjornn TC, Meehan WR, Hetrick NJ, Brusven MA. 1998. Response of juvenile salmonids to riparian and instream cover modifications in small streams flowing through second-growth forests of southeast Alaska. *Transactions of the American Fisheries Society*. **127**: 889–907. DOI: 10.1577/1548-8659(1998)127<0889:ROJSTR>2.0.CO;2

Kelleher C, Wagener T, Gooseff M, McGlynn B, McGuire K, Marshall L. 2012. Investigating controls on the thermal sensitivity of Pennsylvania streams. *Hydrological Processes*. **26**: 771–785. DOI: 10.1002/hyp.8186

Kennard MJ, Pusey BJ, Olden JD, MacKay SJ, Stein JL, Marsh N. 2010. Classification of natural flow regimes in Australia to support environmental flow management. *Freshwater Biology*. **55**: 171–193. DOI: 10.1111/j.1365-2427.2009.02307.x

Kent M, Coker P. 1992. *Vegetation description and analysis: A practical approach*. Wiley: Chichester, 363pp.

Klein R. 1979. Urbanization and Stream Quality Impairment. *Water Resources Bulletin*. **15**: 948–963.

Krause S, Hannah DM, Blume T. 2011. Interstitial pore-water temperature dynamics across a pool-riffle-pool sequence. *Ecohydrology*. **4**: 549–563. DOI: 10.1002/eco.199

Kurylyk BL, Bourque CP-A, MacQuarrie KTB. 2013. Potential surface temperature and shallow groundwater temperature response to climate change: an example from a small forested catchment in east-central New Brunswick (Canada). *Hydrology and Earth System Sciences*. **17**: 2701–2716. DOI: 10.5194/hess-17-2701-2013

Kurylyk BL, MacQuarrie KTB, Voss CI. 2014. Climate change impacts on the temperature and magnitude of groundwater discharge from shallow, unconfined aquifers. *Water Resources Research*. **50** : 3253–3274. DOI: 10.1002/2013WR014588

Laize CLR, Hannah DM. 2010. Modification of climate-river flow associations by basin properties. *Journal of Hydrology*. **389**: 186–204. DOI: 10.1016/j.jhydrol.2010.05.048

Langan SJ, Johnston L, Donaghy MJ, Youngson AF, Hay DW, Soulsby C. 2001. Variation in river water temperatures in an upland stream over a 30-year period. *Science of the Total Environment*. **265**: 195–207. DOI: 10.1016/S0048-9697(00)00659-8

Leach JA, Moore RD. 2010. Above-stream microclimate and stream surface energy exchanges in a wildfire-disturbed riparian zone. *Hydrological Processes*. **24**: 2369–2381. DOI: 10.1002/hyp.7639

Leach JA, Moore RD. 2011. Stream temperature dynamics in two hydrogeomorphically distinct reaches. *Hydrological Processes*. **25**: 679–690. DOI: 10.1002/hyp.7854

Leach JA, Moore RD. 2014. Winter stream temperature in the rain-on-snow zone of the Pacific Northwest: influences of hillslope runoff and transient snow cover. *Hydrology and Earth System Sciences*. **18**: 819–838. DOI: 10.5194/hess-18-819-2014

Leach JA, Moore RD, Hinch SG, Gomi T. 2012. Estimation of forest harvesting-induced stream temperature changes and bioenergetic consequences for cutthroat trout in a coastal stream in British Columbia, Canada. *Aquatic Sciences*. **74**: 427–441. DOI: 10.1007/s00027-011-0238-z

Lee TY, Huang JC, Kao SJ, Liao LY, Tzeng CS, Yang CH, Kalita PK, Tung CP. 2012. Modeling the effects of riparian planting strategies on stream temperature: Increasing suitable habitat for endangered Formosan Landlocked Salmon in Shei-Pa National Park, Taiwan. *Hydrological Processes*. **26**: 3635–3644. DOI: 10.1002/hyp.8440

Macdonald JS, MacIsaac EA, Herunter HE. 2003. The effect of variable-retention riparian buffer zones on water temperatures in small headwater streams in sub-boreal forest ecosystems of British Columbia. *Canadian Journal of Forest Research*. **33**: 1371–1382. DOI: 10.1139/X03-015

MacDonald RJ, Boon S, Byrne JM, Robinson MD, Rasmussen JB. 2014. Potential future climate effects on mountain hydrology, stream temperature, and native salmonid life history. *Canadian Journal of Fisheries and Aquatic Sciences*. **71**: 189–202. DOI: 10.1139/cjfas-2013-0221

Maderich V, Heling R, Bezhenar R, Brovchenko I, Jenner H, Koshebutskyy V, Kuschan A, Terletska K. 2008. Development and application of 3D numerical model THREETOX to the prediction of cooling water transport and mixing in the inland and coastal waters. *Hydrological Processes*. **22**: 1000–1013. DOI: 10.1002/hyp.6985

Malcolm IA, Hannah DM, Donaghy MJ, Soulsby C, Youngson AF. 2004a. The influence of riparian woodland on the spatial and temporal variability of stream water temperatures in an upland salmon stream. *Hydrology and Earth System Sciences*. **8** : 449–459. DOI: 10.5194/hess-8-449-2004

Malcolm IA, Middlemas CA, Soulsby C, Middlemas SJ, Youngson AF. 2010. Hyporheic zone processes in a canalised agricultural stream: implications for salmonid embryo survival.

Fundamental and Applied Limnology / Archiv für Hydrobiologie. **176**: 319–336. DOI: 10.1127/1863-9135/2010/0176-0319

Malcolm IA, Soulsby C, Hannah DM, Bacon PJ, Youngson AF, Tetzlaff D. 2008. The influence of riparian woodland on stream temperatures: implications for the performance of juvenile salmonids. *Hydrological Processes*. **22**: 968–979. DOI: 10.1002/hyp.6996

Malcolm IA, Soulsby C, Youngson AF, Hannah DM. 2005. Catchment-scale controls on groundwater–surface water interactions in the hyporheic zone: implications for salmon embryo survival. *River Research and Applications*. **21**: 977–989. DOI: 10.1002/rra.861

Malcolm IA, Soulsby C, Youngson AF, Hannah DM, McLaren IS, Thorne A. 2004b. Hydrological influences on hyporheic water quality: implications for salmon egg survival. *Hydrological Processes*. **18**: 1543–1560. DOI: 10.1002/hyp.1405

Marsh T, Black A, Acreman M, Elliot C. 2000. River flows. In *The Hydrology of the UK*, Acreman M (ed). Routledge: London; 101–133.

Marsh T, Cole G, Wilby R. 2007. Major droughts in England and Wales, 1800–2006. *Weather*. **62**: 87–93. DOI: 10.1002/wea.67

McGurk BJ. Predicting Stream Temperature After Riparian Vegetation Removal. In: *Proceedings of the Californian Riparian Systems Conference on Protection, Management, Restoration for the 1990s*. Davis, California, 157-164.

Meisner JD, Rosenfeld JS, Regier HA. 1988. The Role of Groundwater in the Impact of Climate Warming on Stream Salmonines. *Fisheries*. **13**: 2–8. DOI: 10.1577/1548-8446(1988)013<0002:TROGIT>2.0.CO;2

Meyer SL. 1992. *Data Analysis for Scientists and Engineers*. 1st Edition. Peer Management Consultants Ltd: Evanston, IL

Mohseni O, Erickson TR, Stefan HG. 1999. Sensitivity of stream temperatures in the United States to air temperatures projected under a global warming scenario. *Water Resources Research*. **35**: 3723–3733. DOI: 10.1029/1999WR900193

Mohseni O, Stefan HG, Eaton JG. 2003. Global warming and potential changes in fish habitat in US streams. *Climatic Change*. **59**: 389–409. DOI: 10.1023/A:1024847723344

Montgomery DR. 1999. Process domains and the river continuum. *Journal of the American Water Resources Association*. **35**: 397–410. DOI: 10.1111/j.1752-1688.1999.tb03598.x

Moore RD, Spittlehouse DL, Story A. 2005a. Riparian microclimate and stream temperature response to forest harvesting: A review. *Journal of the American Water Resources Association*. **41**: 813–834.

Moore RD, Sutherland P, Gomi T, Dakal A. 2005b. Thermal regime of a headwater stream within a clear-cut, coastal British Columbia. *Hydrological Processes*. **19**: 2591-2608. DOI: 1 0.1002/hyp.5733

O'Driscoll MA, DeWalle DR. 2006. Stream-air temperature relations to classify stream-ground water interactions. *Journal of Hydrology*. **329**: 140–153. DOI: 10.1016/j.jhydrol.2006.02.010

Opperman JJ, Luster R, McKenney BA, Roberts M, Meadows AW. 2010. Ecologically Functional Floodplains: Connectivity, Flow Regime, and Scale. *Journal of the American Water Resources Association*. **46**: 211–226. DOI: 10.1111/j.1752-1688.2010.00426.x

Ormerod SJ. 2009. Climate change, river conservation and the adaptation challenge. *Aquatic Conservation: Marine and Freshwater Ecosystems*. **19**: 609–613. DOI: 10.1002/aqc.1062

Orr HG, Des Clers S, Simpson GL, Hughes M, Battarbee RW, Cooper L, Dunbar MJ, Evans R, Hannaford J, Hannah DM, Laize C,Watts G, Wilby RL. 2010. Changing water temperatures: a surface water archive for England and Wales. In *British Hydrological Society's Third International Symposium, 'Role of Hydrology in Managing Consequences of a Changing Global Environment'*, Kirby C(ed). British Hydrological Society. BHS: Newcastle University.

Orr HG Simpson GL, des Clers S, Watts G, Highes M, Hannaford J, Dunbar MJ, Laize C, Wilby RL, Battarbee RW, Evans R. 2014. Detecting changing river temperatures in England and Wales. *Hydrological Processes.* DOI: 10.1002/hyp.10181

Payn RA, Gooseff MN, McGlynn BL, Bencala KE, Wondzell SM. 2012. Exploring changes in the spatial distribution of stream baseflow generation during a seasonal recession. *Water Resources Research*. **48**: W04519. DOI: 10.1029/2011WR011552

Picard CR, Bozek MA, Momot WT. 2003. Effectiveness of using summer thermal indices to classify and protect brook trout streams in northern Ontario. *North American Journal of Fisheries Management*. **23**: 206–215. DOI: 10.1577/1548-8675(2003)023<0206:EOUSTI>2.0.CO;2

Pilgrim JM, Fang X, Stefan HG. 1998. Stream temperature correlations with air temperatures in Minnesota: Implications for climate warming. *Journal of the American Water Resources Association*. **34**: 1109–1121. DOI: 10.1111/j.1752-1688.1998.tb04158.x

Poff NL, Tokar S, Johnson P. 1996. Stream hydrological and ecological responses to climate change assessed with an artificial neural network. *Limnology and Oceanography*. **41**: 857–863.

Poole GC, Berman CH. 2001. An Ecological Perspective on In-Stream Temperature: Natural Heat Dynamics and Mechanisms of Human-CausedThermal Degradation. *Environmental Management*. **27**: 787–802. DOI: 10.1007/s002670010188

Poole GC, O'Daniel SJ, Jones KL, Woessner WW, Bernhardt ES, Helton AM, Stanford JA, Boer BR, Beechie TJ. 2008. Hydrologic spiralling: The role of multiple interactive flow paths in stream ecosystems. *River Research and Applications*. **24**: 1018–1031. DOI: 10.1002/rra.1099

Prata AJ. 1996. A new long-wave formula for estimating downward clear-sky radiation at the surface. *Quarterly Journal of the Royal Meteorological Society*. **122**: 1127–1151. DOI: 10.1002/qj.49712253306

R Core Team. 2013. R: A language and Environment for Statistical Computing. R Foundation for Statistical Computing, Vienna, Asutria. Available at: http://www.R-project.org. Last Accessed: 27/05/2014.

Ramanathan V. 1981. The Role of Ocean-Atmosphere Interactions in the CO_2 Climate Problem. *Journal of the Atmospheric Sciences*. **38**: 918–930. DOI: 10.1175/1520-0469(1981)038<0918:TROOAI>2.0.CO;2

Roth TR, Westhoff MC, Huwald H, Huff JA, Rubin JF, Barrenetxea G, Vettereli M, Parriaux A, Selker JS, Parlange MB. 2010. Stream temperature response to three riparian vegetation scenarios by use of a distributed temperature validated model. Environmental Science and Technology. **44**: 2072-2078. DOI: 10.1021/es902654f

Rutherford JC, Marsh NA, Davies PM, Bunn SE. 2004. Effects of patchy shade on stream water temperature: how quickly do small streams heat and cool? *Marine and Freshwater Research*. **55**: 737–748. DOI: 10.1071/MF04120

Ryan DK, Yearsley JM, Kelly-Quinn M. 2013. Quantifying the effect of semi-natural riparian cover on stream temperatures: implications for salmonid habitat management. *Fisheries Management and Ecology*. **20**: 494–507. DOI: 10.1111/fme.12038

Sand-Jensen K, Pedersen NL. 2005. Differences in temperature, organic carbon and oxygen consumption among lowland streams. *Freshwater Biology*. **50**: 1927–1937. DOI: 10.1111/j.1365-2427.2005.01436.x

Soetaert K, Petzoldt T, Woodrow Setzer R. 2010. Solving differential equations in R: package deSolve. *Journal of Statistical Software*. **33**: 1-25.

Story A, Moore RD, Macdonald JS. 2003. Stream temperatures in two shaded reaches below cutblocks and logging roads: downstream cooling linked to subsurface hydrology. *Canadian Journal of Forest Research*. **33**: 1383–1396. DOI: 10.1139/x03-087

Stott T, Marks S. 1999. Effects of plantation forest clearfelling on stream temperatures in the Plynlimon experimental catchments, mid-Wales. *Hydrology and Earth System Sciences*. **4**: 95–104. DOI: 10.5194/hess-4-95-2000

Stull RB. 2000. *Meteorology for Scientists and Engineers*. Brooks/ Cole: Pacific Grove.

Subehi L, Fukushima T, Onda Y, Mizugaki S, Gomi T, Terajima T, Kosugi K, Hiramatsu S, Kitahara H, Kuraji K, Ozaki N. 2009. Influences of forested watershed conditions on fluctuations in stream water temperature with special reference to watershed area and forest type. *Limnology*. **10**: 33–45. DOI: 10.1007/s10201-008-0258-0

Tague C, Farrell M, Grant G, Lewis S, Rey S. 2007. Hydrogeologic controls on summer stream temperatures in the McKenzie River basin, Oregon. *Hydrological Processes*. **21**: 3288–3300. DOI: 10.1002/hyp.6538

Tait C, Li J, Lamberti G, Pearsons T, Li H. 1994. Relationships Between Riparian Cover and the Community Structure of High Desert Streams. *Journal of the North American Benthological Society*. **13**: 45–56. DOI: 10.2307/1467264

Taylor CA, Stefan HG. 2009. Shallow groundwater temperature response to climate change and urbanization. *Journal of Hydrology*. **375**: 601–612. DOI: 10.1016/j.jhydrol.2009.07.009

Tetzlaff D, Soulsby C, Gibbins C, Bacon PJ, Youngson AF. 2005. An approach to assessing hydrological influences on feeding opportunities of juvenile Atlantic salmon (Salmo salar): a case study of two contrasting years in a small, nursery stream. *Hydrobiologia*. **549**: 65–77. DOI: 10.1007/s10750-005-4166-6

Tetzlaff D, Soulsby C, Waldron S, Malcolm IA, Bacon PJ, Dunn SM, Lilly A, Youngson AF. 2007. Conceptualization of runoff processes using a geographical information system and tracers in a nested mesoscale catchment. *Hydrological Processes*. **21**: 1289–1307. DOI: 10.1002/hyp.6309

Theurer FD, Voos KA, Miller WJ. 1984. Instream water temperature model. Instream Flow Information Paper 16. *US Fish and Wildlife Service*. FWS/OBS.84/15/v.p.

Torgersen CE, Price DM, Li HW, McIntosh BA. 1999. Multiscale thermal refugia and stream habitat associations of chinook salmon in northeastern Oregon. *Ecological Applications*. **9**: 301–319. DOI: 10.2307/2641187

Uehlinger U, Malard F, Ward JV. 2003. Thermal patterns in the surface waters of a glacial river corridor (Val Roseg, Switzerland). *Freshwater Biology*. **48**: 284–300. DOI: 10.1046/j.1365-2427.2003.01000.x

UK Meteorological Office. 2014. MIDAS Land Surface Stations data (1853–current). *NCAS British Atmospheric Data Centre*. 06/01/2014. Available from: http://badc.nerc.ac.uk/view/badc.nerc.ac.uk_ATOM_dataent_ukmo-midas.

University of Manchester/University of London. 2001. Original ERS data ©ESA 1999/2000 (2010). Received and distributed by QinetiQ under licence from the European Space Agency.

Upper Dee riparian scheme, The River Dee Trust: http://www.theriverdeetrust.org.uk/information/our_work.asp, last accessed: 05/06/214, 2011.

Van Vliet MTH, Franssen WHP, Yearsley JR, Ludwig F, Haddeland I, Lettenmaier DP, Kabat P. 2013a. Global river discharge and water temperature under climate change. *Global Environmental Change*. **23**: 450–464. DOI: 10.1016/j.gloenvcha.2012.11.002

Van Vliet MTH, Ludwig F, Zwolsman JJG, Weedon GP, Kabat P. 2011. Global river temperatures and sensitivity to atmospheric warming and changes in river flow. *Water Resources Research*. **47**: W02544. DOI: 10.1029/2010WR009198

Van Vliet MTH, Voegele S, Ruebbelke D. 2013b. Water constraints on European power supply under climate change: impacts on electricity prices. *Environmental Research Letters*. **8**: 035010. DOI: 10.1088/1748-9326/8/3/035010

Van Vliet MTH, Yearsley JR, Ludwig F, Voegele S, Lettenmaier DP, Kabat P. 2012. Vulnerability of US and European electricity supply to climate change. *Nature Climate Change*. **2**: 676–681. DOI: 10.1038/NCLIMATE1546

Watanabe M, Adams RM, Wu JJ, Bolte JP, Cox MM, Johnson SL, Liss WJ, Boggess WG, Ebersole JL. 2005. Toward efficient riparian restoration: integrating economic, physical, and biological models. *Journal of Environmental Management*. **75**: 93–104. DOI: 10.1016/j.jenvman.2004.11.005

Weatherley NS, Ormerod SJ. 1990. Forests and the temperature of upland streams in Wales: a modelling exploration of the biological effects. *Freshwater Biology*. **24**: 109–122. DOI: 10.1111/j.1365-2427.1990.tb00312.x

Webb BW. 1996. Trends in stream and river temperature. *Hydrological Processes*. **10**: 205–226.

Webb BW, Clack PD, Walling DE. 2003. Water–air temperature relationships in a Devon river system and the role of flow. *Hydrological Processes*. **17**: 3069–3084. DOI: 10.1002/hyp.1280

Webb BW, Crisp DT. 2006. Afforestation and stream temperature in a temperate maritime environment. *Hydrological Processes*. **20**: 51–66. DOI: 10.1002/hyp.5898

Webb BW, Hannah DM, Moore RD, Brown LE, Nobilis F. 2008. Recent advances in stream and river temperature research. *Hydrological Processes*. **22**: 902–918. DOI: 10.1002/hyp.6994

Webb BW, Nobilis F. 1994. Water Temperature Behavior in the River Danube During the 20th-Century. *Hydrobiologia*. **291**: 105–113. DOI: 10.1007/BF00044439

Webb BW, Nobilis F. 2007. Long-term changes in river temperature and the influence of climatic and hydrological factors. *Hydrological Sciences Journal*. **52**: 74–85. DOI: 10.1623/hysj.52.1.74

Webb BW, Walling DE. 1986. Spatial variation of water temperature characteristics and behavior in a Devon river system. *Freshwater Biology*. **16**: 585–608. DOI: 10.1111/j.1365-2427.1986.tb01002.x

Webb BW, Walling D. 1992. Long-Term Water Temperature Behavior and Trends in a Devon, Uk, River System. *Hydrological Sciences Journal*. **37**: 567–580. DOI: 10.1080/02626669209492624

Webb BW, Walling DE. 1997. Complex summer water temperature behaviour below a UK regulating reservoir. *Regulated Rivers-Research & Management* **13**: 463–477. DOI: 10.1002/(SICI)1099-1646(199709/10)13:5<463::AID-RRR470>3.0.CO;2-1

Webb BW, Walsh AJ. 2004. Changing UK river temperatures and their impact on fish populations. In: *Hydrology: Science and practice for the 21st century Volume II* (Proceedings of the British Hydrological Society International Conference, Imperial College, London, July 2004), Webb B, Acreman M, Maksimovic C, Smithers H, Kirby, C (eds). British Hydrological Society, 177-191.

Webb BW, Zhang Y. 1997. Spatial and seasonal variability in the components of the river heat budget. *Hydrological Processes*. **11**: 79–101. DOI: 10.1002/(SICI)1099-1085(199701)11:1<79::AID-HYP404>3.3.CO;2-E

Webb BW, Zhang Y. 1999. Water temperatures and heat budgets in Dorset chalk water courses. *Hydrological Processes*. **13**: 309–321. DOI: 10.1002/(SICI)1099-1085(19990228)13:3<309::AID-HYP740>3.0.CO;2-7

Webb BW, Zhang Y. 2004. Intra-annual variability in the non-advective heat energy budget of Devon streams and rivers. *Hydrological Processes*. **18**: 2117–2146. DOI: 10.1002/hyp.1463

Wehrly KE, Wang L, Mitro M. 2007. Field-based estimates of thermal tolerance limits for trout: Incorporating exposure time and temperature fluctuation. *Transactions of the American Fisheries Society*. **136** : 365–374. DOI: 10.1577/T06-163.1

Westhoff MC, Gooseff MN, Bogaard TA, Savenije HHG. 2011. Quantifying hyporheic exchange at high spatial resolution using natural temperature variations along a first-order stream. *Water Resources Research*. 47. DOI: 10.1029/2010WR009767

Wilby RL, Orr H, Watts G, Battarbee RW, Berry PM, Chadd R, Dugdale SJ, Dunbar MJ, Elliott JA, Extence C, Hannah DM, Holmes N, Johnson AC, Knights B, Milner NJ, Ormerod SJ, Solomon D, Timlett R, Whitehead J, Wood PJ. 2010. Evidence needed to manage freshwater ecosystems in a changing climate: Turning adaptation principles into practice. *Science of the Total Environment*. **408**: 4150–4164. DOI: 10.1016/j.scitotenv.2010.05.014

Wild M, Ohmura A, Cubasch U. 1997. GCM-simulated surface energy fluxes in climate change experiments. *Journal of Climate*. **10**: 3093–3110. DOI: 10.1175/1520-0442(1997)010<3093:GSSEFI>2.0.CO;2

Wood SN. 2006. Generalized Additive Models: An Introduction with R. Boca Raton, Chapman and Hall/ CRC, Boca Raton. 391 pp.

Xin Z, Kinouchi T. 2013. Analysis of stream temperature and heat budget in an urban river under strong anthropogenic influences. *Journal of Hydrology*. **489**: 16–25. DOI: 10.1016/j.jhydrol.2013.02.048

Young KA. 2000. Riparian Zone Management in the Pacific Northwest: Who's Cutting What? *Environmental Management*. **26**: 131–144. DOI: 10.1007/s002670010076

APPENDIX: PEER-REVIEWED ARTICLES ACCEPTED FOR PUBLICATION

Garner G, Hannah DM, Sadler JP, Orr HG. 2013. River temperature regimes of England and Wales: spatial patterns, inter-annual variability and climatic sensitivity. *Hydrological Processes.* DOI: 10.1002/hyp.9992

Garner G, Malcolm IA, Sadler JP, Millar CP, Hannah DM. 2014. Inter-annual variability in the effects of riparian woodland on micro-climate, energy exchanges and water temperature of an upland Scottish stream. *Hydrological Processes*. DOI: 10.1002/hyp.10223.

Hannah DM, **Garner G**. In Press. River water temperature in the United Kingdom: changes over the 20th century and possible changes over the 21st century. *Progress in Physical Geography*. DOI: 10.1177/0309133314550669.

Watts G, Battarbee R, Bloomfield JP, Crossman J, Daccache A, Durance I, Elliot A, **Garner G**, Hannaford J, Hannah DM, Hess T, Jackson CR, Kay AL, Kernan M, Knox J, Mackay JD, Marianne SE, Monteith D, Ormerod S, Rance J, Wade A, Wade S, Weatherhead K, Whitehead P, Wilby RL. In Press. Climate change and water in the UK- past changes and future prospects. *Progress in Physical Geography*.